

The morphological effects of Sediment Diversions on the Lower Mississippi River



Final Report

MSc-thesis

M.F.M. (Matthijs) Bos

May 30, 2011

Delft University of Technology
Faculty of Civil Engineering and Geosciences
Department of Hydraulic Engineering

Graduation committee:

Prof. H.J. de Vriend,
Dr. C.J. Sloff,
Dr. E. Mosselman,
Dr. M. van Ledden MBA,
Dr. A. Blom,
Dr. I.Y. Georgiou,

Delft University of Technology
Delft University of Technology, Deltares
Delft University of Technology, Deltares
Royal Haskoning
Delft University of Technology
University of New Orleans



Preface and Acknowledgments

This report contains the Msc-thesis for the Master Hydraulic Engineering at Delft University of Technology. The study was commissioned and funded by Royal Haskoning and Deltares. This research was done in the time frame of 8 months, from September 2010 to May 2011. As part of the thesis, three months from November to January was spent in New Orleans. Royal Haskoning hosted this stay. A blog about this stay is enclosed in Appendix J.

The visit to New Orleans made it possible to cooperate with several researchers in the US and to experience the Mississippi in real life. Therefore many thanks goes to all who made a contribution to this research. First of all the colleagues at Haskoning Inc. in New Orleans, and especially Mr. Kluyver Mrs. Wise. They really assured a good foundation for this study and a nice stay in New Orleans. I also would like to thank the researchers, Mr. Pereira, Ms. Davis of UNO and Mr. Karadogan of LSU who gave access to additional field data and model results. Moreover thanks goes to Dr. Yossef for helping with the model setup, grid design and all the software programming behind the scenes.

I am also thankful to my Graduation Committee: Dr. Van Ledden for giving the opportunity to start this study and to make it possible to go New Orleans, Dr. Sloff and Dr. Mosselman for all the theoretical assistance and finding a way through Delft3D, Dr. Blom and Prof. De Vriend for giving the necessary assistance from the University, and Dr. Georgiou for helping to get an understanding of the Lower Mississippi River behavior and the introduction to other researchers.

Finally I especially wish to thank my girlfriend and friends and family, who were of helping hand, supportive and gave confidentiality.

Executive summary

The wetlands in the Mississippi delta (USA) are drastically subsiding and eroding. Many projects and researches are ongoing to determine how this “drowning effect” of the delta can be stopped. One of the solutions that could be feasible is implementing sediment diversions in the levees of the Lower Mississippi River in order to divert sediment into the delta.

This thesis addresses the morphological effects of river diversions on the Lower Mississippi River. The main objective is to analyze and optimize trade-offs between delta building and river navigability.

For this purpose a 2DH numerical model with Delf3D has been created; the model simulates the hydro- and morphodynamic behavior. The river reach which has been studied is the final 110 km of the river from Point a la Hache at River Kilometer 78 (RK 78) down to the mouth of the river (RK -30). The hydrodynamic model has been calibrated and verified with flow and stage data from daily observations on the river. With the available sediment data a calibration has been carried out of the morphological behavior in the river. The model has been used to simulate several scenarios to get insight in the problems in the delta.

From analysis of the model results the river bed in the study area can be divided into three categories. Upstream of RK 4 the bed is subject to erosion, around RK 4 the bed is practically in equilibrium and downstream of RK 4 the bed is subject to sedimentation. The reach downstream of RK 4 is the dredging reach; after analyzing the long-term simulation of 20 years it is not expected that the dredging quantities will decrease in the future. Closing off West Bay diversion has a positive effect on the dredging quantities.

The best diversion site for this study area is found in the inner bend of the river upstream of Empire (RK 47). This site is most efficient and diverts the largest quantities of sand through the diversion.

Keywords:

Lower Mississippi River, Sediment diversion, numerical modeling, Delft3D, hydrodynamic and morphodynamic behavior, maintenance dredging

Table of contents

<i>Preface and Acknowledgments</i>	<i>i</i>
<i>Executative summary</i>	<i>ii</i>
<i>List of figures.....</i>	<i>vi</i>
<i>List of tables.....</i>	<i>ix</i>
 Chapter 1. Introduction.....	 1
1.1 Background of the Mississippi River Delta	1
1.2 Objective	6
1.3 Methodology and Research outline	6
1.4 Explanation of Conversions	7
 Chapter 2. The Mississippi River	 8
2.1 General.....	8
2.2 Hydrodynamics.....	10
2.3 Morphodynamics	13
2.4 Mississippi delta	17
2.4.1. Problems in delta	17
2.4.2. Creating a sustainable delta	17
2.4.3. Extensive research	21
2.5 Navigation and dredging activities	23
 Chapter 3. Set-up of numerical model.....	 26
3.1 Introduction	26
3.2 Model assumptions	26
3.3 Study Area.....	27
3.4 Delft3D Grid design	28
3.4.1 Grid layout.....	28
3.4.2 Grid requirements.....	29
3.4.3 Main grid and Distributaries.....	30
3.5 Model bed topography.....	32
 Chapter 4. Hydrodynamic calibration & verification	 34
4.1 Flow Boundary conditions	34
4.1.1 Upstream boundary conditions.....	34
4.1.2 Downstream boundary condition	37
4.1.3 Distribution of flow over the distributaries.....	38
4.2 Stage data	39
4.2.1 Data sets and vertical datum	40
4.2.2 Observed stages	41

4.3	Method of calibration.....	42
4.3.1	Changing the roughness parameter	42
4.3.2	Results.....	42
4.3.3	Conclusions of hydrodynamic calibration	44
4.4	Method of verification.....	45
4.4.1	Flow boundary conditions.....	45
4.4.2	Results.....	45
4.5	Conclusions of Hydrodynamic Calibration & Verification.....	46
Chapter 5. Morphological calibration		47
5.1	Bed material of the river	47
5.2	Sediment transport Boundary conditions	48
5.2.1	Suspended sediment transport.....	48
5.2.2	Boundary conditions	50
5.2.3	Bed-load transport	51
5.2.4	Boundary conditions	51
5.3	Transport formulas.....	51
5.3.1	Sand transport formula.....	52
5.3.2	Mud transport formula	53
5.4	Morphological schematization	55
5.5	Method of calibration.....	56
5.5.1	1D Calibration	57
5.5.2	2D Calibration	61
5.5.3	Calibration of the dredging quantities	65
5.5.4	Calibration of the mud deposition processes.....	68
5.5.5	Results.....	70
5.6	Conclusions of Morphodynamic calibration.....	72
Chapter 6. Assessment of sediment diversion strategies.....		74
6.1	Introduction	74
6.2	The need of dredging, maintain navigability.....	75
6.3	Closing off West Bay diversion	79
6.4	Implementation of a sediment diversion.....	82
6.5	Impact of sediment diversions.....	86
6.6	Optimizing the sediment diversion in the inner bend of river.....	89
Chapter 7. Conclusions & Recommendations.....		91
7.1	Conclusions	91
7.2	Recommendations	92
Chapter 8. References.....		95

<i>Appendix A: Port of New Orleans</i>	<i>1</i>
<i>Appendix B: Lower Mississippi River control structures</i>	<i>2</i>
<i>Appendix C: Dredging Strategy</i>	<i>5</i>
<i>Appendix D: Fundamental 2D equations used by Delft3D.....</i>	<i>7</i>
<i>Appendix E: River Navigation Maps</i>	<i>9</i>
<i>Appendix F: Topography/ Bathymetry data set.....</i>	<i>12</i>
<i>Appendix H: Results of Dredging Simulations</i>	<i>14</i>
<i>Appendix I: Suspended Transport at Diversion Sites</i>	<i>16</i>
<i>Appendix J: Nedeco Blog</i>	<i>18</i>

List of figures

Figure 1.1: Evolution of Mississippi delta. Delta lobes of the Mississippi [Day <i>et al.</i> , 2007]	1
Figure 1.2: Galloway's delta classification [Galloway, 1992]	2
Figure 1.3: Present Mississippi Delta [Parker, 2009].....	2
Figure 1.4: Mississippi delta, historical and projected land change in coastal Louisiana, 1932-2050 [U.S. Geological Survey, National Wetlands Research Center, 2003]	4
Figure 1.5: Evolution of the Atchafalaya	5
Figure 1.6: Evolution of the Wax Lake Delta (left) and Atchafalaya Bay (right) as documented in satellite images from 1990, 2000, and 2005, and modeling results for shoreline positions with the sediment supply rates of 25 (dotted line) and 38 Mt/yr (solid lines) in the corresponding years. [Kim <i>et al.</i> , 2008]	5
Figure 2.1: Lower Mississippi River Basin [Kesel, 2003]	8
Figure 2.2: Lateral migration of the Mississippi River [Parker, 2009]	9
Figure 2.3: Upper and lower part of the Lower Mississippi River [Parker, 2009]	9
Figure 2.4: Mississippi discharge hydrograph 1938-2011 [USACE, 2011a].	10
Figure 2.5: Seasonal flow-duration curves at Talbert Landing (1963-2005) [Thorne <i>et al.</i> , 2008].	11
Figure 2.6: Mississippi River, Schematized with design floods [America's Wetland Resources Center, 2011]. ...	12
Figure 2.7: Sediment starved Mississippi River [Dean, 2006]	13
Figure 2.8: Transport mechanism [Jansen <i>et al.</i> , 1979]	13
Figure 2.9: Surface slope & Bed slope, Lower Mississippi River (RK 78 down to RK -30)	14
Figure 2.10: Consequence of water withdrawal [De Vriend <i>et al.</i> , 2010]	15
Figure 2.11: Consequence of sediment withdrawal [De Vriend <i>et al.</i> , 2010]	15
Figure 2.12: Representation of flow and sediment distribution in 1850 [Kesel, 2003]	17
Figure 2.13: Representation of flow and sediment distribution in 1990 [Kesel, 2003]	17
Figure 2.14: Mississippi Delta, Louisiana US, HOP is Head of Passes [Google Earth, 2011].....	18
Figure 2.15: Dredging West Bay Diversion, black box is anchorage area, Modified [USACE, 2003]	19
Figure 2.16: West Bay Diversion, opening [Wilson, 2008]	19
Figure 2.17: Simulation; West Bay Diversion, black box is anchorage area, Modified [USACE, 2009b]	20
Figure 2.18: Simulation; Excluding West Bay Diversion, black box is anchorage area, Modified [USACE, 2009b]	20
Figure 2.19: Small Scale Physical Model Lower Mississippi River, in blue the diverted sediment after running a simulation, modified [Wilson, 2008]	21
Figure 2.20: Model representation of growing delta, modified [Kim <i>et al.</i> , 2008]	22
Figure 2.21: Large sea going vessel in the Southwest Pass at the Gulf of Mexico (photograph Bos)	23
Figure 2.22: Overview dredging strategies (top view) [USACE 2010]	23
Figure 2.23: Dredging reach of 45 km, from downstream Venice to the mouth of the river (bird view) [Google Earth, 2011; Open Earth Tools, 2011]	24
Figure 2.24: Dredging quantities and costs [Ulm, 2010]	24
Figure 2.25: Maintenance work on breakwater in December 2010, at the mouth of the river at the Gulf of Mexico (photograph Bos)	25
Figure 3.1: Lower Mississippi River, Study area, Modified [Google maps, 2011]	27
Figure 3.2: Grid of model reach in Delft3D (the main grid is cyan, the distributaries are red. The land boundary of the delta and the river is in white and yellow) [Google Earth, 2011; Open Earth Tools, 2011]	28
Figure 3.3: Visualization of the grid. Trifurcation; Main stem, Pass a Loutre and South Pass in white, purple and red respectively. [Google Earth, 2011; Open Earth Tools, 2011]	30
Figure 3.4 Representation of flow velocities and direction	31
Figure 3.5 Trifurcation at Head of Passes [Google Maps],	31

Figure 3.6: Trifurcation at Head of Passes (photograph Bos)	31
Figure 3.7: Delft3D, representation of topography and bathymetry of study area (white indicates missing data)	32
Figure 3.8, Lower Mississippi River: initial bed level.....	33
Figure 4.1: Lower Mississippi, location Talbert Landing [Allison & Meselhe, 2010]	34
Figure 4.2: Observed discharge at Talbert landing from 2001-2009	34
Figure 4.3: Measured duration curve of discharge data set	35
Figure 4.4: The distribution function of the discharge data.....	36
Figure 4.5: Observed stages plotted against discharge	37
Figure 4.6 East Jetty Gage station (RK -30) at Gulf of Mexico (photograph, Bos).....	37
Figure 4.7: Discharge distribution in percentage of discharge at Venice [Davis, In Press]	38
Figure 4.8: Discharge distribution in percentage of Venice [Davis, In Press].....	38
Figure 4.9: Model reach and gage stations pointed out, Modified [Google maps, 2011]	40
Figure 4.10: Discharge rating curve gage station Pt a la Hache	41
Figure 4.11: Discharge rating curve gage station Empire.....	41
Figure 4.12: Discharge rating curve gage station Venice	41
Figure 4.13: Discharge rating curve gage station Head of Passes	41
Figure 4.14: Simulated and observed stage of the model reach for three discharge levels.....	43
Figure 4.15: Difference between measured stages at Venice and Head of Passes form 2001-2010, for low, intermediate and high flow (red, blue and green).	43
Figure 4.16: Discharge distribution of calibration and verification data set.....	45
Figure 4.17: Verification of the model	46
Figure 5.1: Bed material grain size in the Lower Mississippi River from Head of Passes until RK 126, 2003 data (low discharge as a line plot) and 2008 (high discharge as triangles), upper axis is River Kilometer, lower axis is sample number [Allison <i>et al.</i> , 2010]	47
Figure 5.2: Lower Mississippi [Allison & Meselhe, 2010].....	48
Figure 5.3: Suspended sediment discharge measured at Talbert Landing, 1987-2010 [Karadogan, 2010].....	49
Figure 5.4: Suspended sediment concentration measured at Talbert Landing, 1987-2010 [Karadogan, 2010] ..	50
Figure 5.5: Relation between discharge and sand in suspended transport.....	50
Figure 5.6: Pattern of suspended sediment concentration from St Francisville to Head of Passes [Mossa, 1996]	54
Figure 5.7: Frequency curve of discharge and sediment load from data set.....	55
Figure 5.8: Observed increased bed level from 2004 to 2010, from Venice (RK 16) down to the Gulf of Mexico (RK -30). Main stem of the Mississippi River.	58
Figure 5.9: Simulation with different calibration parameters, maximum bed level change (8 years), in centreline of the river (black circle is figure 5.10)	59
Figure 5.10: Calibration: bed level gradient, difference between imposed upstream boundary condition for bed level change, 0.10 and 0.50 m/year.	59
Figure 5.11: River bends in the model, green are the riverbanks with its non-erodible layer. Blue is the river bed	61
Figure 5.12: Non-erodible layer included into the model.....	61
Figure 5.13: Dynamic system in the river [Kleinhans <i>et al.</i> 2008]	62
Figure 5.14: Cross-section RK10.....	64
Figure 5.15: Cross-section RK 3	64
Figure 5.16: Cross-section RK -1.....	64
Figure 5.17: Cross-section RK -20.....	64

Figure 5.18: Cumulative sediment transport at Head of Passes with varying calibration parameters, during the intermediate discharge level, $Q=20000 \text{ m}^3/\text{s}$	65
Figure 5.19: Results of Simulation, representation of cumulative dredging quantities	66
Figure 5.20: Dredges only cell centres	67
Figure 5.21: Dredges at least one corner	67
Figure 5.22: Differences between two dredge options	67
Figure 5.23: Simulation with no mud deposition	68
Figure 5.24: Simulation with enhanced mud deposition	68
Figure 5.25: Simulated bed levels, no mud deposition vs. enhanced mud deposition.....	69
Figure 5.26: Simulated vs. Observed bed level dredging reach	71
Figure 6.1: Centreline and Dredge reach, within grid design [Google Earth, 2011; OET, 2011]	75
Figure 6.2: Simulated long-term Morphological Response, without dredging activities.....	76
Figure 6.3: Simulated long-term Morphological Response, including dredging activities.....	76
Figure 6.4: Velocities in the lower reach RK 18 – RK -30; understanding the sedimentation process	77
Figure 6.5: Initial navigation channel of 2004 vs. simulated navigation channel in 2010 at Head of Passes	78
Figure 6.6: Initial navigation channel of 2004 vs. simulated navigation channel in 2010 at the mouth of the river	78
Figure 6.7: Flow velocity pattern [m/s]	79
Figure 6.8: Flow velocity pattern [m/s]	79
Figure 6.9: Differences in flow velocities for two scenarios [m/s], the direction implies which scenario has relatively higher values. The downward direction of the arrows refers to the open- and upward to the closed scenario.	80
Figure 6.10: Differences in sediment transport rates for two scenarios [kg/ms], the direction implies which scenario has relatively higher values. The downward direction of the arrows refers to the open- and upward to the closed scenario.	80
Figure 6.11: RK 4, Simulated bed levels for Open, Closed off West Bay diversion and without dredging	81
Figure 6.12: RK -2, Simulated bed levels for Open, Closed off West Bay diversion and without dredging	81
Figure 6.13: Schematization of three basic types of controlled river diversions: A. Siphon; B. Gated diversion; and C. Controlled subdelta. [Wilson, 2008].....	82
Figure 6.14: Location of diversion sites 1 to 4, Modified [Google maps, 2011].....	83
Figure 6.15: top view of the model at diversion site 1 (RK 53), the arrows in the direction perpendicular to the flow represent the released suspended sediment (in the red circle).	84
Figure 6.16: Diversion site 1 (RK 53); small size	84
Figure 6.17: Diversion site 1 (RK 53); doubled size	84
Figure 6.18: First simulated Dredging Activities for the scenarios (according calibration settings)	86
Figure 6.19: Second simulated Dredging Activities for the scenarios (according to mud sensitivity scenario)	87
Figure 6.20: Helical flow in river bends, Modified	89
Figure 6.21: Submerged vanes in the river	89
Figure 6.22: Preliminary design a sediment of diversion [Dijkman, 2007]	90
Figure 6.23: Control structure [Harrison <i>et al.</i> , 2009].....	90
Figure 7.1: Topography obtained from a multibeam survey in the Mississippi River at Lower English turn (RK 132-137).	94
Figure 7.2: River training structures in the developed model	94

List of tables

Table 1.1: Conversion table, Metric vs. English	7
Table 2.1: Sediment fractions and their particle grain size.....	14
Table 4.1: Flow distribution along the distributaries [Davis, In Press].....	39
Table 4.2: Gage station facts.....	40
Table 4.3: Coefficient for Q-h lines for verification.....	46
Table 5.1: Obtained sediment discharges and concentrations for flow boundary conditions	51
Table 5.2: Model MorFACs.....	56
Table 5.3: Results of sediment transport through model	60
Table 5.4: Results from Dredging Simulations	66
Table 5.5: Summary of morphological parameters.....	70
Table 5.6: Summary of calibration parameters.....	70
Table 6.1: Results for diversion sites.....	85
Table 6.2: Results from Dredging Simulations	87

Chapter 1. Introduction

1.1 Background of the Mississippi River Delta

The Mississippi Delta in Louisiana State (USA) is formed over the past ten million years. The delta has been built up during several interglacial periods. During these 10 million years the Mississippi River carried large quantities of sediments and deposited them in the Gulf of Mexico. The Mississippi Delta has been formed with these river-borne sediments. The delta has been on different places through history and shifted its location. Every time the Mississippi River found its way to the Gulf of Mexico. The present delta is only 3000-6000 years old. The evolution of the delta can be divided in delta lobes. A lobe is a distinct area of sediment deposits, relates to a specific course of the river to the sea, see figure 1.1. The different lobes have different locations of the mouth of the river. Six lobes can be identified over the past 6000 years. The Mississippi “Bird Foot” Delta is only 600 years old and is the present course of the river to the Gulf of Mexico.

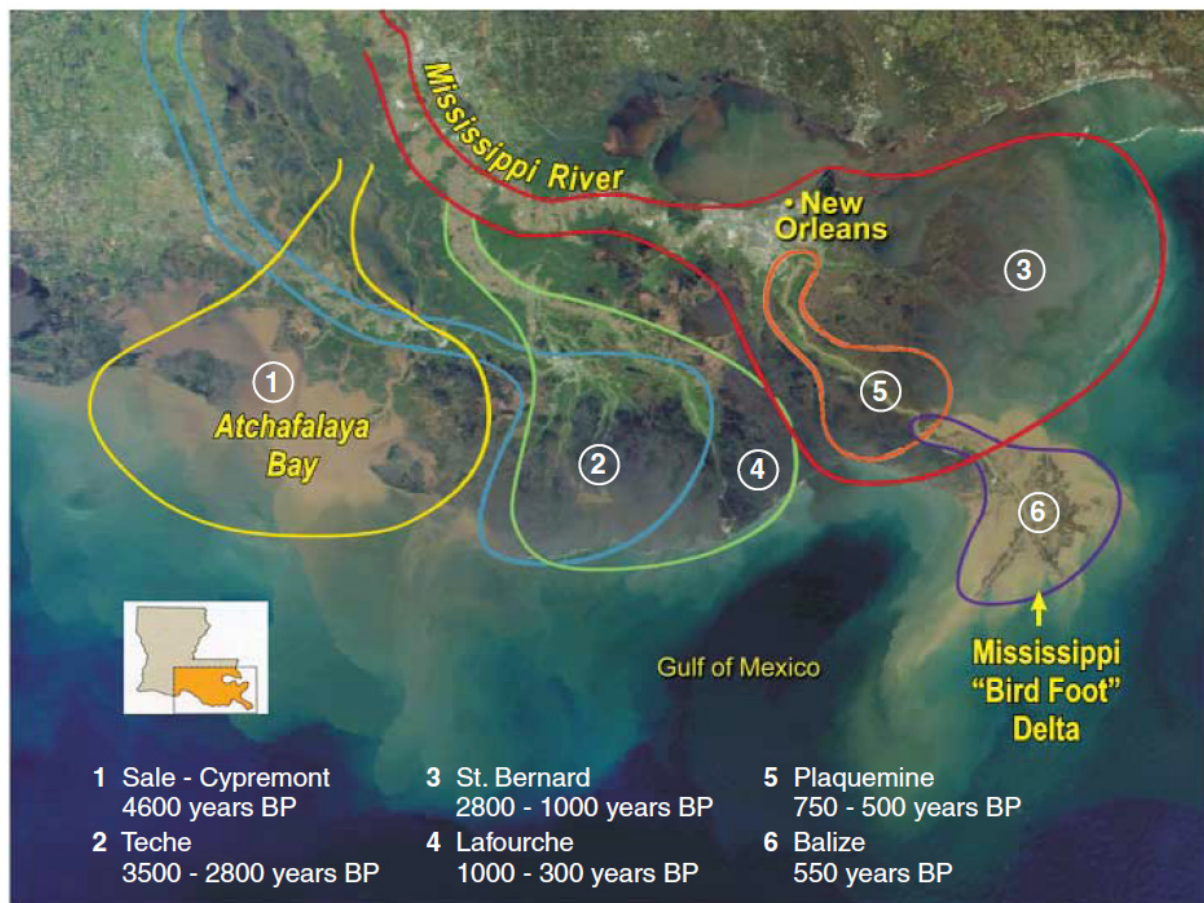


Figure 1.1: Evolution of Mississippi delta. Delta lobes of the Mississippi [Day *et al.*, 2007]

The Atchafalaya Bay and Mississippi “Bird Foot” Delta are presently the active deltas of the Mississippi River. The Teche- and Lafourche lobes are cut off and consequently inactive. The Atchafalaya River diverts 30% of the flow to the Atchafalaya Bay. The Mississippi River diverts 70% through the “Bird Foot” Delta to the Gulf of Mexico, see figure 1.1. The distribution of the flow is controlled by the Old River structure, see Appendix B.

Delta Classification

According to Galloway's delta classification (see figure 1.2) the Mississippi delta is river dominant, which implies that tide and wave action are not of great importance compared to the forces of the river in terms of delta formation [Galloway, 1992]. Therefore the delta was able to grow into the Gulf of Mexico creating the "Bird Foot" Delta, see figure 1.3. The Danube delta, which is situated in the Black Sea (Romania) is another example of a river dominated delta.

The tidal amplitude is around 1 ft (30 cm) near the mouth of the Mississippi River. The tide penetrates until Empire (RK 47) during the intermediate and high flow season (Feb.-Jun.), which is the dominant season for the river [Allison *et al.*, 2010].

The tidal amplitude is too low to penetrate far upstream. If the river would be tide dominated, the tidal forcing should be able to generate a reverse flow at the downstream boundary of the river, but the forcing is too weak. During low flow the tide is able to penetrate from Head of Passes (RK 0) up to RK 400. The tidal penetration influences the stages [Allison *et al.*, 2010]. Wave dominated deltas are subjected to a high erosion rate. Therefore they form a more sheltered delta behind a cliff, like the São Francisco (Brazil).

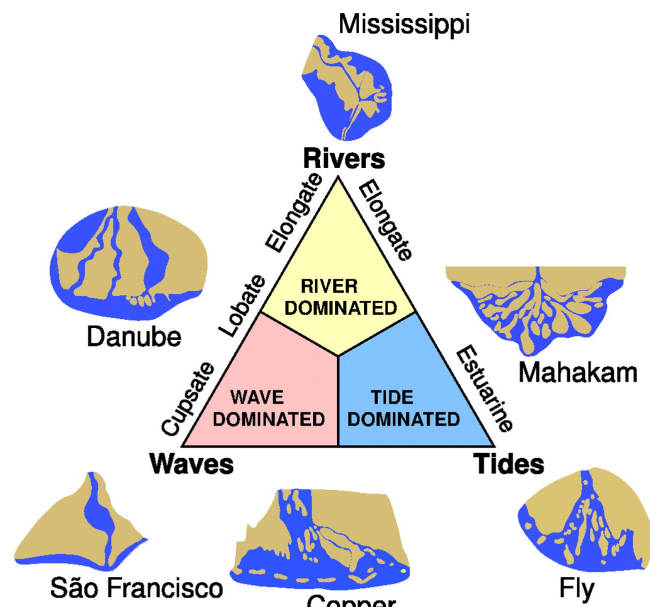


Figure 1.2: Galloway's delta classification [Galloway, 1992]



Figure 1.3: Present Mississippi Delta [Parker, 2009]

Problems in the Mississippi Delta

Since 1930 4,900 km² of the delta has disappeared into the Gulf of Mexico (GOM). Between 1978 and 2000 USGS reported 1704 km² of wetland loss. The wetlands in the Mississippi Delta consist of marshes and swamps. Marshes are in a salt water environment, due to the connection to sea. The swamps are in a fresh water environment fed by the river and ground water. USGS predicts a land loss in the wetlands of another 1300 km² by 2050 [Barras *et al.*, 2003].

The land loss is caused by subsidence and erosion. Subsidence occurs due to consolidation of the soil and the exploration of oil. Erosion, besides wave action, is mainly caused by the hurricanes that struck the delta. To counteract these effects the river needs to deliver sediment. Unfortunately the river delivers too little sediment to the system.

The declining effect of the delta would continue unless people would interfere. A prediction has been made what the delta will look like in 2050, see figure 1.4. All land colored in red is lost between 1932 and 2000, the green is gained land.

Observations indicated a land loss of 560 km² after hurricanes Katrina and Rita in 2005 [USGS, 2006]. These observations have made it clear something must be done in the near future to prevent the delta from further declining. In addition the wetlands also have to counteract the upcoming sea level rise and subsidence in the future, with rates of 2-4 mm/year [IPCC, 2007] and 1.4-11 mm/year [Kim *et al.*, 2008] respectively.

Many projects and researches try to assess how this “drowning effect” of the delta can be stopped or even reversed. Researchers have stated that the delta is not sustainable anymore; an approach needs to be established to restore the delta and create new land [Parker and Sequeiros, 2006; Day *et al.*, 2007; Reed, 2009].

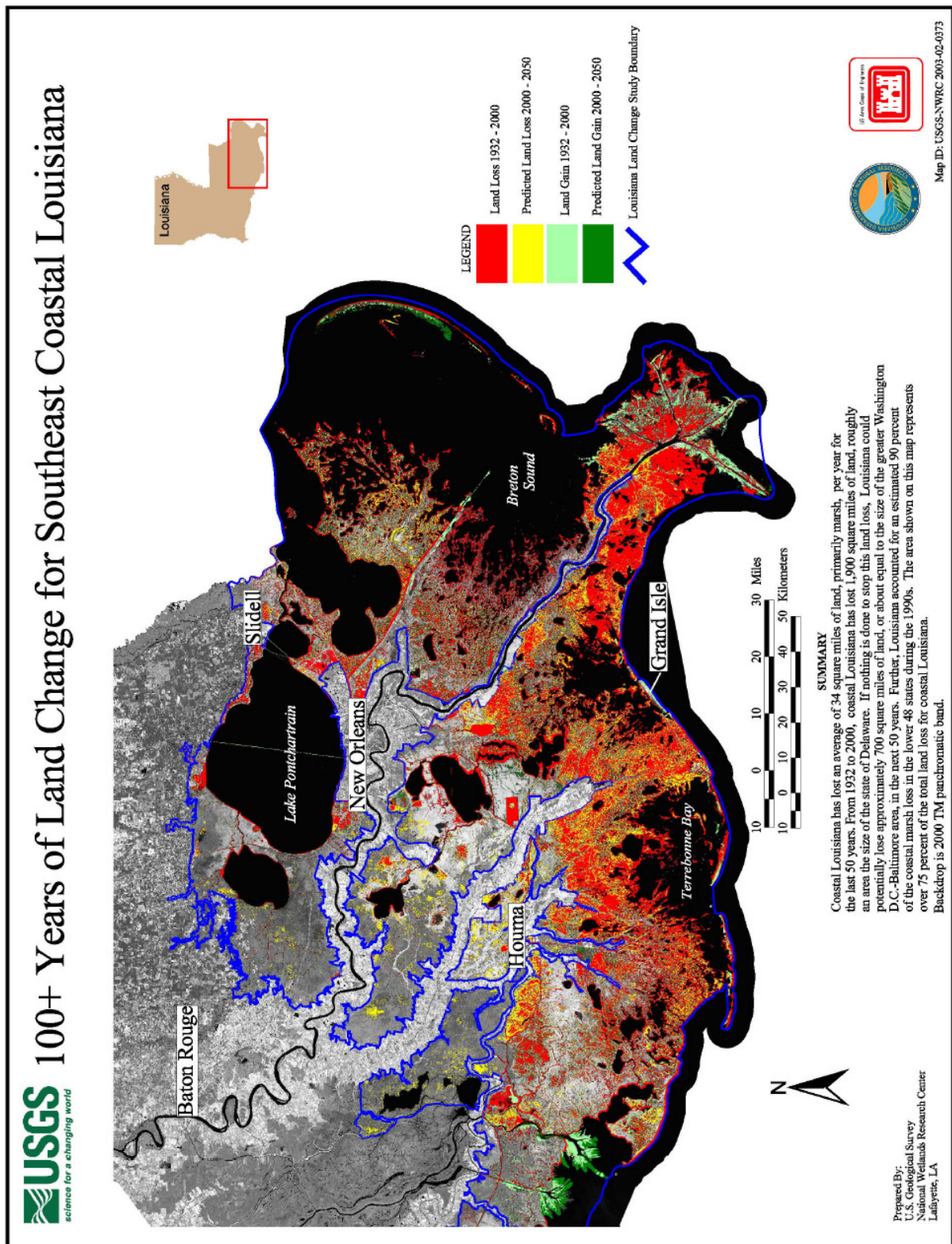


Figure 1.4: Mississippi delta, historical and projected land change in coastal Louisiana, 1932-2050 [U.S. Geological Survey, National Wetlands Research Center, 2003]

Canalization of the Lower Mississippi River

New Orleans was founded in 1717. From that time the delta has been actively used for navigation. Due to this active use the delta has been through a lot of development. The Lower Mississippi has been canalized since the 19th century for navigability. The canalization of the Lower Mississippi River causes the problems in the delta. This effect is explained in detail in section 2.4.

The shipping industry demands 100% navigability through the Mississippi River because the entire inner land has to be accessible at any time. For many years the US Army Corps of Engineers (USACE) maintains a river channel depth of 45 ft (14 m) for navigation by maintenance dredging.

Creation of new wetlands

As stated before, the wetlands have to deal with land loss. Therefore wetlands have to be created to counteract this loss. One of the solutions to create wetlands is to build river sediment diversions in the levees of the Lower Mississippi. Generally speaking, river sediment diversions convey sediments from the river to the wetlands. Strategically building diversions helps to create new land in the wetlands. With the use of new diversions sediments will be conveyed from the river to the wetlands.

Besides creating new land the sediment diversions contribute in an additional way: they reduce saltwater intrusion into the fresh water swamps. Therefore favorable salinity levels can be re-established. This improves the fish and wildlife habitat and also the marsh vegetation.

Practical example

The Atchafalaya River is a distributary of the Mississippi River. The Wax Lake Delta and Atchafalaya bay are at the mouth of the Atchafalaya River and are an example of monitored delta growth. The grow rate is about $4 \text{ km}^2/\text{year}$ [Kim *et al.*, 2008]. The delta of the Atchafalaya River is also shown in figures 1.1 and 1.4. In figure 1.4 the delta is shown in the left. The areas are in green (delta growth). Figures 1.5 and 1.6 show the presence of the delta in 1973 and its evolution until 2005. As from the 1970s the Atchafalaya River diverts 30% of the flow and sediments (see Appendix B), which enhanced the delta formation. As can be seen the delta has grown extremely. The sediment supply to the delta is $38 \text{ Mt}/\text{year}$ as shown in figure 1.6 [Kim *et al.*, 2008].

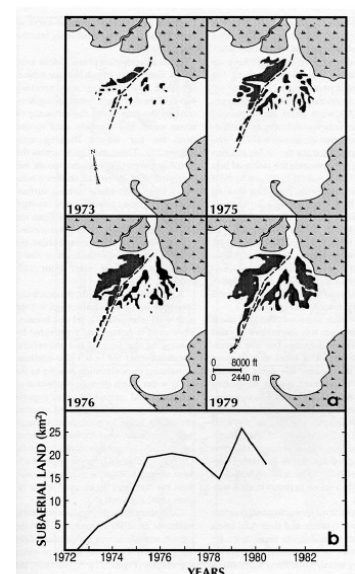


Figure 1.5: Evolution of the Atchafalaya Bay [Wilson, 2008]

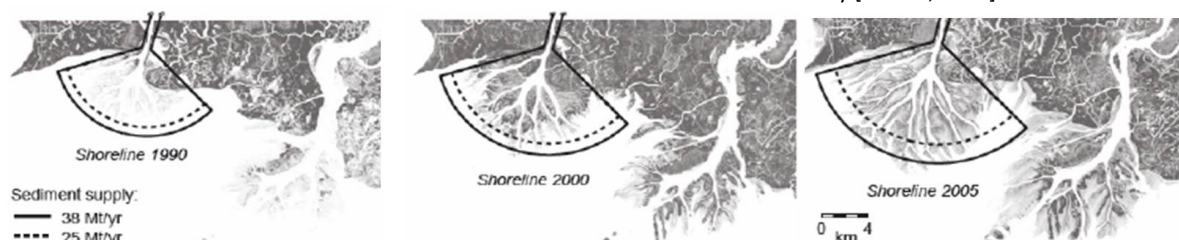


Figure 1.6: Evolution of the Wax Lake Delta (left) and Atchafalaya Bay (right) as documented in satellite images from 1990, 2000, and 2005, and modeling results for shoreline positions with the sediment supply rates of 25 (dotted line) and 38 Mt/yr (solid lines) in the corresponding years. [Kim *et al.*, 2008]

The effects of sediment diversions

The effects of implementing river diversions in the Lower Mississippi River are not well known. These engineering interventions could cause problems for the navigability of the river in term of extra deposition and maintenance dredging. This thesis addresses the physical effects of these interventions in the river.

1.2 Objective

The objective is to study a sediment diversion in the Mississippi River and to assess the amount of sediment that can be diverted from the river, for delta building purposes, while minimizing the impact on navigability of the river (i.e. no significant increase in maintenance dredging efforts).

The following questions will be addressed:

1. What would be the impact of the implementation of diversions to the river system?
2. What would be the best location for the implementation of river diversions for delta building purposes, with minimum impacts?
3. Is it possible to sustain a navigable fairway in the Mississippi River with limited dredging cost?

1.3 Methodology and Research outline

First the Mississippi River drainage basin with the tributaries and distributaries is discussed in Chapter 2. It specifies various elements of the river system to get an understanding of the system and its problems. An overview of ongoing extensive research is reviewed and one of the research gaps is formulated.

Previous studies have shown numerical modeling efforts help to understand the impact of diversions on the Mississippi River system. Moreover the development of new numerical models is encouraged by the river managers (USACE). Therefore a new numerical model is developed and applied for this research.

The approach of the study is to make a 2D numerical model using Delft3D, which simulates the hydrodynamic and morphological behavior of the river. The model design and set-up is described in chapter 3. The model simulations represent 10 to 20 years in real life time. The hydrodynamic and morphodynamic data available is schematized to ensure it is simplified for this research purpose i.e. long-term morphological behavior of the Lower Mississippi River.

In chapter 4 the flow boundary conditions are discussed. A description is given about the set up of the boundary condition for calibration and verification. Next the outcome of the calibration and verification is presented. This outcome represents the settings and parameters that are used for morphological computations.

Chapter 5 describes how the input parameters of morphology are formulated and the way the morphodynamic calibration is done. It gives an overview of the available sediment transport data and describes the initial and boundary conditions.

In chapter 6 the complete model is applied to management scenarios. This chapter shows the capabilities of the model in terms of its predictive capabilities for sediment erosion and deposition. Next the modeling addresses the capacity of delta formation by sediment diversions.

Sediment diversions at four different locations with different scenarios are assessed using the model. These scenarios and strategies are reviewed and the impact of the diversions is studied. In addition an overview is given of how to efficiently extract sediment from the river. Giving insight into the effect of the sediment diversions is the goal of this model. The model can contribute to proposing a strategy on how to manage the river in the future.

Finally conclusions and recommendations are summarized in chapter 7.

1.4 Explanation of Conversions

English vs. Metric units

This report will use the metric system. The original available data and figures are used from literature. When figures present the English units, those figures are be used in the report and a conversion is made to the metric system. In table 1.1 the conversions are listed.

Table 1.1: Conversion table, Metric vs. English

metric	English
1 m ³ /s	35.31467 cfs
1 m	0.3048 ft
1 m ³	1.30795 cubic yards
1 hectares	2.47 acres

Suspended sediment concentration

The concentration in parts per million (PPM) can be converted by multiplying with a factor which includes the specific relative density of the sediment in order to get mg/l. The factor ranges from 1.5-1.7 for this study. For example 250 PPM converts into 400 mg/l.

In general:

- Concentration: [mg/l] = 1000 [kg/m³]
- Bed shear stress: [kg/m, s²] = [N/m²] = [Pa]

Chapter 2. The Mississippi River

2.1 General

The Mississippi River has already been for centuries a great resource of fresh water supply, sediments and nutrients to the Louisiana coastal delta. It is also very important from an economic point of view, because many ports are situated at the banks of the river e.g. the Port of New Orleans, Port of South Louisiana and Baton Rouge, see appendix A for some port facts. The Mississippi river is the major river in the United States and the third largest river in the world. Together with the Missouri and Ohio River, which are its major tributaries, its length is 6236¹ km. It drains 41% of the US, which is an area of over 3.2×10^6 km², covering 31 states and even 2 Canadian provinces, see figure 2.1 (upper left corner) for the entire drainage basin. The Lower Mississippi has its origin in Cairo, see top of Figure 2.1, and finds its way to the Gulf of Mexico. It has a length of 1,600 km and is one of the world's most regulated rivers [Kesel, 2003; Karadogan *et al.*, 2009].

Figure 2.1 shows the Lower Mississippi River divided in two sections, the alluvial valley and the deltaic plain respectively. The upper 2/3 of the Lower Mississippi River is strongly meandering and meanders freely through a flood plain that ranges from 40 to 200 km wide. The river has a shallow alluvial channel and has an average annual lateral migration of 25 m/year and higher, see figure 2.2 [Kesel *et al.*, 1992; Hudson and Kesel, 2000; Parker, 2009] The lower third is the deltaic plain (Figure 2.1). This part is not flowing freely, as it flows between high artificial levees. The artificial levees strongly reduce the average annual lateral migration to only 3 m/year to negligible values. The levees cause a deep alluvial channel without floodplains. [Kesel *et al.*, 1992].

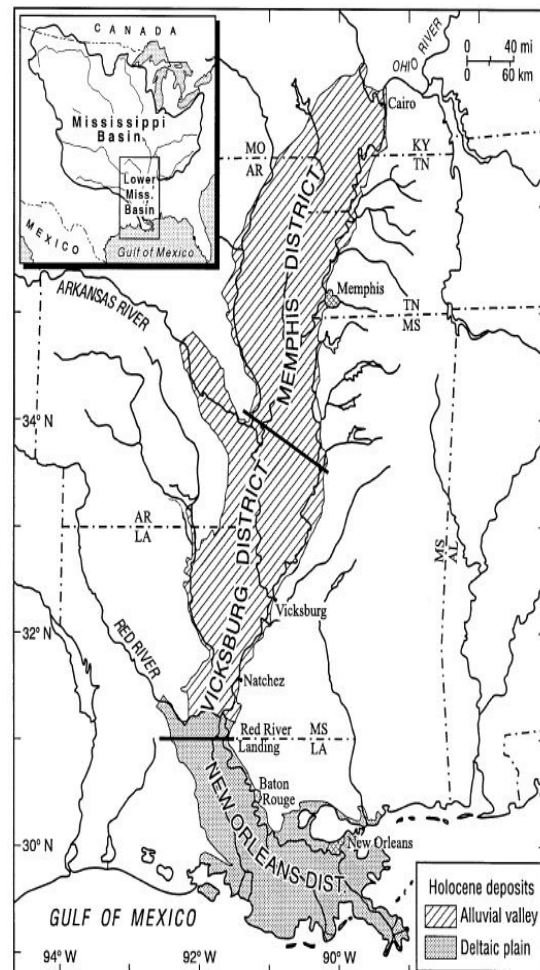


Figure 2.1: Lower Mississippi River Basin [Kesel, 2003]

¹ Eaglespeak: <http://www.eaglespeak.us/2010/02/waterways.html>, Accessed: January 2011

Figure 2.2 shows the longitudinal lateral migration rate per kilometer. The upper 2/3 of the river (RK 1100 to RK 492) has a high lateral migration rate. As from RK 492 to RK 0, which is the deltaic plain (Old River structure, see appendix B). The lateral migration rate is minor. River kilometer 0 corresponds with Head of Passes at the mouth of the river.

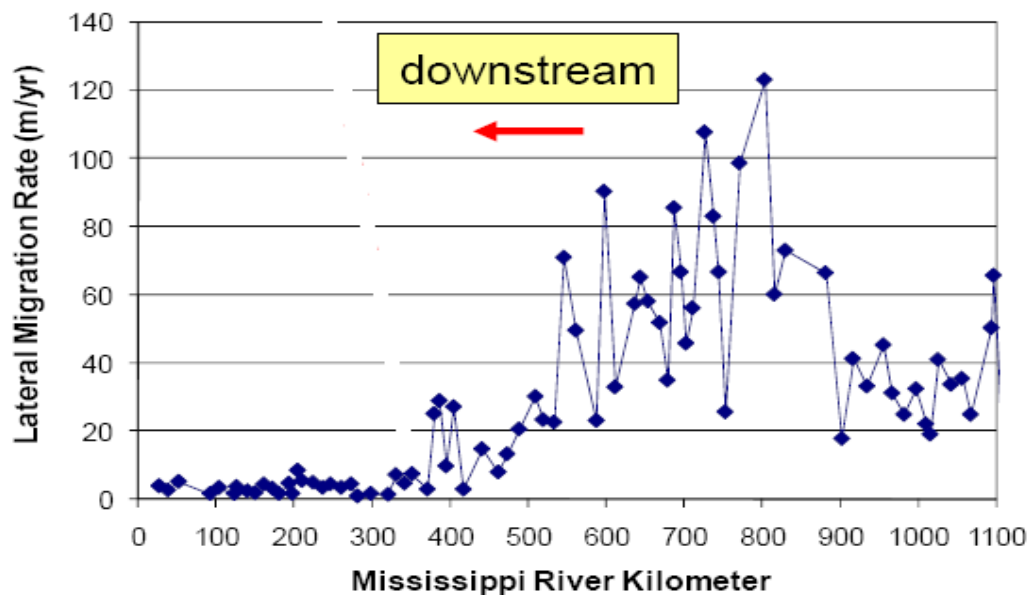


Figure 2.2: Lateral migration of the Mississippi River [Parker, 2009]

In figure 2.3 the top figure represents a cross-section of the upper 2/3 alluvial part of the Lower Mississippi. As can be seen and stated before, the river has a wide stretch and is relatively shallow. Also floodplains are present. The lower figure is the lower 1/3, which is restricted. The river is kept in place by the artificial levees and is relatively deep. The geometry of the river highly affects the river response. This is explained in section 5.5.2.

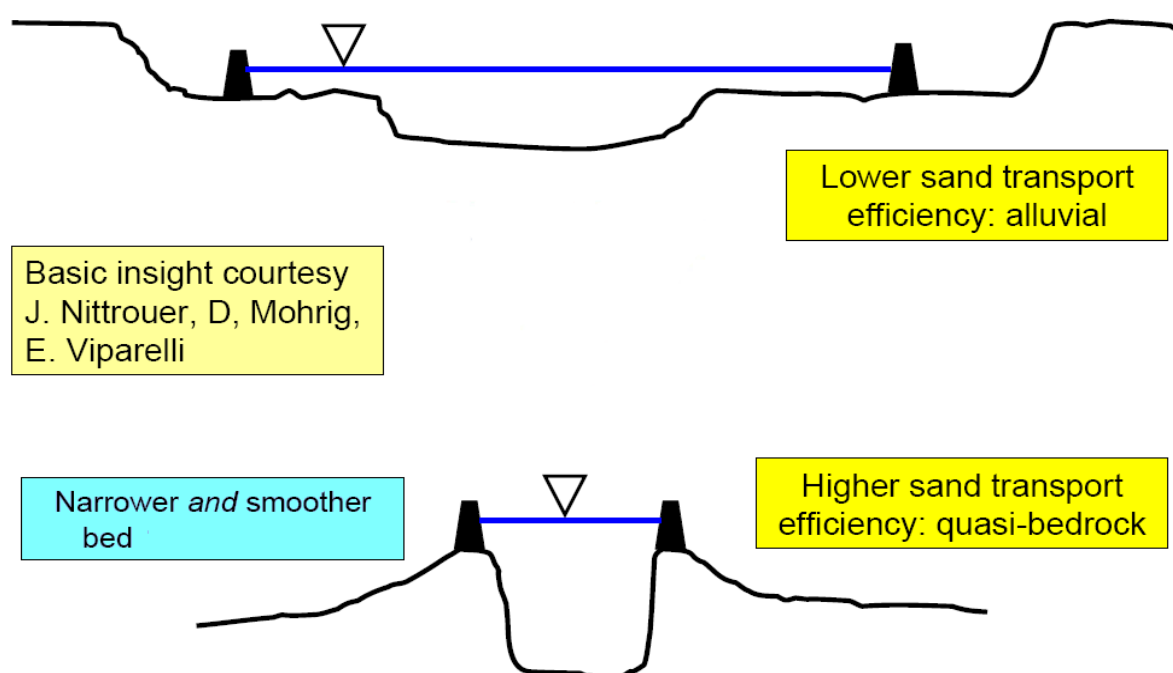


Figure 2.3: Upper and lower part of the Lower Mississippi River [Parker, 2009]

2.2 Hydrodynamics

Discharge regime

The Mississippi River is a large river with large year to year variations. Figure 2.4 gives an overview of the discharge data of the Mississippi at Talbert Landing (RK 492) from 1938-2010. The flow peaks at 1,500,000 cfs ($\sim 42,500 \text{ m}^3/\text{s}$) and can be as low as 100,000 cfs ($\sim 2,900 \text{ m}^3/\text{s}$). The difference between the high and low discharge regime is therefore of great importance. The average discharge of the Lower Mississippi River is about $14,500 \text{ m}^3/\text{s}$. The duration of the high flow peak is usually two weeks [Allison *et al.*, 2010].

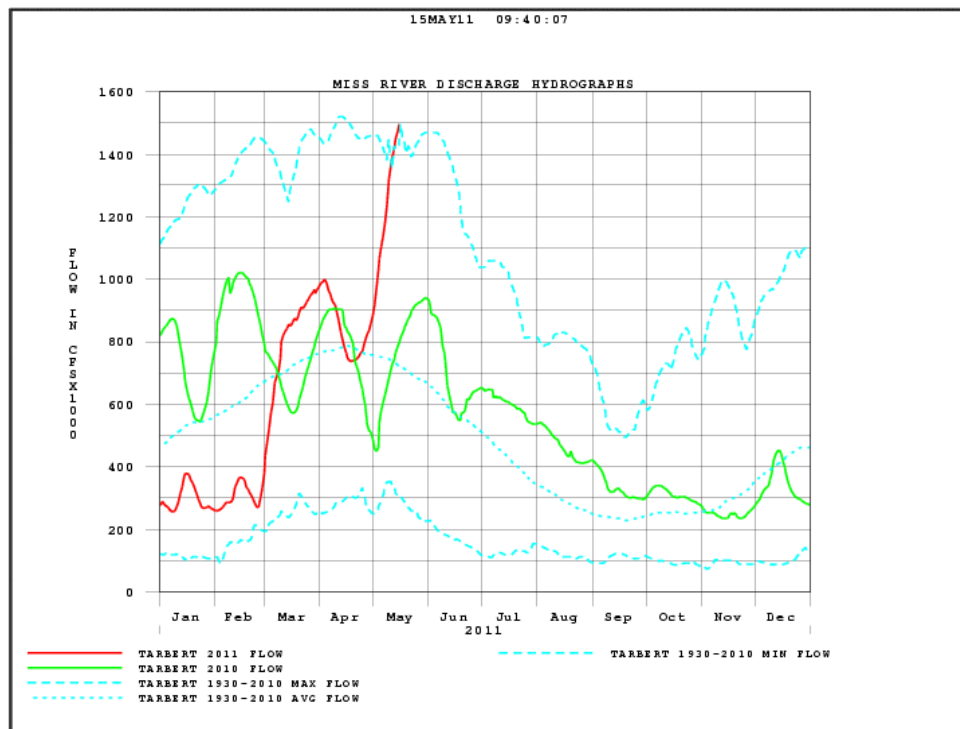


Figure 2.4: Mississippi discharge hydrograph 1938-2011 [USACE, 2011a].

In figure 2.4 a pattern can be seen in the behavior of the river. High flows occur during spring (flood season) and low flows during the autumn (dry season). The winter and summer have an intermediate flow. Figure 2.5 gives a more detailed picture and shows which discharges are most likely to happen in each season. Winter season has the largest variability of discharges that can occur. The intermediate flow season is the dominant flow season, which was referred to in section 1.1, with respect to the Delta Classification.

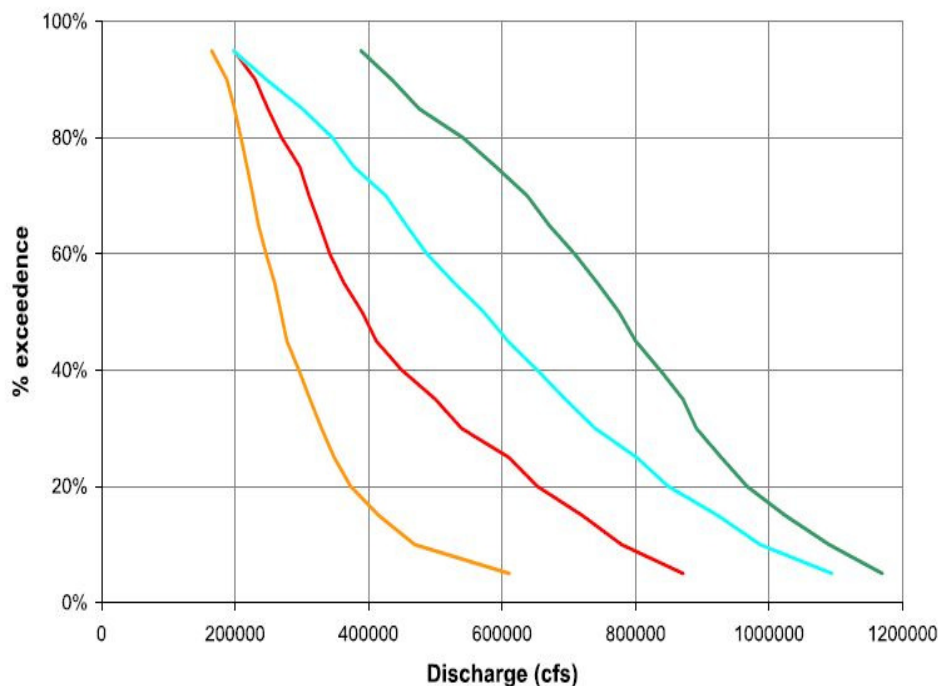


Figure 2.5: Seasonal flow-duration curves at Talbert Landing (1963-2005) [Thorne *et al.*, 2008].

Saltwater wedge

The saltwater wedge is present during the low flow condition in the autumn ($< 8500 \text{ m}^3/\text{s}$) and migrates up to Venice (RK 16, see figure 1.3) for about 96 days a year [Allison *et al.*, 2010]. In June the saltwater wedge comes to Head of Passes (RK 0). The saltwater wedge is not able to migrate all the way up to Venice because of higher flow velocities. It can be assumed that the saltwater wedge is always present in the Southwest Pass, which is the navigable Pass from RK 0 down to RK -30. The presence of this saltwater wedge influences the morphodynamics in the Southwest Pass because the saltwater wedge initiates flocculation of mud. This flocculation process enhances the sedimentation in the Southwest Pass. Next to the saltwater wedge reduces the near bed flow velocities, which also initiates more sedimentation of the sediments. Maintenance dredging contributes to the intrusion of the saltwater because of a deepened river channel [Galler and Allison, 2008].

During extreme low flow events $< 3000 \text{ m}^3/\text{s}$ the saltwater wedge can migrate all the way up to New Orleans (RK 165). This gives a lot of trouble for the drinking water intakes. USACE even had to place an earthen thalweg sill at RK 116 in 1988 and 1999 to prevent that from happening [Allison *et al.*, 2010].

Schematization of the Mississippi River

In figure 2.6 the regulated flow in the Mississippi River can be seen. The design flood discharges in the figure are given in cubic feet per second (cfs). At the upstream boundary a design discharge of 2.25 million cfs enters the system from the Ohio River and could reach to 2.89 million cfs, only 1.25 million cfs flows along New Orleans into the Gulf of Mexico. Water is diverted by several control structures such as the Bonnet Carre Spillway and the Morganza Spillway, which are only open if necessary. The control structures divert percentages of the flow in different directions; see Appendix B for more information about these structures, i.e. the Old River Control structure and the Bonnet Carre Spillway.

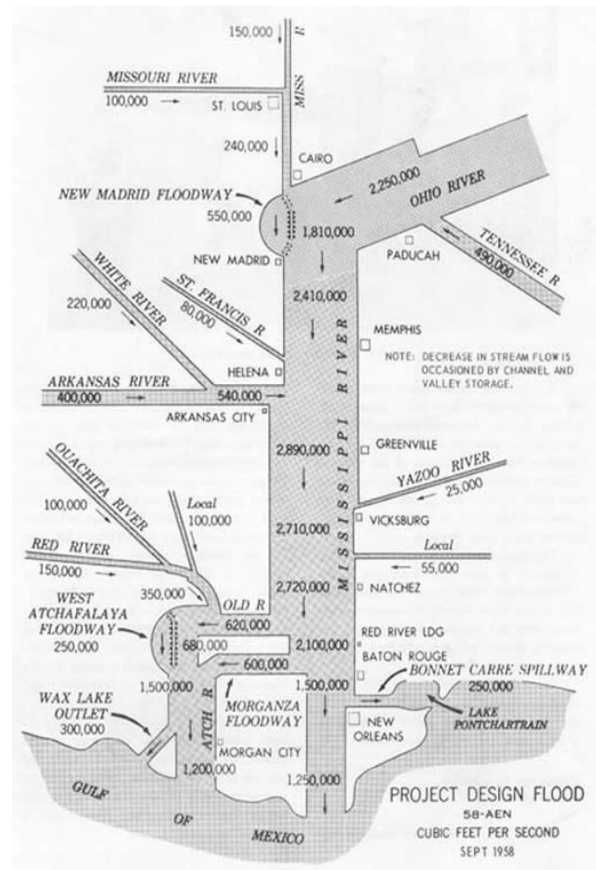


Figure 2.6: Mississippi River, Schematized with design floods [America's Wetland Resources Center, 2011].

2.3 Morphodynamics

Sediment starved river

The Mississippi sediment availability has decreased enormously in the past centuries after the construction of dams, locks, hydropower plants and levees in its major tributaries. The sediment storage capacity is also decreased because the river is no longer allowed to meander [Kesel, 2003]. Figure 2.7 represents the fact of a sediment starved river in one glance. The sediment transport decreased from 500 Mton/year in 1950 to approximately 100 Mton/year in 2010 [Allison *et al.*, 2010].

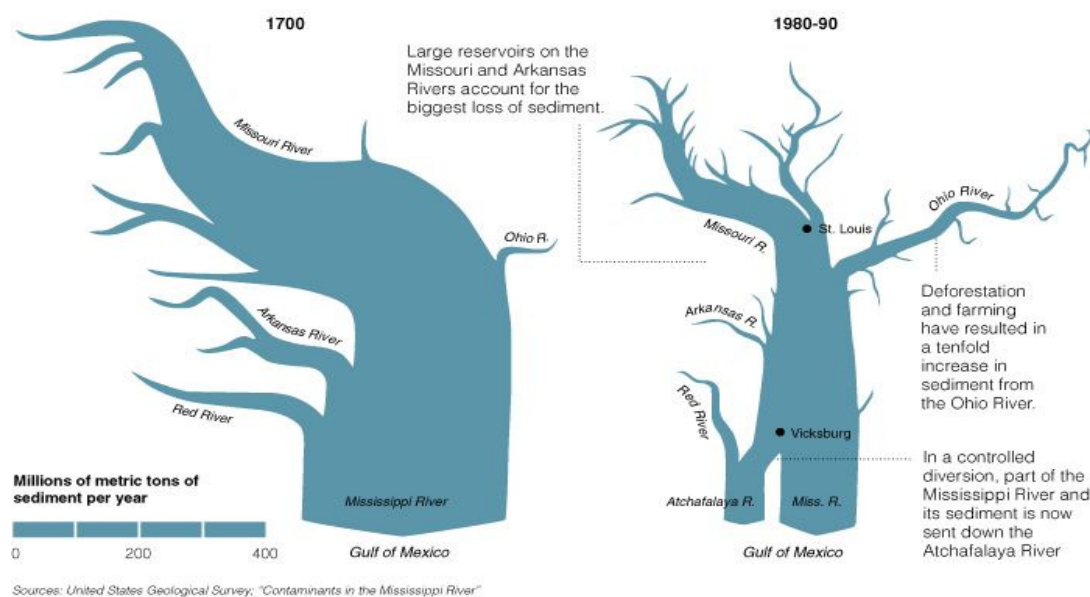


Figure 2.7: Sediment starved Mississippi River [Dean, 2006]

Transport mechanism

Sediment transport is classified into bed-load and suspended load. The sum of both loads is the total sediment transport of the river, see figure 2.8 for schematization. The suspended load transports the very fine sediment fractions by advection and turbulent motion in the water column. The coarse sediment fractions are mainly transported as bed-load along the river bed.

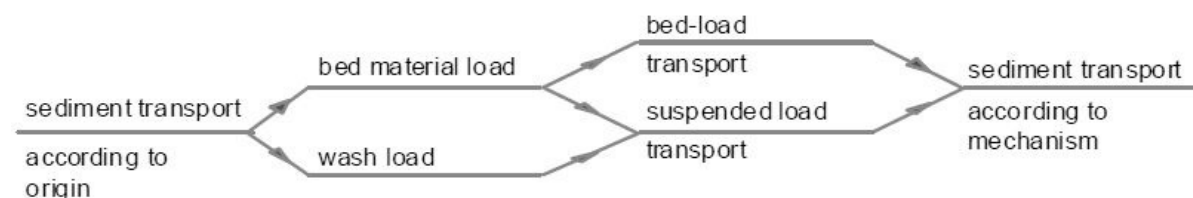


Figure 2.8: Transport mechanism [Jansen *et al.*, 1979]

Sediment fractions and transport load

The Mississippi River bed-load consists of non-cohesive sand particles, classified as fine sand and medium sand respectively. The suspended load consists of fine and medium sand particles and cohesive clay. See table 2.1 for their particle grain size.

Table 2.1: Sediment fractions and their particle grain size

Sediment fraction	Grain size
Sand (non-cohesive)	63 μm -20 mm
Silt (non-cohesive)	4-62 μm
Clay (cohesive)	<3 μm

The average suspended load of the Lower Mississippi River at Talbert Landing is estimated as $91 \cdot 10^6$ ton/year and the bed-load transport is on average $2.2 \cdot 10^6$ ton/year, which is equivalent to about 2.5% of the suspended load [Nittrouer *et al.*, 2008]. The average sediment concentration is about 200 mg/l [Allison *et al.*, 2010].

Bed topography

Only limited field data is available of the bed topography in the river. The bed topography is gained from 2004. Recent bed topography data is only available from the dredging reach (RK 18 to -30, see figure 2.9)

River is turning shallow

Figure 2.9 shows the centerline of the river over the longitudinal section of the Lower Mississippi River from RK 78 at Point a la Hache down to the Gulf of Mexico at RK -30 (Below Head of Passes, RK 0). The figure clearly shows that the bed form RK 78 up to RK -30 of the Lower Mississippi River turns shallow; i.e. at upstream part the river is deeper (30-35 m) than at the mouth of the river (10-15 m).

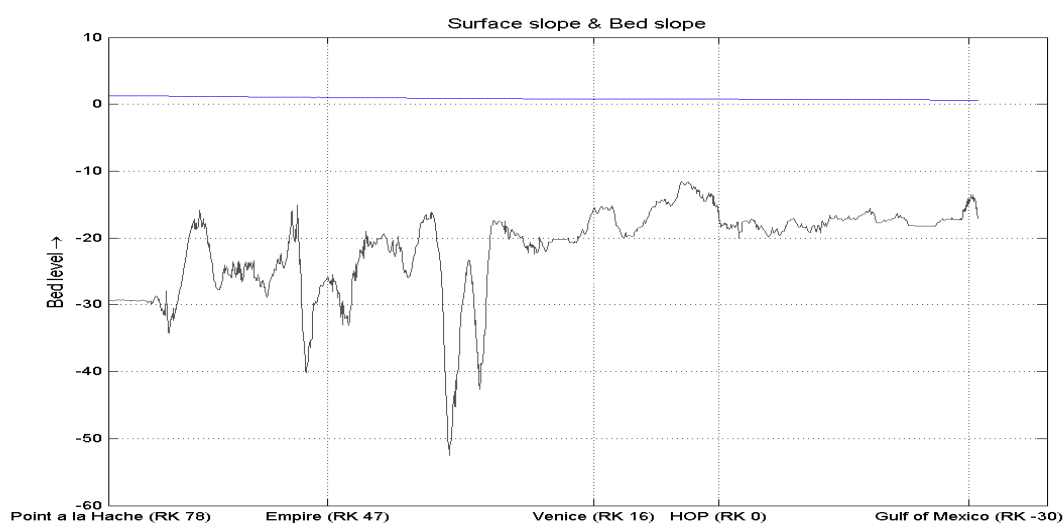


Figure 2.9: Surface slope & Bed slope, Lower Mississippi River (RK 78 down to RK -30)

As shown in figure 2.10 water withdrawal induces an increase of the downstream bed elevation, a reduction of the depth and an increasing slope. Moreover the consequence of sediment withdrawal induces a degradation of the bed, an increase of the depth and a decrease of the bed slope, see figure 2.11. These simplified principles show general river engineering rules (Forget-me-nots²) can be relatively applied to the Lower Mississippi River. This makes it possible to get a quick insight with basic analytical computations.

Water withdrawal is represented by the distributaries in the downstream reach, which can be related to the bed elevation and the shallow water depth in the downstream reach. Locally placed sediment diversions could provide a degradation of the bed.

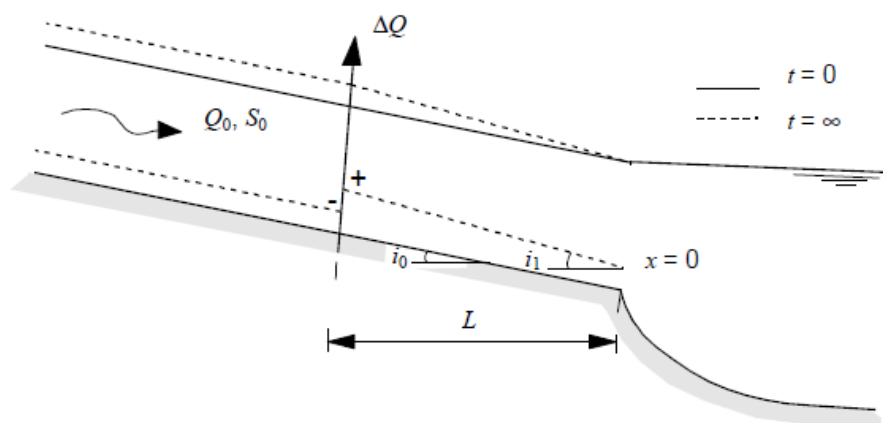


Figure 2.10: Consequence of water withdrawal [De Vriend *et al.*, 2010]

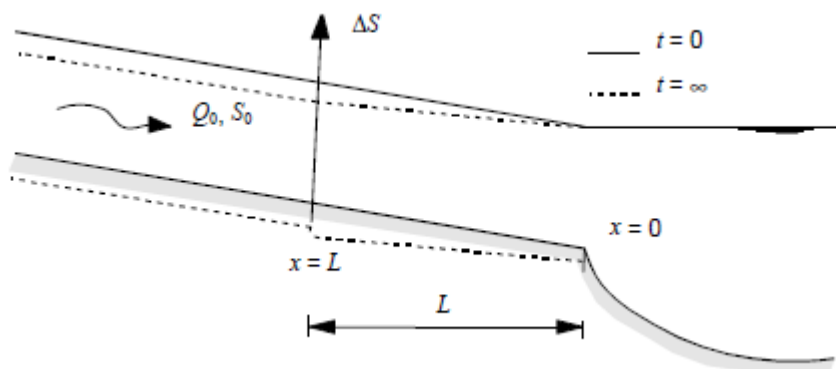


Figure 2.11: Consequence of sediment withdrawal [De Vriend *et al.*, 2010]

² 'For-get-me-nots', long term morphological response [De Vriend, 2010] .

Length and time scales

Characteristic length and time scales can be computed. The length scale gives insight into the scales for backwater curves. The scale indicates how far disturbances downstream can be noticed upstream. It is assumed the length of the model should be order magnitude of the length scale for intermediate/ high flow. This way the disturbances at the downstream boundary can travel through the entire model. The time scale indicates 50% of the time the morphological response needs to (computed with the sediment transport rate) to travel over the length scale from upstream to downstream. They can be computed with the following formulas:

$$L_{lengthscale} = \frac{1}{4} \frac{h_0}{i_b} \quad (2.1)$$

$$T_{timescale} = \frac{3i_b L_{lengthscale}}{q_s b} \quad (2.2)$$

in which h_0 is the depth [m] at the mouth of the river, i_b is the bed slope, q_s is the sediment transport [m^2/s] and b is a non-linearity coefficient (ranging from 3 to 5).

The length scale varies from 375 to 100 km for low and high flow respectively. The scale show that during low flow the disturbances from downstream can be noticed far upstream.

The time scale varies from 740 to 5.5 years for low and high flow respectively. The time scale shows that morphological disturbances take several years to centuries to travel through the river.

Furthermore the adaptation length scales (L_a) and time scales (T_a) can be compute. These scales give inside into the behavior of suspended sediment (sand) particles. The length scale refers to the distance a particle travels over the water depth before it settles on the river bed and the time scale refers to what time it takes [Galappatti and Vreugdenhil, 1985]:

$$L_a = \frac{hu}{w_s} \quad (2.3)$$

$$T_a = \frac{h}{w_s} \quad (2.4)$$

in which h is the water depth [m], u is the depth averaged flow velocity [m/s] and w_s is the settling velocity of the sediment particles [m/s].

The adaptation length (L_a) varies from 2 to 5 km for low and high flow respectively and the adaptation time (T_a) is approximately 55 min.

2.4 Mississippi delta

2.4.1. Problems in delta

Several researchers have stated that the Mississippi delta is not sustainable anymore. It is rapidly subsiding and it needs to be restored [Parker *et al.*, 2006; Day *et al.*, 2007; Reed, 2009]. The wetland loss rates are estimated up to 77 km²/year [Barras *et al.*, 2003].

Without human interference a delta maintains itself by two counteracting processes; sediment deposition and avulsions of the river. Unfortunately both processes are blocked because of the canalization of the river. The Mississippi river has been canalized since the 19th century from upstream Cairo to downstream New Orleans and further to the coast far into the Gulf of Mexico. Figure 2.12 and 2.13 give an overview of change in the delta. In 1850 the river had dozens of sediment pathways. In 1990 there are only three sediment pathways left. These figures show that sediment has been transported straight into the Gulf of Mexico for already 150 years.

The pathways to the delta are blocked. The river cannot deposit its sediment in the delta, which makes it unable to replenish the delta with sediments and create new land [Kesel, 2003; Parker *et al.*, 2006; Kim *et al.*, 2008]. Besides that the installation of many control structures (see Appendix B) in the Lower Mississippi River changed the behavior of the river. The sediment delivery in the delta decreased by a factor five over the last 60 years due to these interventions. These measures were necessary to provide navigability and flood protection.

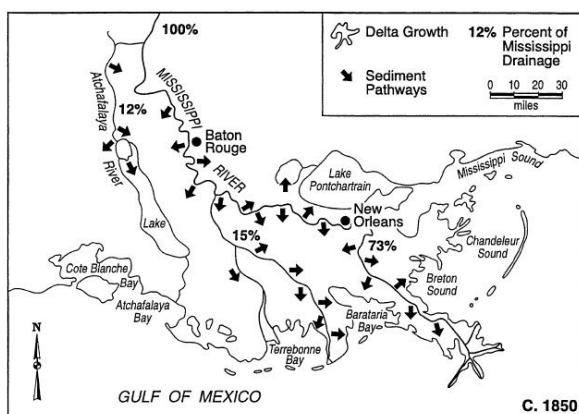


Figure 2.12: Representation of flow and sediment distribution in 1850 [Kesel, 2003]

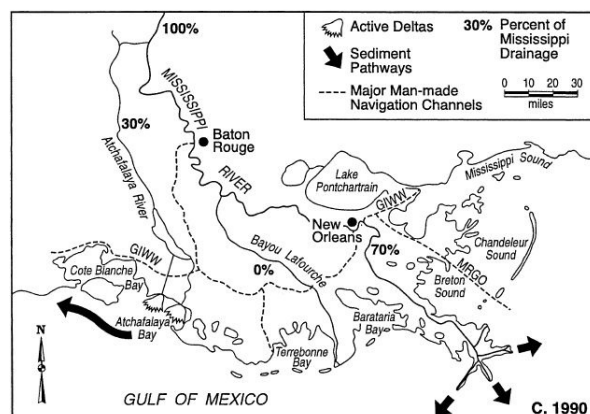


Figure 2.13: Representation of flow and sediment distribution in 1990 [Kesel, 2003]

2.4.2. Creating a sustainable delta

To create a sustainable delta it is necessary to restore the delta in a way nature would do if there were no human interventions. The sediments that are delivered by the Mississippi River need to be distributed over the delta plains, the so called marshes and swamps. This is possible by creating diversions in the Mississippi River channel at the spots where new land has to be built.

Louisiana Coastal Protection and Restoration (LACPR) Program

LACPR program is the post Hurricane Katrina work document of the USACE for all the restoration plans of the Mississippi delta. The report of LACPR contains strategies, plans and technical designs [USACE, 2009a]. The National Research Committee did a review on the final report of LACPR program. Below a relevant list of interesting key findings and recommendations is given [National Research Committee, 2009]:

1. The USACE should have a better scientific understanding of the uncertainties of the implications of the Mississippi diversions. Numerical modeling efforts could provide a better quantitative understanding.
2. The USACE should monitor and evaluate the already existing diversions and draw lessons from that.
3. The LACPR team should think of a good trade-off between coastal restoration by diversions and navigability of the river.

Pilot diversion program: West Bay Diversion

The US Army Corps of Engineers (USACE) is responsible for the maintenance and operations of the river. As part of the LCA program (LCA is the pre-Katrina Coastal restoration program) USACE built in 2003 a pilot sediment diversion, West Bay Diversion, to study the effect of a sediment diversion.

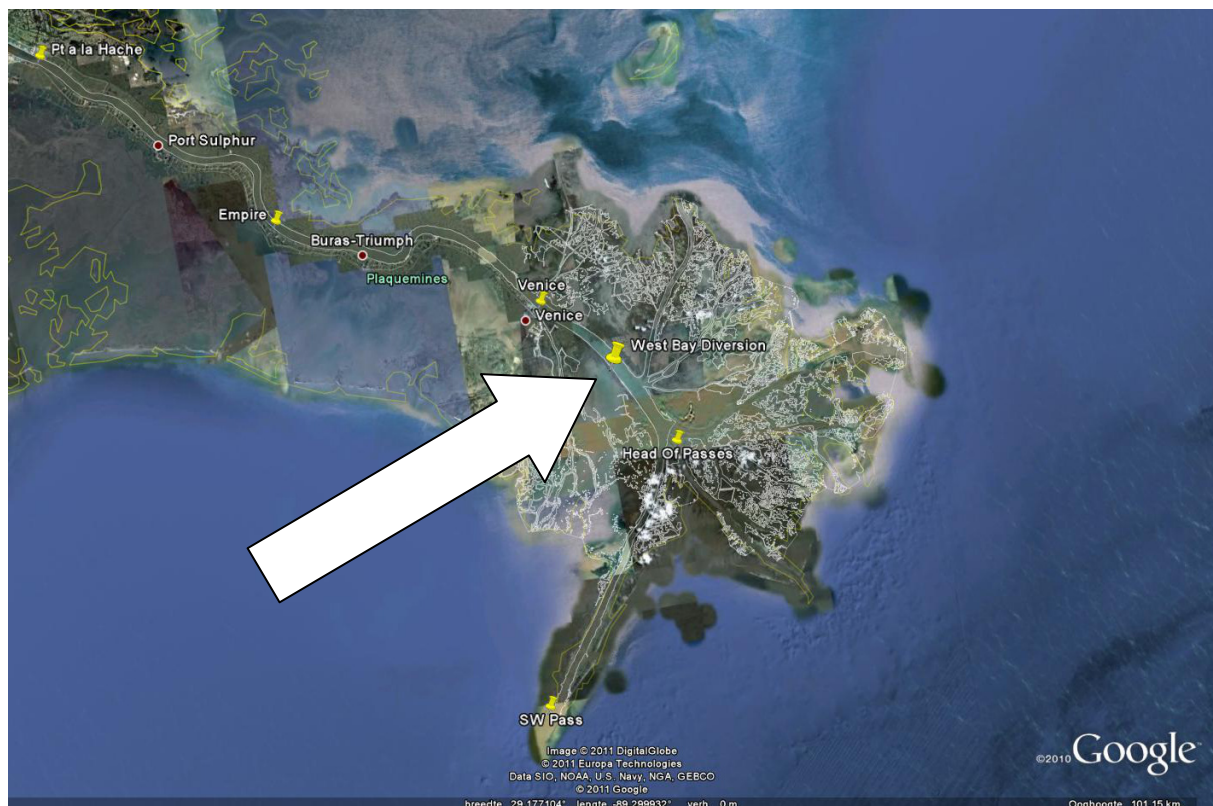


Figure 2.14: Mississippi Delta, Louisiana US, HOP is Head of Passes [Google Earth, 2011]

A gap was dredged in the river levee (figure 2.14) and bank protection was added at the openings of the diversion to prevent the opening from scouring (figure 2.16). The USACE also

monitors and analyses the behavior of the diversion. The sediment diversion is made at the West bank of the main stem of the Mississippi River at RK 8 above of Head of Passes, see figure 2.14, which is at the trifurcation of the river. The delta grow rate of the West Bay diversion is observed by Ashurst and has been estimated as $2 \text{ km}^2/\text{year}$ [Ashurst, 2007].

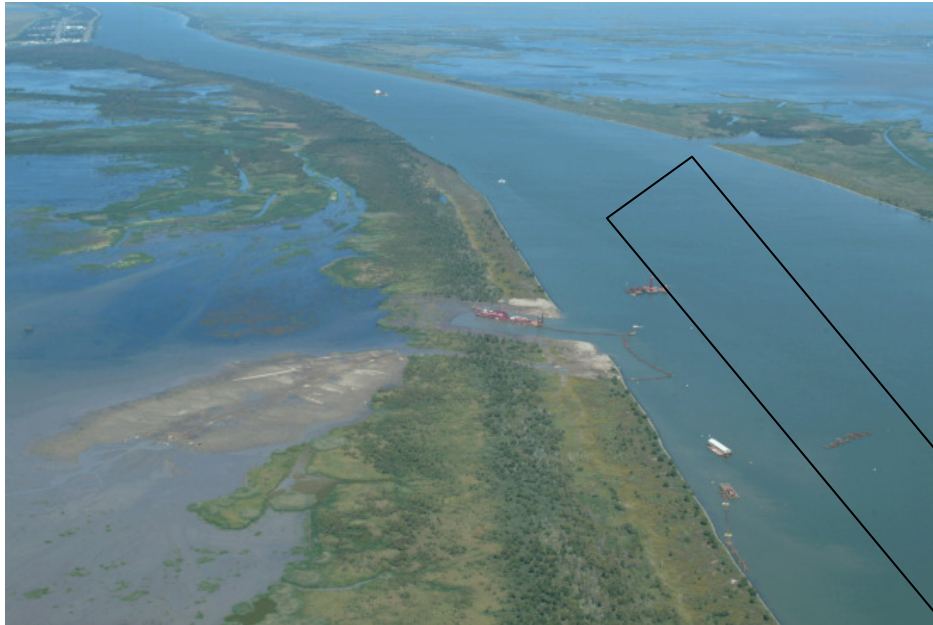


Figure 2.15: Dredging West Bay Diversion, black box is anchorage area, Modified [USACE, 2003]

The diversion is causing problems to the anchorage area (see Appendix E) for ocean-going vessels, which is situated at the opening of the diversion, see figures 2.15, 2.17 and 2.18 (black box). The diversion is blamed for increased aggregation of the bed [National Research Council, 2009]. Every three years the bed has to be extensively dredged which costs over millions of dollars. Probably the diversion has been built too close to the mouth of the river [Schleifstein, 2010].



Figure 2.16: West Bay Diversion, opening [Wilson, 2008]

USACE (2009b) modeled the silting up phenomena of the anchorage area, see figures 2.17 and 2.18 for the model representation. The red color shows relative sedimentation and aggregation of the bed, green shows no changes and blue erosion and degradation between start and end of simulation (reference year is 2009, simulations ran for 1 year). According to this study the West Bay diversion is 100% responsible for the siltation of the anchorage area. [USACE, 2009b]. The figures show there is a real difference between the situation with and without the West Bay Diversion. The situation without the West Bay Diversion is desirable.

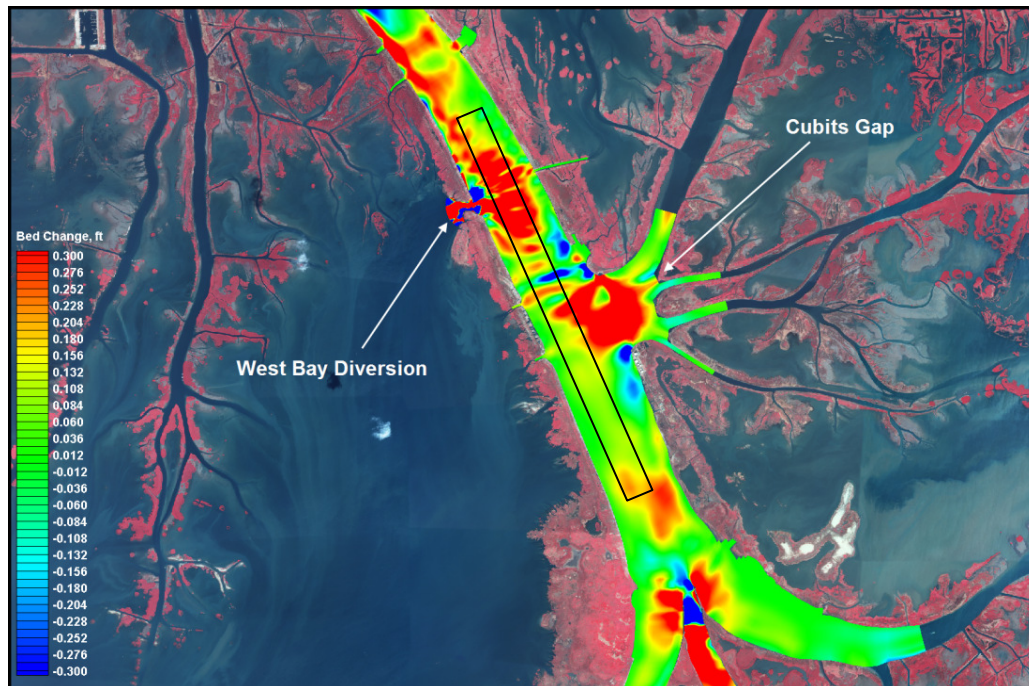


Figure 2.17: Simulation; West Bay Diversion, black box is anchorage area, Modified [USACE, 2009b]

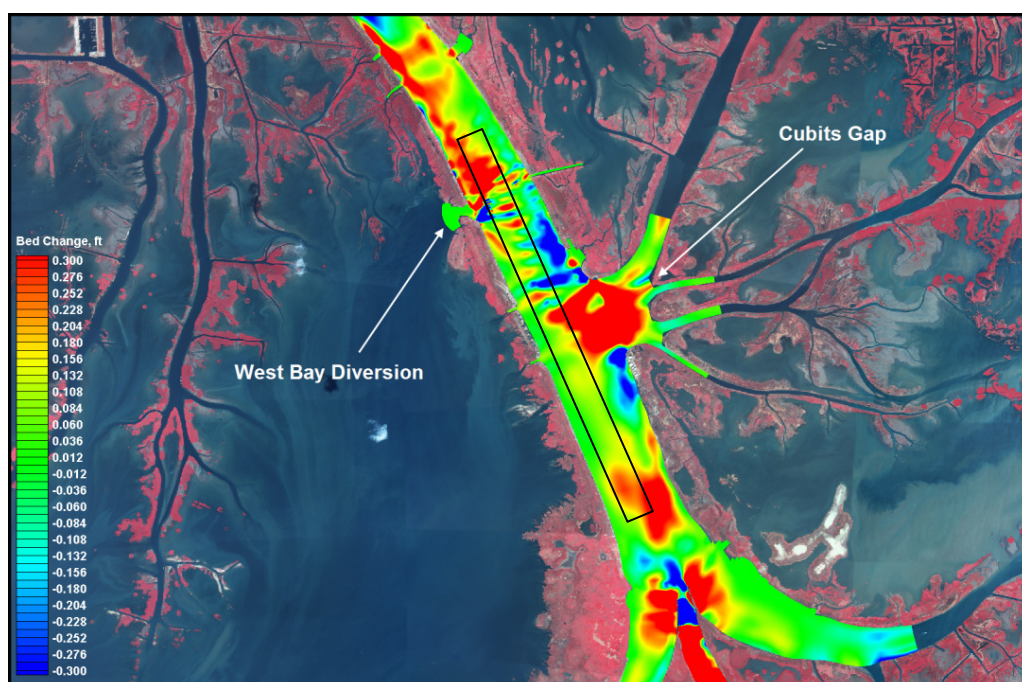


Figure 2.18: Simulation; Excluding West Bay Diversion, black box is anchorage area, Modified [USACE, 2009b]

The USACE claims it is a real life experiment, to apply lessons learned in future projects [Schleifstein, 2010]. Presently the USACE discusses whether to maintain the diversion or to close it. Closing the diversion is considered to be a waste of money. This is an interesting case because this study is also about the implementation of a diversion, with the objective of minimizing the impacts on navigability. The site location of the diversion seems to be of great importance. This lesson is taken into account in this study and is further treated in detail in chapter 6.

2.4.3. Extensive research

There are many ongoing research projects that try to assess the effects of diversions and the capabilities for delta building. A brief summary is given to indicate to what extent research has been done thus far. Numerical models are used to simulate the effects of implementing diversions. The 2D (quasi 3D) numerical models of Karadogan, Pereira and Meselhe are still in development [Pereira *et al.*, 2009; Pereira *et al.*, 2010; Pereira *et al.*, in Press; Karadogan *et al.*, 2009; Karadogan, 2010; Meselhe *et al.* In Press] Karadogan uses the USACE Adaptive Hydraulics Model (ADH), an unstructured finite element model. Pereira uses ECOMSED which has a structured grid [HydroQual, 2002]. Meselhe uses 3-D Flow3D, this modeling suite also uses a structured grid, Meselhe mainly focuses on influences of the already in 2001 approved Myrtle Grove Diversion. The construction of the Myrtle Grove diversion (RK 92), within the LCA program is proposed for 2013 [USACE, 2011].

Next to this also Small Scale Physical Modelling (SSPM) is done by Louisiana State University (LSU) [Wilson *et al.*, 2008]. The research project shows that it is possible to build land by implementing diversions in the system and the impact on bed morphology. It visualises the sediment processes for different scenarios; an example can be seen in figure 2.19.

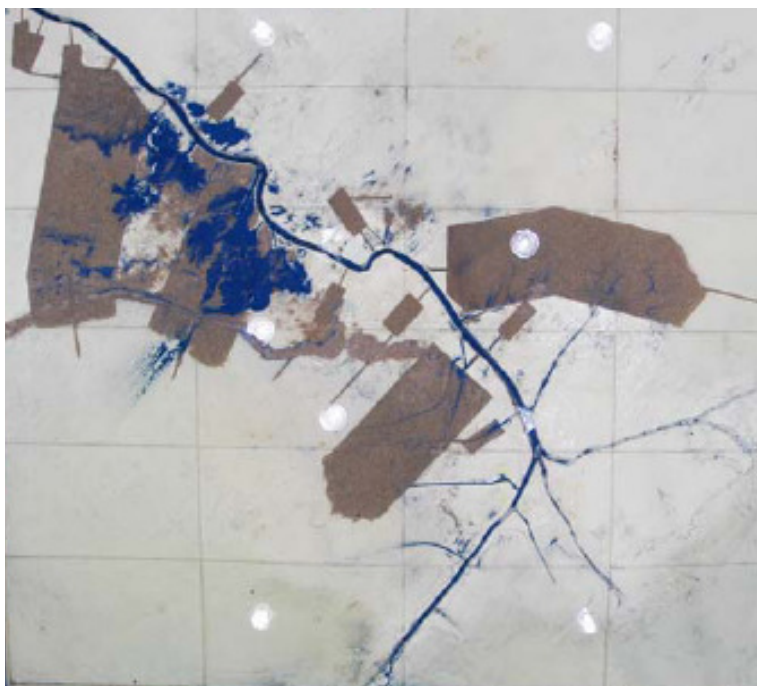


Figure 2.19: Small Scale Physical Model Lower Mississippi River, in blue the diverted sediment after running a simulation, modified [Wilson, 2008]

Another research is done by CLEAR on delta formation capacity. CLEAR (Coastal Louisiana Ecosystem Assessment and Restoration) is a science based organization where State, USACE and Universities together collaborate. The model of Kim *et al.* (2008) represents two diversions, one on each side of the river in the delta. The diversions divert 45% of the discharge and sediment during the high flow season. Control structures will divert the water and sediment into the delta. During low flow the control structures are closed to secure navigation. The implementation of a diversion could result in land accretion in the order of 1,000 km² in about a century (10 km²/year), or a rate of 913 km³/year, see figure 2.20. This is a factor 2.5 more than the grow rate of the Wax lake delta, which seems a lot. The fans in the figure show the accreted land [Kim *et al.*, 2008]. The modeled creation of the fans should be put in perspective. The grow rate (10 km²/year per diversion) seems promising and representative compared the grow rate of the West Bay diversion (2 km²/year), because the modeled diversions convey 5,000 m³/s compared to the West Bay Diversion which conveys 1,000 m³/year. The same multiplication can be found. It is a start against the current land losses of 77 km²/year.

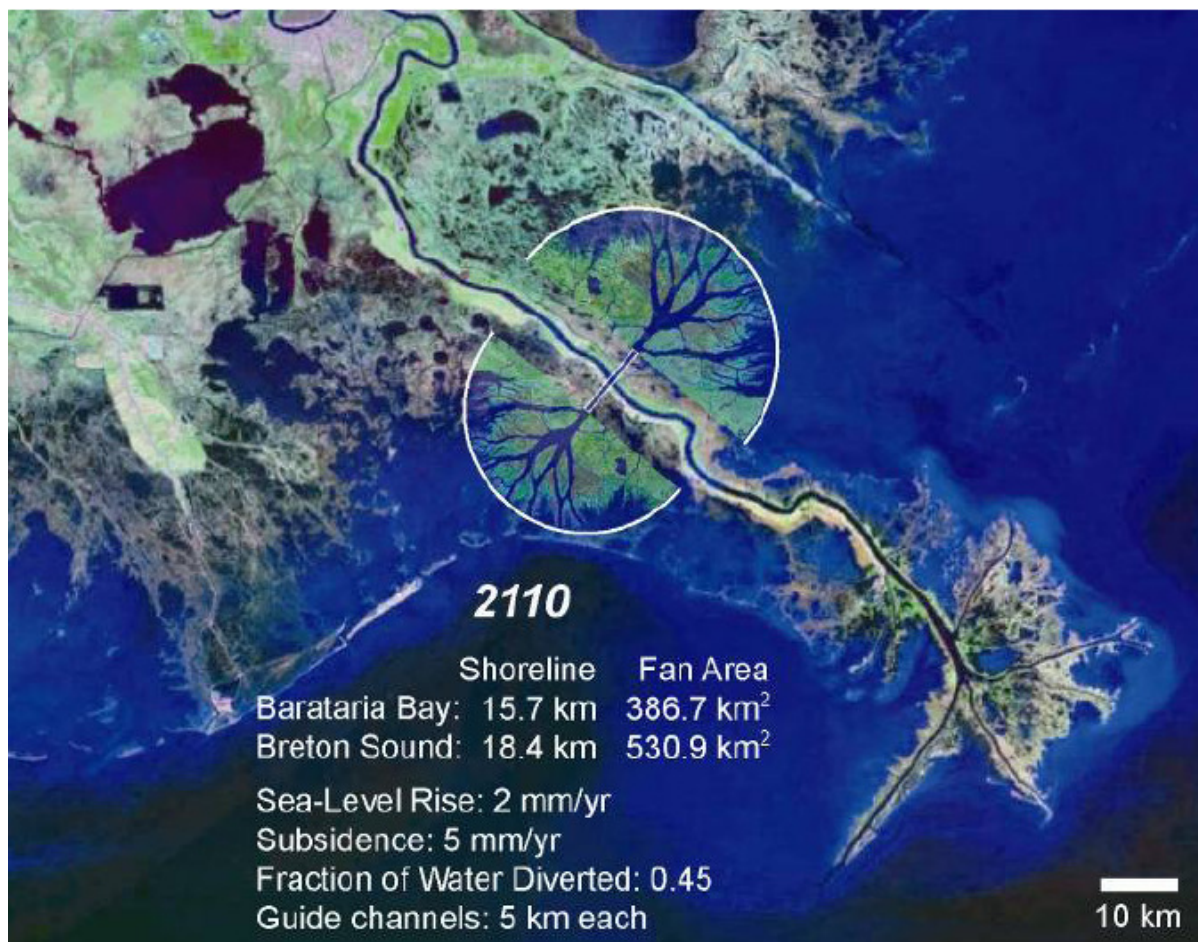


Figure 2.20: Model representation of growing delta, modified [Kim *et al.*, 2008]

2.5 Navigation and dredging activities

Dredging activities

The shipping industry is a very strong player that is concerned about large engineering interventions in the river. They demand 100% navigability on the Mississippi outlet/ inlet River channel because the inner land has to be accessible at any time.

The USACE maintains a deep channel fairway of 14 m (45 ft) by maintenance dredging, in order to give access to deep ocean going vessels and oil tankers. Maintenance dredging of the Lower Mississippi started already in the 19th century. The deep channel fairway is maintained from Baton Rouge RK 376 to the Gulf of Mexico (GOM) RK -35.2. The dredging of the Southwest Pass begins when the river starts to rise (usually December, January or February) and will continue usually until June or July. The crossings between Baton Rouge and New Orleans usually are dredged when the river falls. The harbor of New Orleans is dredged once or twice a year (in spring and end of summer/early fall) [pers. comm. Ulm, 2010].



Figure 2.21: Large sea going vessel in the Southwest Pass at the Gulf of Mexico (photograph Bos)

Dredging strategy of the Southwest Pass

In figure 2.22 and 2.23 the dredging reach is shown in top and bird view. The dredging reach is from RK 10 above Head of Passes, down to RK 35 below Head of Passes. The dredging reach starts right after the point the main stem has to distribute its flow over the distributaries. From this point the river turns shallower than the upstream part.

The plots with the dredging strategy are enclosed in Appendix C. In those plots it can be seen the dredged material is used to create new land in the delta with the intention to counteract the problems in the delta.

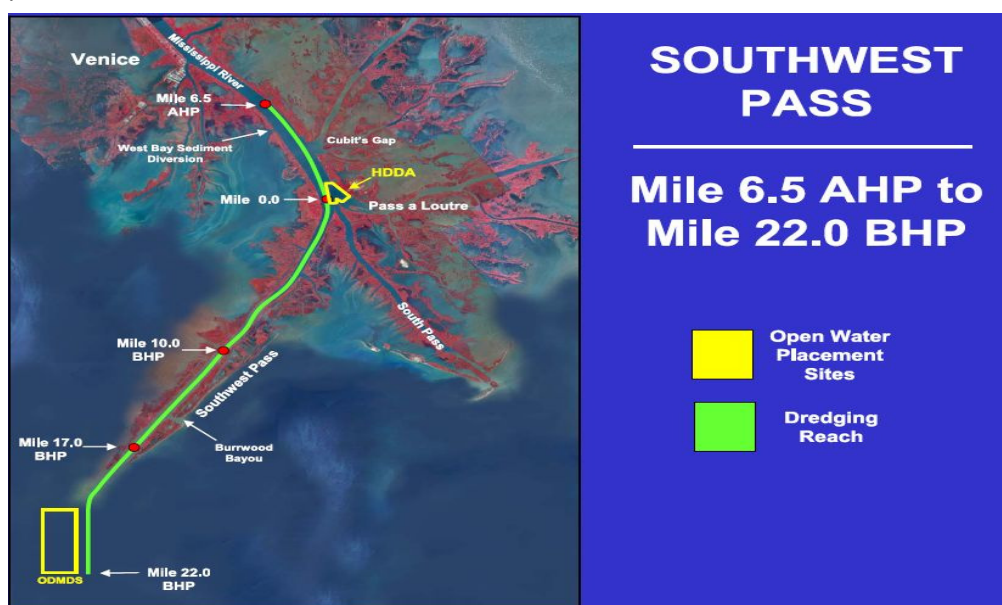


Figure 2.22: Overview dredging strategies (top view) [USACE 2010]

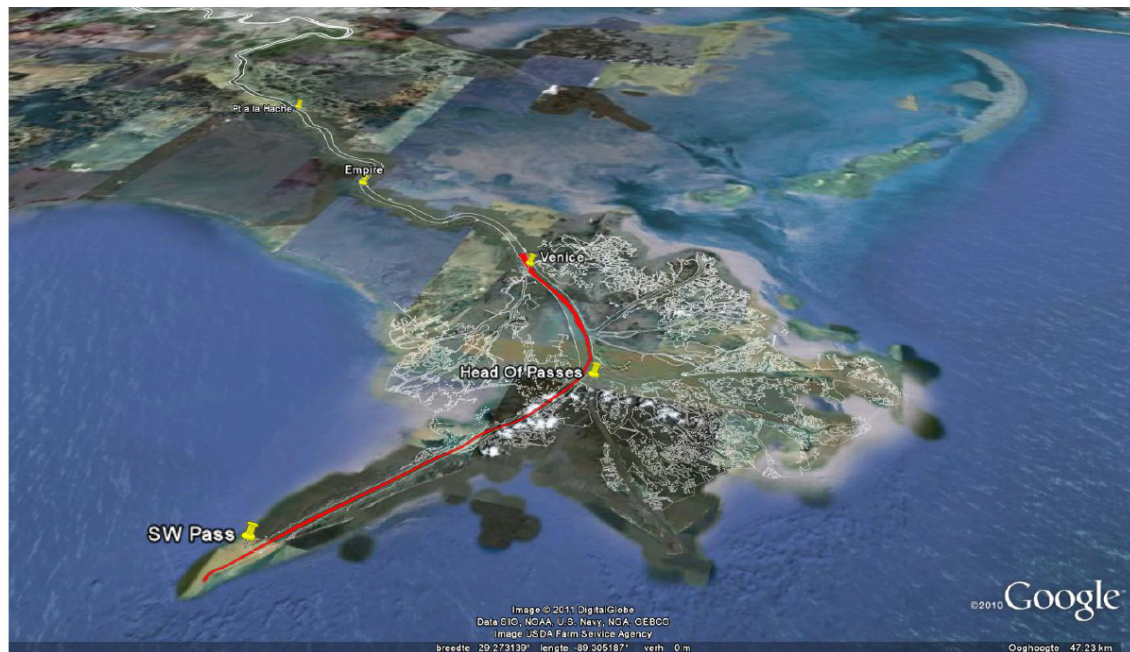


Figure 2.23: Dredging reach of 45 km, from downstream Venice to the mouth of the river (bird view) [Google Earth, 2011; Open Earth Tools, 2011]

Dredging budget

The dredged quantities and costs over the past 20 years are presented in figure 2.24. The average dredged material over these 20 years is 13 million m^3 . From 2006 to 2010 the quantities and costs are increasing. The quantities and costs do not increase simultaneously, because the price per cube dredge material became higher over the last few years. This has to do with increasing costs of fuel etc.

The increasing dredged quantities refer to the effect that the dredged channel is filling up faster than before. The reason why this process goes faster and therefore more material needs to be dredged is not well known. However 2008 and 2009 are relatively flood years, in these years the quantities abruptly increase. It could be assumed that the increasing dredging quantities are related to high discharges, because the flow transports more sediments to the downstream reach in the delta. Chapter 6 provides into more details.

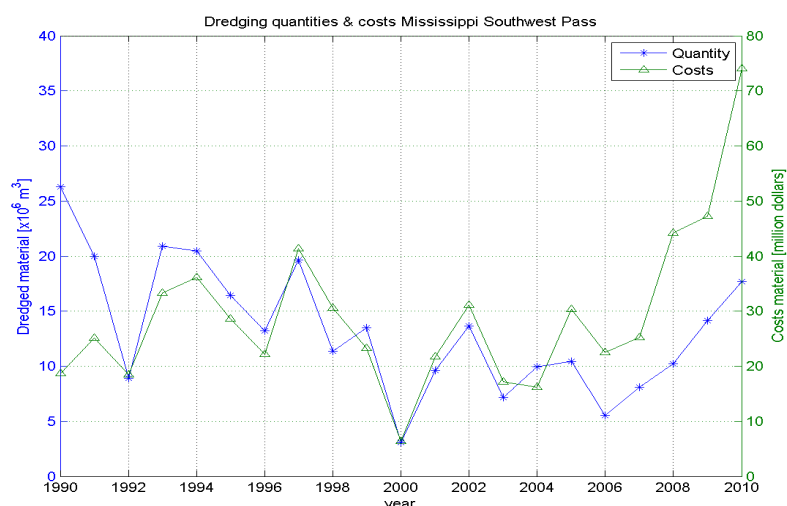


Figure 2.24: Dredging quantities and costs [Ulm, 2010]

River survey

Within the available resources the navigation channel of the Southwest Pass (dredging reach in figure 2.22) is surveyed every work day. Hereby, the USACE is able to see if maintenance dredging is needed in certain areas. The purpose of these surveys is to inspect the navigation channel and therefore to determine when dredging is required [pers. comm. Ulm, 2010].

River training structures

River training structures are built along the entire Lower Mississippi River; e.g. rock bend protections, fore shore rock protections, jetties, lateral pile dikes and bank revetments, see Appendix E for the river maps. The river training structures are indicated in these maps. These measures are done to prevent the river from changing its course and prevent the banks and river bed from eroding.

The building of these structures started back in the early 1850s. Maintenance of all of these structures is included in the navigation channel project that is managed by the USACE. Figure 2.25 shows maintenance work on the breakwater at the mouth of the river in the Gulf of Mexico.



Figure 2.25: Maintenance work on breakwater in December 2010, at the mouth of the river at the Gulf of Mexico (photograph Bos)

Chapter 3. Set-up of numerical model

3.1 Introduction

Delft3D is the numerical modeling software which is used to model the hydro- and morphodynamic Lower Mississippi River. The model provides in the understanding the river behavior and the impact of interventions. Delft3D is a state of the art numerical modeling software package developed by Deltares, formerly WL | Delft Hydraulics.

The software makes use of a finite-difference numerical approach in a form equivalent to finite volume. Delft3D is a modeling suite to investigate e.g. hydrodynamics, sediment transport and morphology. It has many advantages such as high runtime efficiency. More about the background of Delft3D can be read in Appendix D [Deltares, 2011].

3.2 Model assumptions

General assumptions have been made in order to schematize the study area and to simplify the model. The model is 2D depth averaged (2DH). In this way the model can be used to assess large scale processes over more than 100 km. The model can help to make predictions and to visualize practical applications. The objective of this study is focused on 2D long-term morphological behavior of the river.

In 2D it is possible to simulate the cross-river processes such as the extraction of sediment by diversions. The bed level behavior around the diversion can be studied. In addition the continuous dredging activities can be included within the long-term simulations.

A 3D model is very inefficient with respect to run time. It should be kept in mind a 10 year long-term simulation has to run for up to 5 days. A 3D model is more interesting for modeling in detail, for instance around structures; e.g. a sediment diversion. Scales of morphological response for 3D modeling is related to the water depth, i.e. up to 50 m.

The model excludes tidal- and wave forcing on the downstream boundary, because the river discharge is dominant as stated in section 1.1. Modeling of salinity is also excluded; therefore no saltwater wedge is modeled as described in section 2.2. In a later phase the salinity could be added to the model.

Simulations were run steady-state with constant discharge levels and corresponding sediment transport, which means the flow throughout the year is schematized as well as the sediment transport in the model. The flow is schematized in three discharge levels and kept the same over the years, as it is explained in chapter 4. The morphological response is also schematized, and how this is done is explained in chapter 5.

3.3 Study Area

The model reach of this study is from Point a la Hache until the mouth of the river at the Gulf of Mexico. The length of the model reach is about 110 km. The main stem of the river is the yellow line in the map of the model reach (figure 3.1). This reach is chosen because at Point a la Hache is a water-level gauge. Besides the so-called Bohemia spillway starts right after this point. This spillway is only active with flows exceeding 20,000 m³/s, see section 4.1. This study is interested in the downstream effect of the sediment diversions in the delta, therefore adding more domain to the model upstream is not necessary.

Moreover, extending the model reach would increase the computation run time, which would make the model slower. This study is done on a PC. From practical experiences a model reach of about 100 km is manageable on a stand-alone computer.



Figure 3.1: Lower Mississippi River, Study area, Modified [Google maps, 2011]

3.4 Delft3D Grid design

3.4.1 Grid layout

This research focuses on the main river channel, which is used for navigation of oceangoing vessels. Considering this objective, the grid of the numerical model is limited to the main stem. The grid design of the model needs to be a structured curvilinear grid. The use of the unstructured grid application of Delft3D, with the triangular elements, is not possible, because the morphological module is not yet available.

The main stem is also the main grid; the distributaries along the river are basically attached to the main grid. Since the considered river reach is trained with revetments on the banks and is constrained with levees, no floodplains are included. The application of domain decomposition in Delft3D is necessary to attach the distributaries to the main grid.

The attached grids of the distributaries are only used to subtract the correct amount of flow from the main stem, to reproduce the hydrodynamic behavior in the river. The sediment transport distribution over the distributaries is dependent on the hydrodynamic behavior. The model itself calculates the corresponding sediment transport over the distributaries.

The distributaries are: Baptiste Collette, Grand Pass-Tiger Pass, Cubits Gap, West Bay Diversion, Pass a Loutre and South Pass. The Southwest Pass is the navigable channel to the Gulf of Mexico and is part of the main stem of the Mississippi River and the main grid.

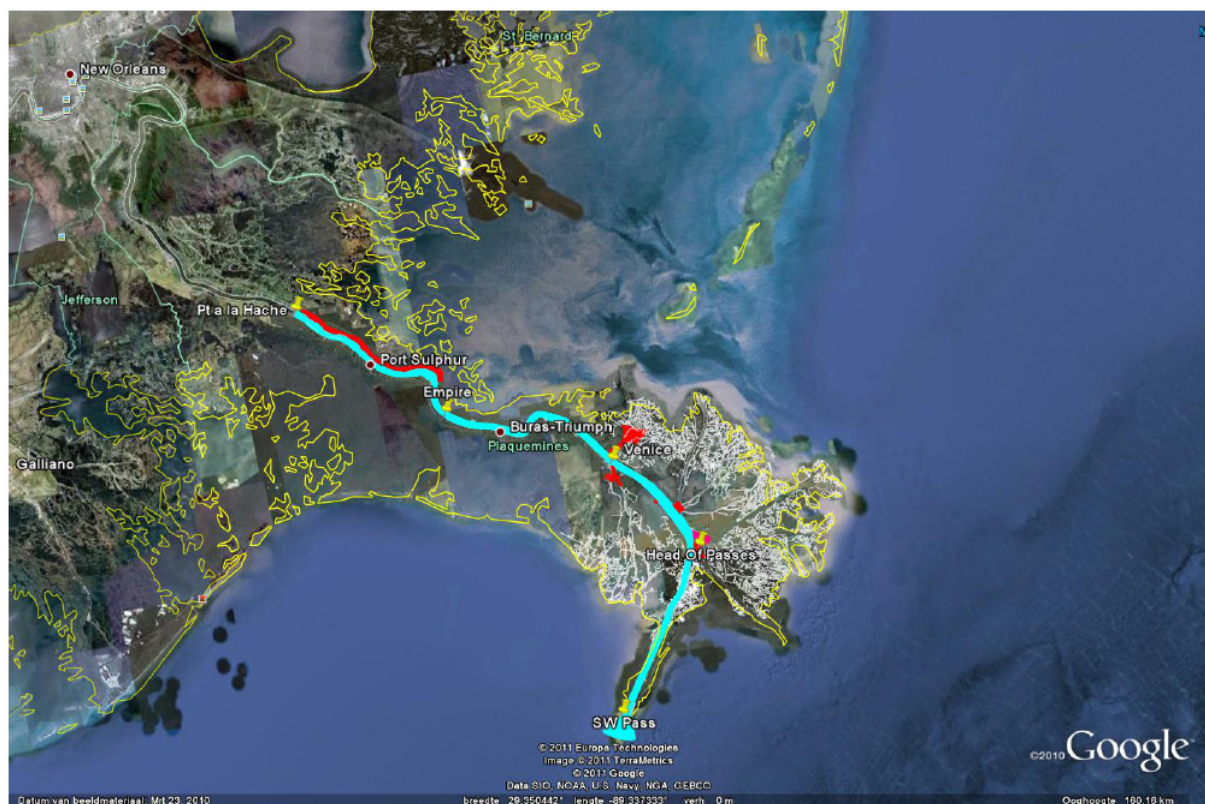


Figure 3.2: Grid of model reach in Delft3D (the main grid is cyan, the distributaries are red. The land boundary of the delta and the river is in white and yellow) [Google Earth, 2011; Open Earth Tools, 2011]

3.4.2 Grid requirements

The structured grid has been designed upon four requirements in a way that the model is able to simulate the 2D hydrodynamic river behavior properly. The four requirements for the grid design are the following and are described in detail by Mosselman *et al.*, 2005 and Ottevanger & Yossef, 2006.

- The alluvial part of the river should be represented with at least 6 grid cells in transverse direction, to be able to compute the transverse profile.
- Aspect ratio <4, which is the length/width ratio of a grid cell
- Orthogonality of $\sin(\alpha) < 0.086$, this means that the angle between consecutive grid line segments should be less than 5°.
- Smoothness <1.2, this is the relative difference in size between two adjacent cells.

The main-grid has 20 cells in the lateral direction and 1662 in the direction of the flow. There is only one grid cell in the vertical direction. Therefore the model is depth-averaged and categorized as a 2DH numerical model. The model has a varying depth of 13 to 55 m and a varying grid size (Δx) of 20-100 m, which is along the main axis and Δy is about 50 m perpendicular to main axis.

The Courant (CFL) condition has to be met to achieve convergence of the numerical simulation. If it does not meet the CFL-condition the model becomes unstable. According to the CFL condition the computations needs a time step (Δt) of approximately 15 s. The formula for the CFL condition reads [Deltares, 2010], CFL condition <8:

$$CFL = \frac{\Delta t}{\Delta x, \Delta y} (u + \sqrt{gh}) \leq 8 \quad (3.1)$$

3.4.3 Main grid and Distributaries

The main structured grid is curvilinear and boundary-fitted. The distributaries have mostly rectangular grid cells and the boundaries are shaped like a staircase (figure 3.3). The rectangular grid for the distributaries is chosen because it can be easily attached to the main-grid. It is sufficient to use these types of grids because this study only focuses on morphological processes in the main stem of the river. The stair case boundaries give small disturbances in the flow pattern, thus disturbances in the calculated bed elevation. Since the morphological processes in the distributaries are not taken in account, this has no effect on the performance of the model. These disturbance in the main grid needs to be avoided, therefore the grid of the main stem is boundary-fitted and curvilinear following the flow stream-lines.



Figure 3.3: Visualization of the grid. Trifurcation; Main stem, Pass a Loutre and South Pass in white, purple and red respectively. [Google Earth, 2011; Open Earth Tools, 2011]

The grid refinement (figure 3.3) in the rectangular grids was necessary for the trifurcation at Head of Passes (RK 0) in order to get a stable model. The extra computation time due to the distributaries is small compared to the computation time already needed for the main-grid.

To give an idea of the distribution of the flow at the trifurcation at Head of Passes see figure 3.3. The flow velocities to the South Pass are relatively high, because the entrance of the pass is rather narrow due to river training structures. Next, the channel of the South Pass to the Gulf of Mexico is short compared to the Southwest Pass. Therefore the South Pass has a larger gradient which will increase the flow velocities. Only a small percentage of the flow goes into the Pass a Loutre.

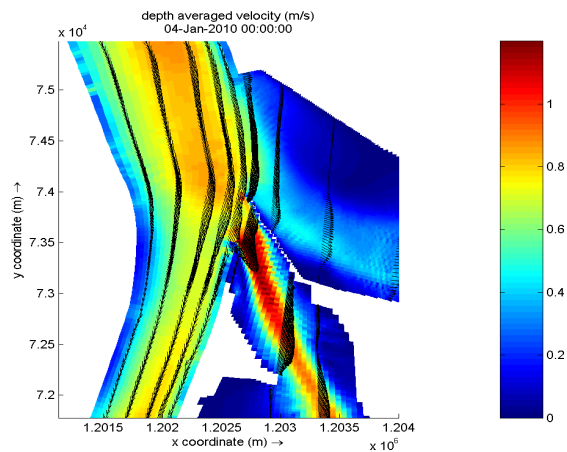


Figure 3.4 Representation of flow velocities and direction ($Q=20000 \text{ m}^3/\text{s}$)



Figure 3.5 Trifurcation at Head of Passes [Google Maps], narrow opening to South Pass

Figure 3.4 is shown to give an idea how the Mississippi stretches out at Head of Passes. The left opening is Pass a Loutre, the middle is the South Pass, and the right is the Southwest Pass (the main channel). Note that the river is 1.5 kilometres wide at Head of Passes.



Figure 3.6: Trifurcation at Head of Passes (photograph Bos)

3.5 Model bed topography

The bed topography for the model originates from two data sets, which are combined. The first data set is the single beam hydrographic survey of 2003 and 2004 in the Mississippi River [USACE, 2007]. The second data set has been extracted from the SL16v18c3 grid of the ADCIRC Model (Appendix F) [Bunya *et al.*, 2010; Notre Dame, 2010]. A conversion is done to NAVD88 (2004.65) vertical datum. The effect of Hurricane Katrina should be taken in account when analysis is done on model results. Because of its tremendous impact, Hurricane Katrina strongly influenced the bed topography. The USACE only does a survey of the entire region once every 10 years; therefore this data set is most recent.

Figure 3.7 shows the topography and the bathymetry of the Mississippi delta. New Orleans is situated in this delta. North of New Orleans is the shallow Lake Pontchartrain. The dark blue lines represent the main stem of the Lower Mississippi River. It can be seen how the River finds his way to the Gulf of Mexico. The green and yellow areas along the river and at the boundary with the Gulf of Mexico represent the swamps and marshes.

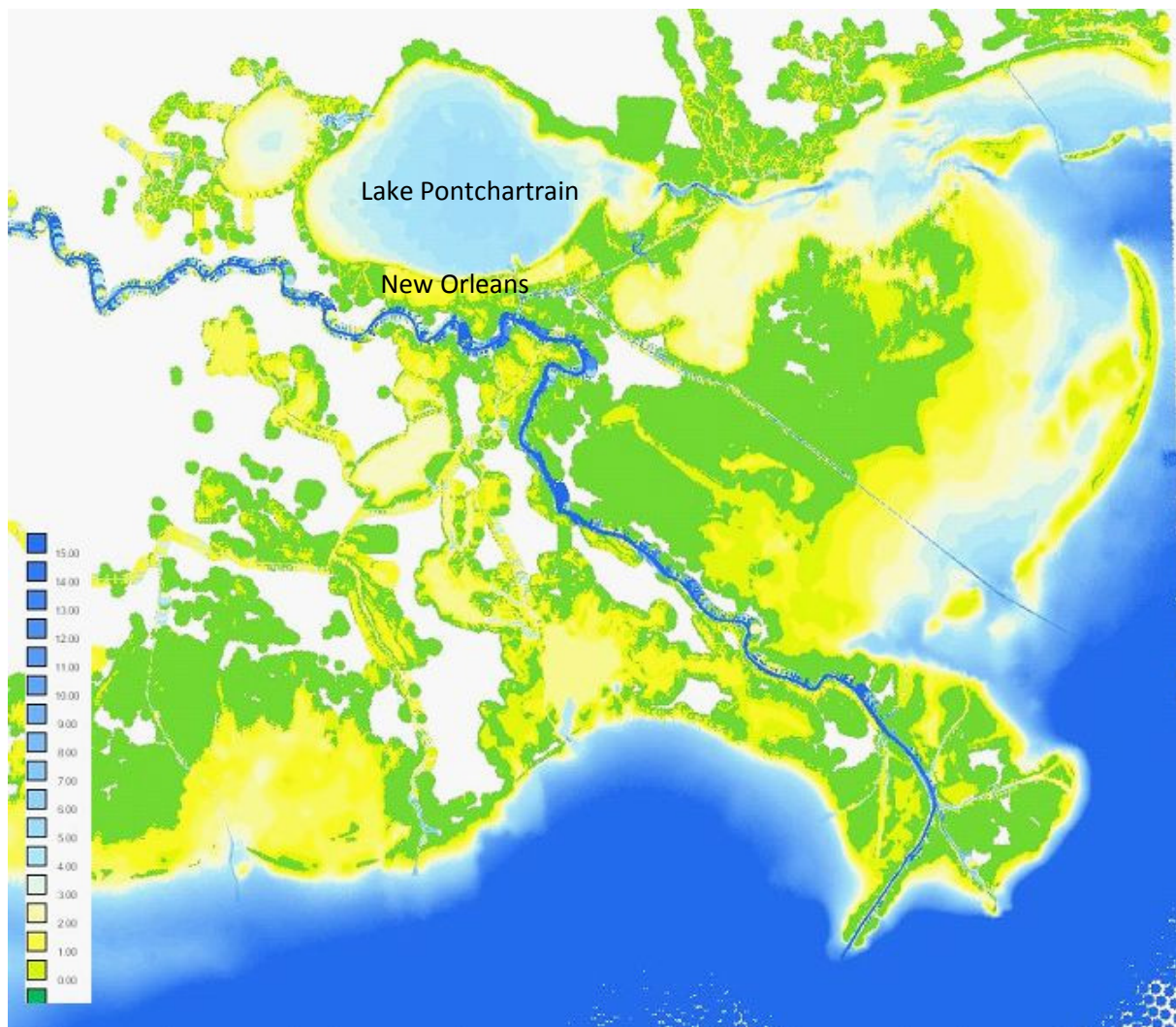


Figure 3.7: Delft3D, representation of topography and bathymetry of study area (white indicates missing data)

Initial bed level

Figure 3.8 shows the bed topography (initial bed level) of the model reach. The data set as shown in figure 3.7 is customized and interpolated to the grid. The depth ranges from 0 – 50 m. The downstream reach of the river is shallower than the upstream parts. This causes problems for navigation. The shallower (orange) river stretch is also the dredging reach, see section 2.5.

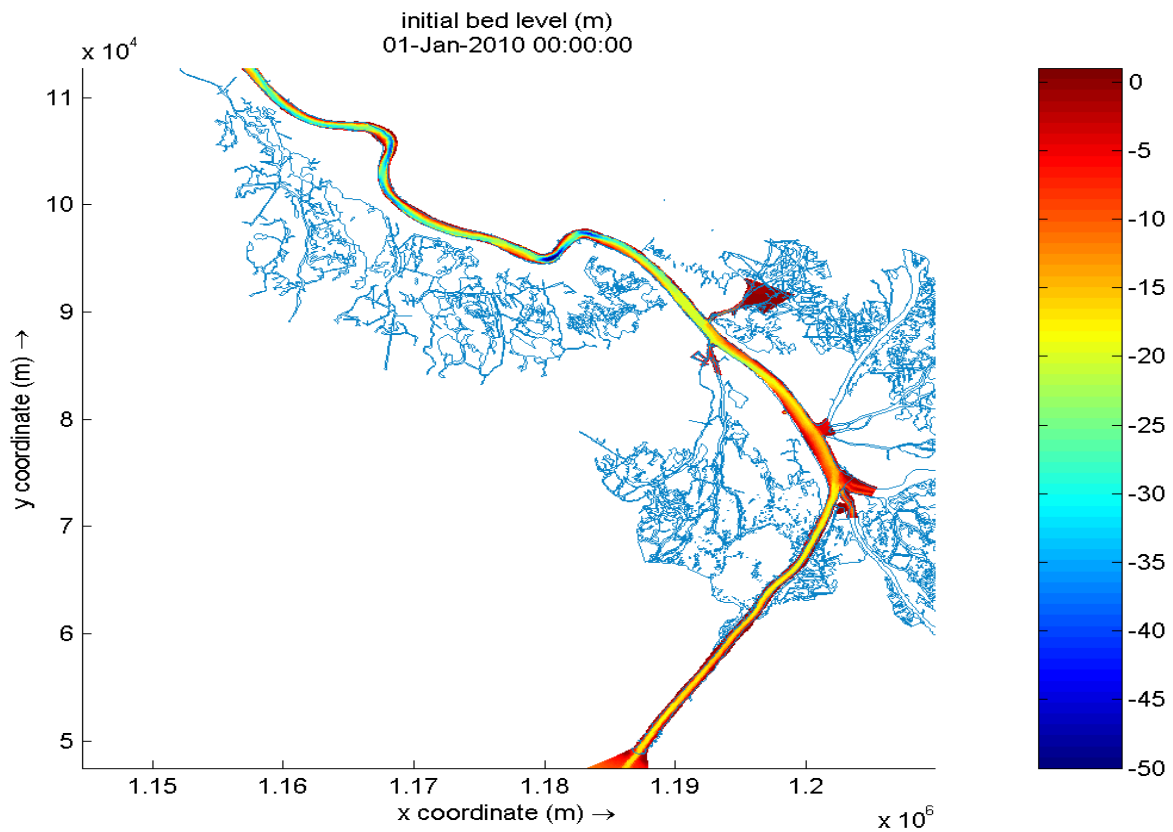


Figure 3.8, Lower Mississippi River: initial bed level

Chapter 4. Hydrodynamic calibration & verification

4.1 Flow Boundary conditions

4.1.1 Upstream boundary conditions

Discharge data for the Mississippi River are available through USACE. The USACE has been observing the river daily since early 1900. These data are open source and easy to download from their websites [USACE, 2011]. The discharge data set is gained from the Talbert Landing gage, see figure 4.1. This gage is downstream of the Old River Control structures which divert 70% of the river flow into the Mississippi Delta and 30% into the Atchafalaya Delta.

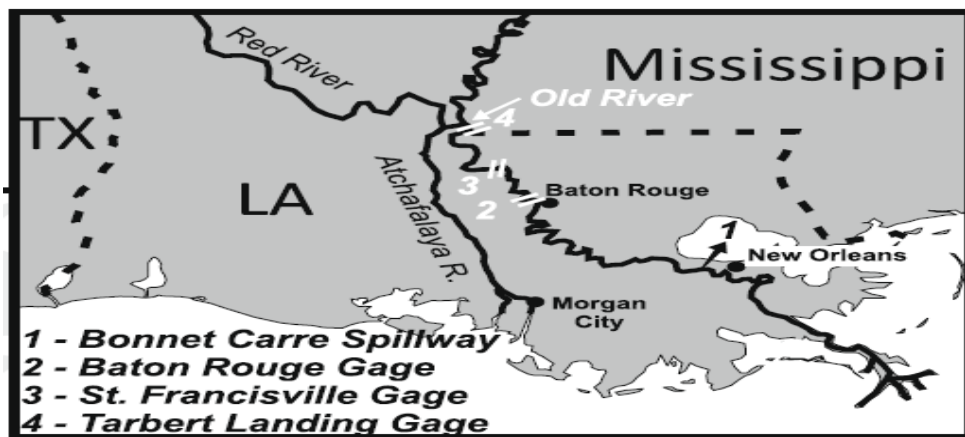


Figure 4.1: Lower Mississippi, location Talbert Landing [Allison & Meselhe, 2010]

The flow regime of the Lower Mississippi River is analyzed based on the discharge data from 2001-2009. Figure 4.2 gives an overview of the discharge regime throughout the whole year. It is noticeable that the discharge is different every year. 2008 was a year with high flows; also the Bonnet Carre Spillway was opened to divert the top of the peak discharges in April 2008. 2001 was a low flow year. These two years represent roughly the range in which the discharge varies.

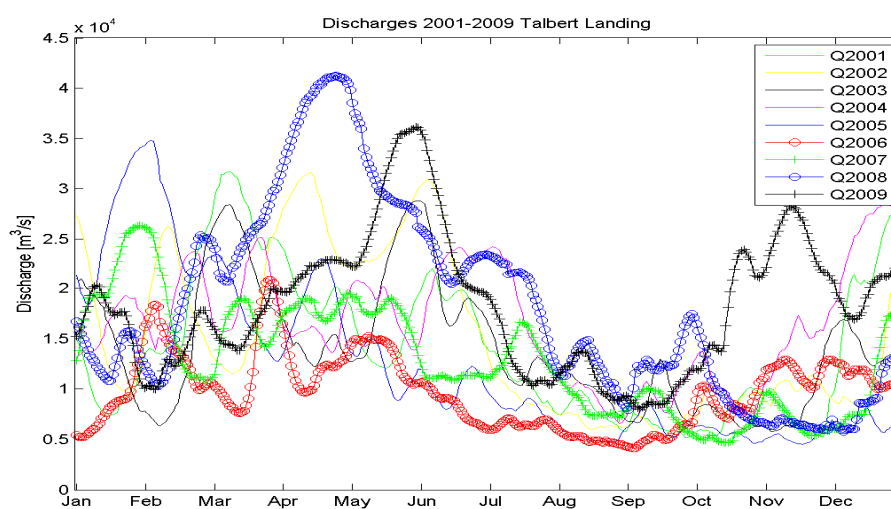


Figure 4.2: Observed discharge at Talbert landing from 2001-2009

The discharge data from 2001 to 2009 have been plotted (figure 4.3) as a frequency curve to see the rate of occurrence. The discharge data set from 2001 to 2009 is distributed in three levels in order to get boundary conditions for the numerical model, see the black line in figure 4.3. The upstream boundary is divided in three levels also to simplify the discharge regime and later on to be able to represent the morphological behavior of the river. The loss of discharge due to the Caernarvon and Davis Pond freshwater diversions is taken in account. The first level is the peak flow, the second is the intermediate flow and the third is the low flow, 33,000, 20,000 and 10,000 m³/s respectively.

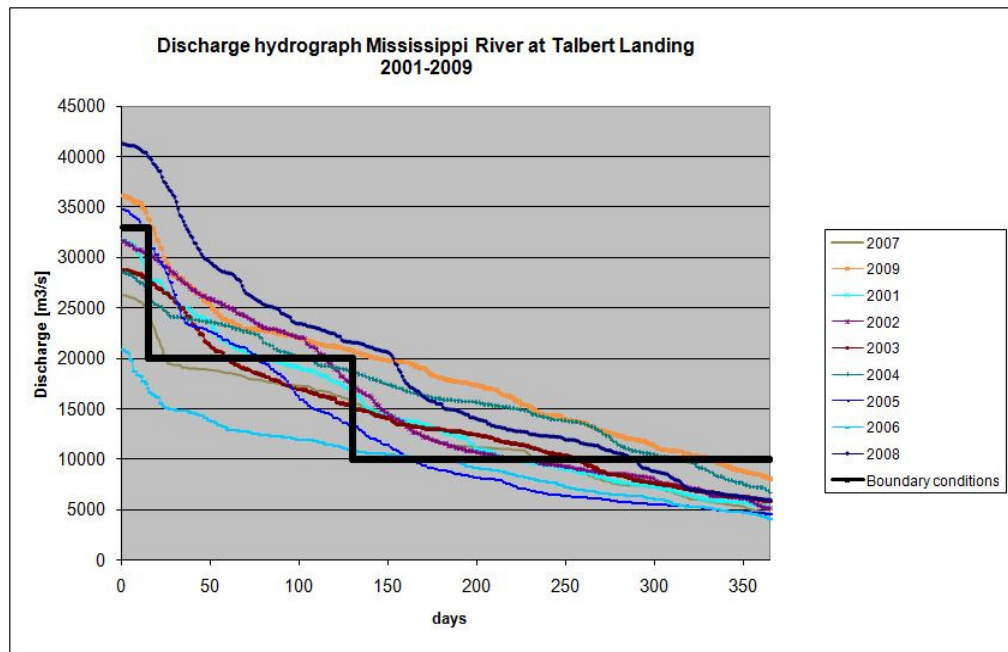


Figure 4.3: Measured duration curve of discharge data set

The peak flow represents the floods, which usually occur two weeks a year, mostly in the month April or May. The peak flow is the top 4% in the distribution function (figure 4.4) which represents two weeks (figure 4.3). The height of the peak flow is based on the average maximum discharge that comes from Talbert Landing and passes the Bonnet Carre Spillway even when it is opened. The peak flow is defined as 33,000 m³/s.

The height of the intermediate flow is based on two assumptions. For discharges between approximately 15,000 and 17,000 m³/s the suspended sediment transport rate is in equilibrium. There is no net re-suspension or deposition of sediment. Most of the suspended sediment stays in the water column. Besides that, the transport capacity of the flow is also too low to have an active moving bed [Mossa, 1996; Ashurst, 2007, Meselhe *et al.* 2011]. The second reason is that for discharge higher than 20,000 m³/s the Bohemia Spillway releases flow. To simplify the intermediate flow, it is chosen to define the intermediate flow as 20,000 m³/s and no flow will be released during the intermediate flow. This flow will also have a significant sediment transport capacity, which is characteristic for an intermediate flow within a morphological year. The intermediate flow occurs about 4 months a year from e.g. January to April and often in the period between May and June

Since the peak- and intermediate flow are defined, the low flow follows from that. The low flow is defined as 10,000 m³/s. The low flow occurs about 7 months of a year from June to January.

The total discharge data set is also plotted as a probability distribution curve (figure 4.4). In this way it is possible to define how often various discharges occur. The distribution shows that the mean discharge over this period is 14,300 m³/s. The standard deviation is 7,300 m³/s. In figure 4.4 the red ellipses represent the data set which is used to determine the discharge levels. The black stars indicate the three selected discharge levels. The red ellipses represent the occurrence of the discharge for this data set.

- 4% of the discharge exceeds 24,000 m³/s, which indicates the flood period.
- 32% of the discharge is higher than 16,000 m³/s and lower than 24,000 m³/s.
- 64% of the discharge is below 16,000 m³/s.

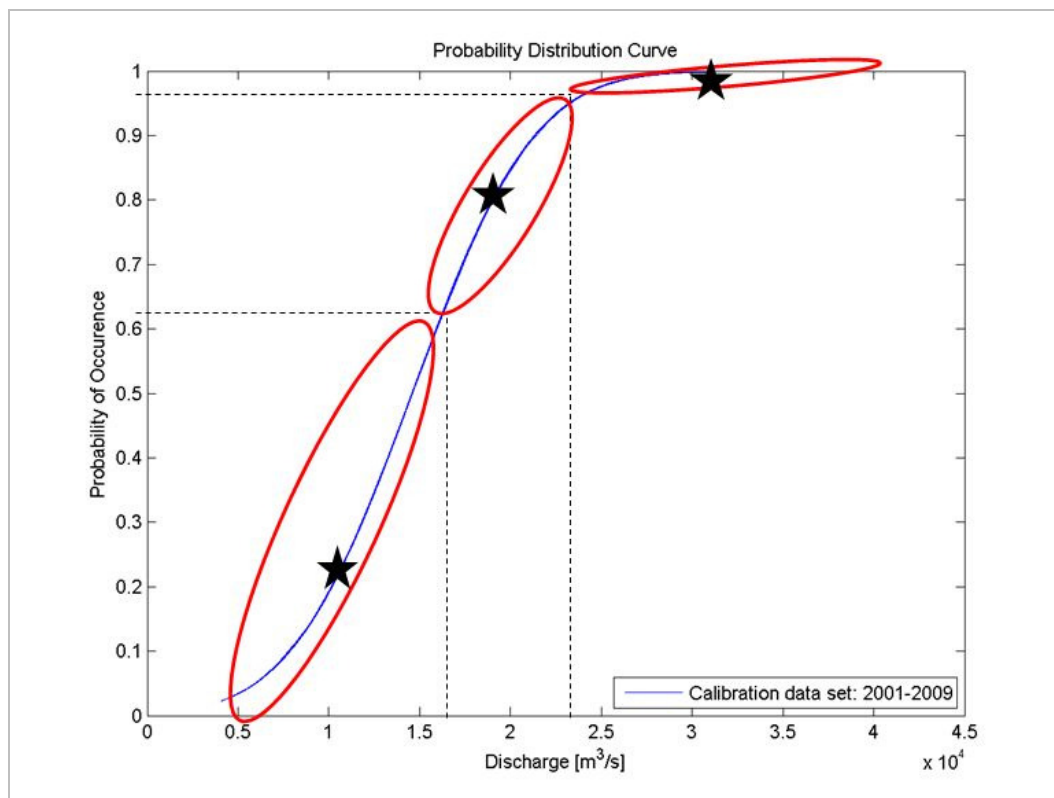


Figure 4.4: The distribution function of the discharge data

4.1.2 Downstream boundary condition

The downstream boundary condition of the model is based on the average stage level (+0.65 m NAVD88) from the East Jetty gage station (RK -30), at the mouth of the river. The tidal effect is schematized as a deviation which describes therefore the uncertainty of the tidal amplitude at the downstream boundary. The standard deviations for the three downstream boundary conditions are 0.28, 0.28 and 0.09 m for low, intermediate and high flow respectively. The regression analysis of the stage data set of 2001 to 2009 shows there is no correlation between the discharge and the stage, because of the tidal effect. Therefore a steady downstream condition is specified. The tidal amplitude is 1 ft (~30 cm), see Figure 4.5.

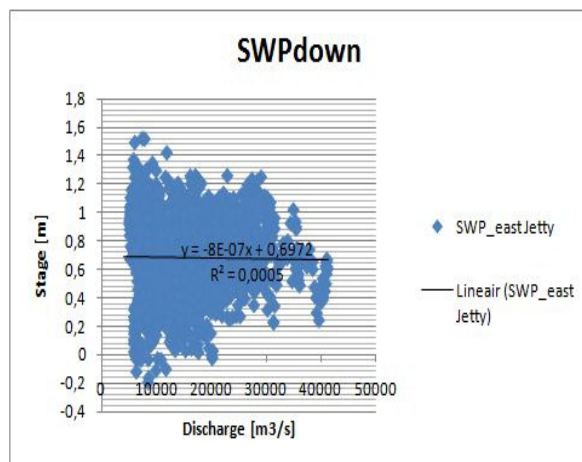


Figure 4.5: Observed stages plotted against discharge From East Jetty, Southwest Pass (RK -30) 2001-2009



Figure 4.6 East Jetty Gage station (RK -30) at Gulf of Mexico (photograph, Bos)

Facts: vertical datum correction: from NGVD29 to NAVD88 is +0.22 ft (0.0671 m), Set on Jan 16, 2008, all prior historic data are at NGVD29.

Highest level measured: +1.70 m NGVD29 on Oct 27, 1985

Lowest level measured: -0.49 m NGVD29 on Jan 25, 1940

4.1.3 Distribution of flow over the distributaries

The downstream boundary conditions of the distributaries, as shown in figure 4.7, are imposed with an extracted discharge instead of a water level. These conditions are obtained from the 1D (HEC-RAS³) Hydrodynamic model of Davis (2010). This model uses the discharge measurements of the survey done for the West Bay project in 2005 [Davis, 2010]. The model is calibrated and verified. Pereira *et al.* (2009) also uses this model for its model calibration [Pereira *et al.*, 2009; Pereira, 2010; Pereira, In Press]. Figures 4.7 and 4.8 represent the distribution to all the distributaries.

The distribution of flow varies continuously. For example the flow through Pass a Loutre changes significantly over the last 50 year from 30 to 12% of the flow at Talbert Landing. For Baptiste Collette and Grand Pass occurs the opposite, they increased from 4 to 10 percent in this period [Kemp, 2010].

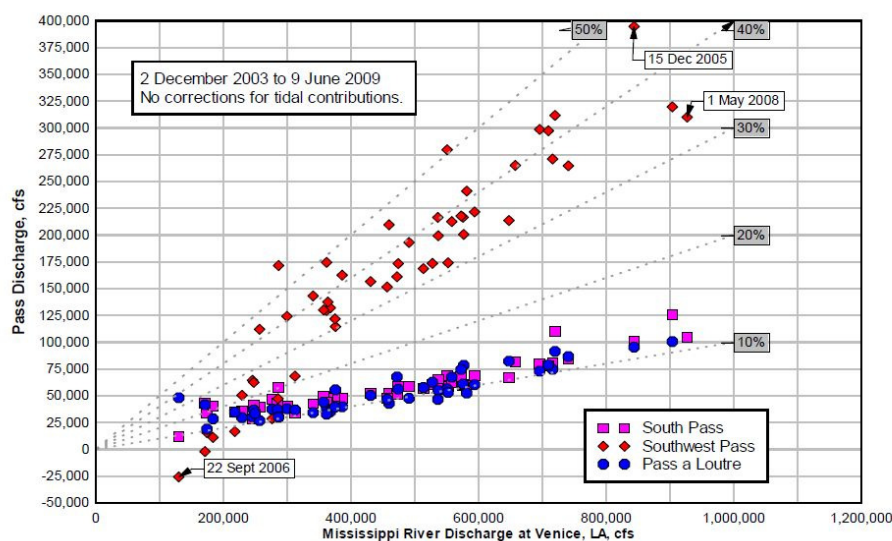


Figure 4.7: Discharge distribution in percentage of discharge at Venice [Davis, In Press]

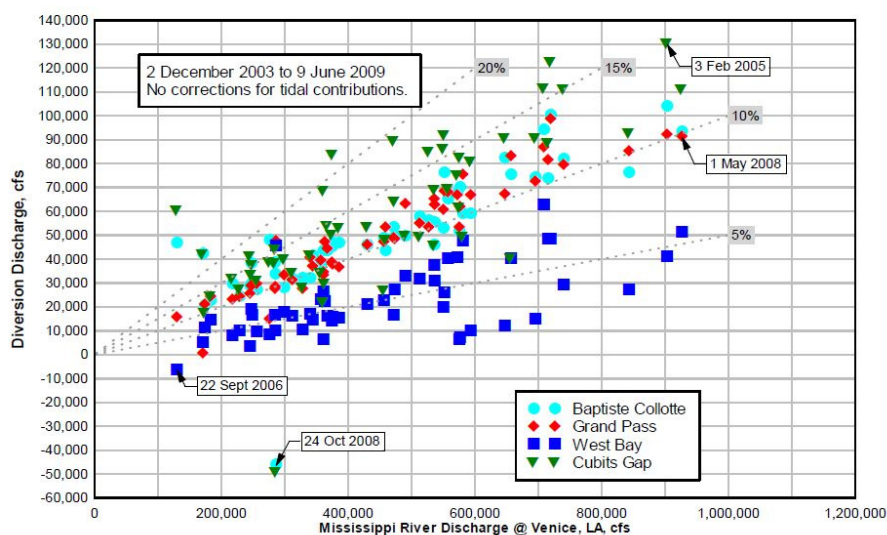


Figure 4.8: Discharge distribution in percentage of Venice [Davis, In Press]

³ HEC-RAS; 1D model software of the USACE

In table 4.1 the distribution over the distributaries is described. These values are used to define the subtraction of flow from the main stem for each distributary. This distribution is valid for all the boundary conditions. The distribution of percentages does not vary for different discharges.

Table 4.1: Flow distribution along the distributaries [Davis, In Press]

Percentages of Venice flow	
Baptiste Collette	15,44%
Grand Pass	10,98%
Main Pass	11,04%
Pass a Loutre	7,81%
South Pass	15,11%
Southwest Pass	34,52%
West Bay	5,10%
	100,00%
Fort St. Philip	1,06%

Bohemia Spillway

The rate of outflow over the Bohemia Spillway for discharges higher than 20,000 m³/s is also obtained from the 1D hydrodynamic model of Davis [Davis, In Press]. A polynomial regression is done on the available data set. The regression analysis provides an outflow rate of 4320 m³/s for the 33,000 m³/s discharge boundary.

4.2 Stage data

Every discharge results in a specific stage in the river. The stage is decreasing in the downstream direction to the mouth of the river. For this study three upstream discharge levels are specified. The next step is to specify the stage at a location for the three different discharges. The stages along the model reach are necessary to ensure a hydrodynamic calibration of the model. These stages can be obtained from the available data set. Four gage stations along the model reach are used: Point a la Hache is station 1 and also the upstream boundary of the model. Empire is station 2, Venice station 3 and Head of Passes station 4. Gage station 5 is only used to determine the downstream boundary of the model as described in the previous section and is excluded from the calibration.

Furthermore the downstream boundary does not vary for the different three discharge levels, specified as upstream boundary conditions. The locations of these stations are pointed in figure 4.9. The data set from Talbert Landing (RK 492), which is used to determine the three boundary conditions for discharge upstream is also used for the calibration of the computed water levels.



Figure 4.9: Model reach and gage stations pointed out, Modified [Google maps, 2011]

4.2.1 Data sets and vertical datum

Special attention needs to be paid to the different vertical datums. Two different vertical datums are used, NGVD29 and NAVD88. After hurricane Katrina most gage datums were set to NAVD88. The correction terms are necessary to convert from NGVD29 to NAVD88 and are different for every location. The correction factor is in some cases already prescribed, for other locations a tool can be used from the National Geodetic Survey (NGS) [NGS, 1999a, b].

In addition the bed level of the river is continuously changing, but this study only uses one reference bed level obtained from the bathymetry data of 2003 to 2004. This affects the sensitivity of the calibration. The used dataset for calibration will only refer to this bed level. This uncertainty needs to be taken in account.

The data set for calibration has been obtained from two websites with the same source [USACE, 2011a, b]. River gages started after Katrina and have the present data; The USACE also has the old database back to early 1900. All the obtained stage data are converted to NAVD88. An overview of the data is given in table 4.2 for each station. Due to Hurricane Katrina some stations were out of operations for some years, that is why no data is available for these periods.

Table 4.2: Gage station facts

Station	RK [km]	ID	Data set	Datum	Correction factor NGVD29 to NAVD88	Max. Stage NGVD29	Min. stage NGVD29	Operation [year]
Pt a la Hache	78	1400	01-05, 08 & 09	NAVD88 since Sept 24, 2006	-0.089 m *	15.25 ft 09/09/1965	-1.06 ft 01/24/1940	1938
Empire	48	1440	03,04,08 & 09	NAVD88 since July 7, 2007	-0.084 m *	10.92 ft 08/17/1969	-1.23 ft 01/19/1981	1960
Venice	17	1480	01-09	NGVD29	-0.1768 m (-58 ft) **	9.11 ft 08/17/1969	-0.77 ft 12/25/1989	1944
Head of Passes	-1	1545	01-04, 08 & 09	NAVD88 since April 17, 2008	+0.0427 m (+14 ft) **	12.03 ft 08/17/1969	-0.87 ft 12/25/1989	1875

* Correction factor based on converter [NGS, 1999b]

** Correction factor prescribed by USACE [River gages, 2010]

4.2.2 Observed stages

To determine an observed water level for the three discharge levels (10,000, 20,000 and 33,000 m³/s), the measured discharges at Talbert Landing (RK 492) from 2001 to 2009 are plotted against the observed stage data for the four different stations. The regression analysis yields the observed stage.

In figure 4.10 to 4.13 dotted lines are drawn at the three discharge levels (10,000, 20,000 and 33,000). The red boxes indicate a cloud with a bandwidth of 500 m³/s with stages for certain discharges. From that cloud a deviation is computed, which will represent the uncertainty due to the tidal amplitude and the uncertainty of the observed stage determined by the regression analysis for the given discharge, see figures 4.10 to 4.13. The uncertainties relate to bedforms and hysteresis.

The correlation between the discharge and the stage data will decrease further downstream because of the tidal influences and the presents of the distributaries. The station Point a la Hache has a good correlation, with $R^2=0.81$. Empire, Venice and Head of Passes have a correlation of resp. 0.63, 0.48 and 0.31. The influence of the tide is noticeable.

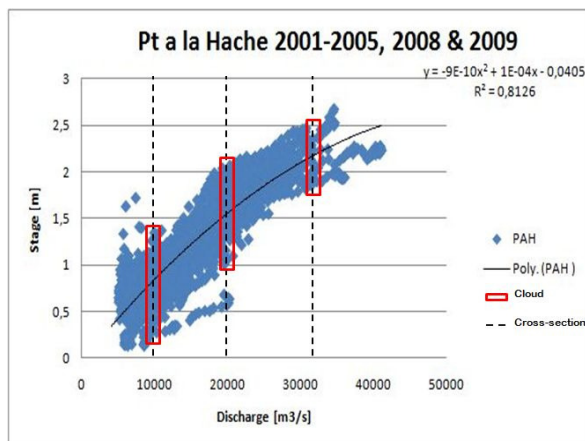


Figure 4.10: Discharge rating curve gage station Pt a la Hache

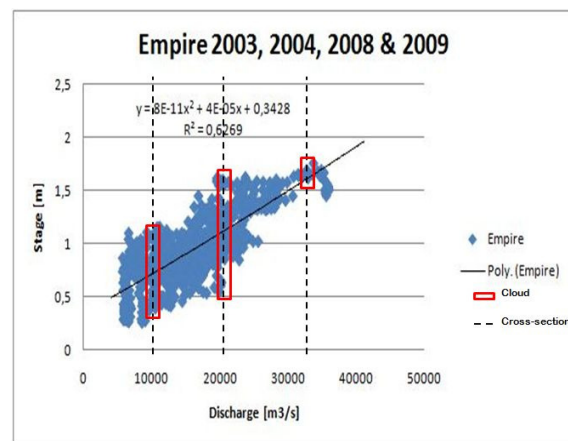


Figure 4.11: Discharge rating curve gage station Empire

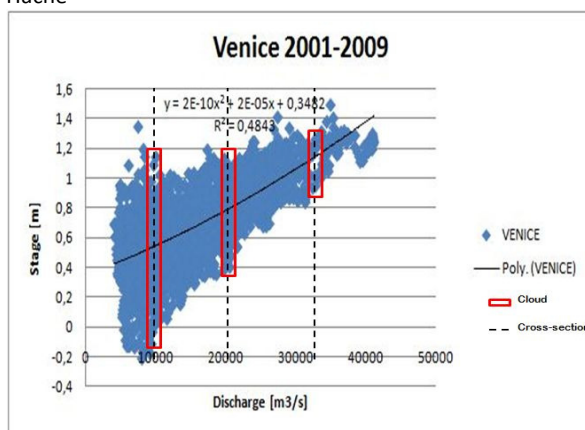


Figure 4.12: Discharge rating curve gage station Venice

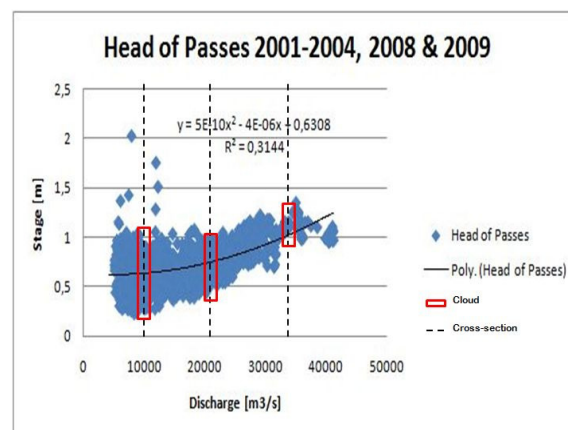


Figure 4.13: Discharge rating curve gage station Head of Passes

4.3 Method of calibration

The observed stages of the four stations are used for model calibration. The model needs approximately 24 hours to get rid of initial effects.

4.3.1 Changing the roughness parameter

The simulations for the three discharge levels only vary from one parameter i.e. the roughness parameter. By increasing or decreasing the roughness parameter the stage at the four stations can be tuned. Several simulations were done with a varying roughness parameter to see which simulation has the best fit with the observations.

A starting Manning value of $0.021 \text{ s/m}^{1/3}$ is used, based on the study of Pereira *et al.* 2009. High flow has larger discharge, which means higher velocities, a steeper surface slope, a higher water depth, and a higher sediment transport rate than low flow relatively. Consequently sediment transport creates bedforms at the river bed. These bedforms are more prominent at higher sediment transport rates, which results in a larger roughness and therefore a higher Manning value. This means high flow has higher Manning values than low flow. During low flow there is only a gentle surface slope and low flow velocities. The Manning value was adjusted in order to get as close to the observed stages. Decreasing the Manning value results in a lower stage and vice versa.

4.3.2 Results

The results of the calibration are shown in figure 4.14. During this calibration the river is divided into three sections, from RK 78 to RK 47, from RK 47 to RK 0 and from RK 0 to RK -30 respectively. All three sections have one Manning value which is kept the same for the three discharge levels. This is desirable for modeling purposes. The highest Manning value is used upstream and it decreases downstream from 0.018 to 0.016 to $0.014 \text{ s/m}^{1/3}$. The decreasing Manning values result from the changing bed material and river behavior e.g. the decreasing, D_{50} (see section 5.1) flow and sediment transport rate.

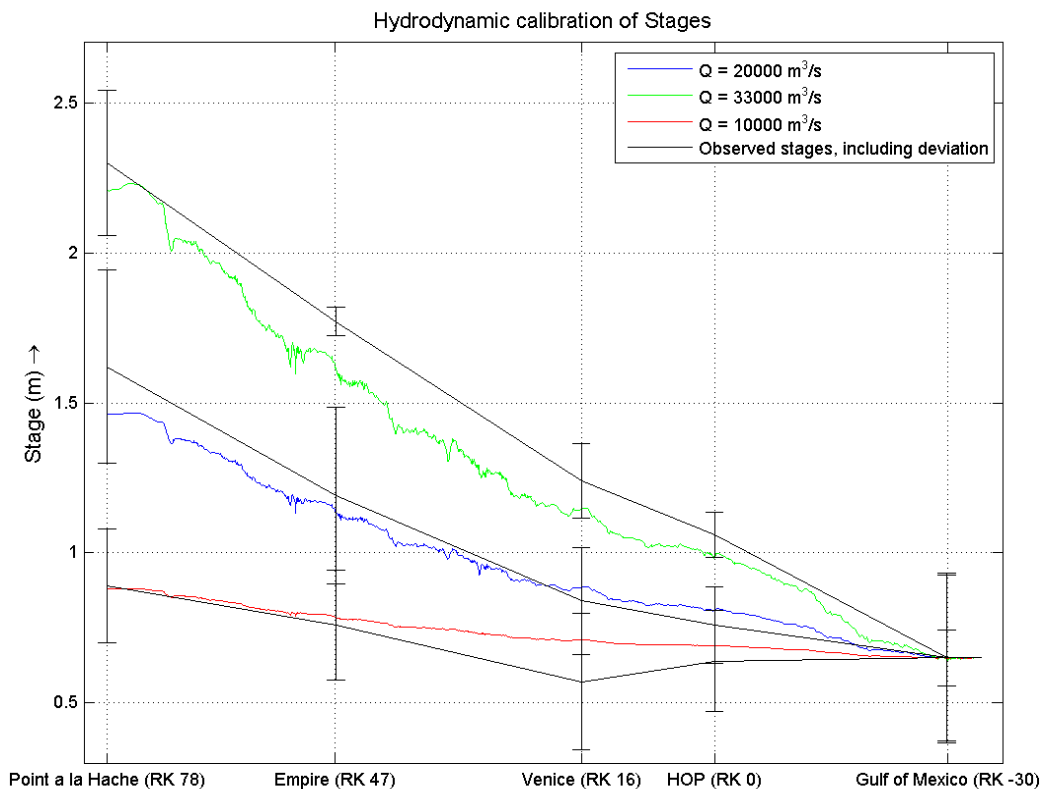


Figure 4.14: Simulated and observed stage of the model reach for three discharge levels

Venice gage station

Table 4.3 shows a large error ($\sim 25\%$) for the Venice station during low flow conditions. An analysis is done on the stage difference between Venice and Head of Passes at the same time over ten years, see 4.15. From this analysis it can be seen that during low flow (red dots) the measured stage at Venice is lower than at Head of Passes. This means a negative surface slope gradient. This effect is never observed in real life and there is also no real physical explanation for this observation. Therefore the Venice gage during low flow is probably not reliable [pers. comm. Georgiou, 2011].

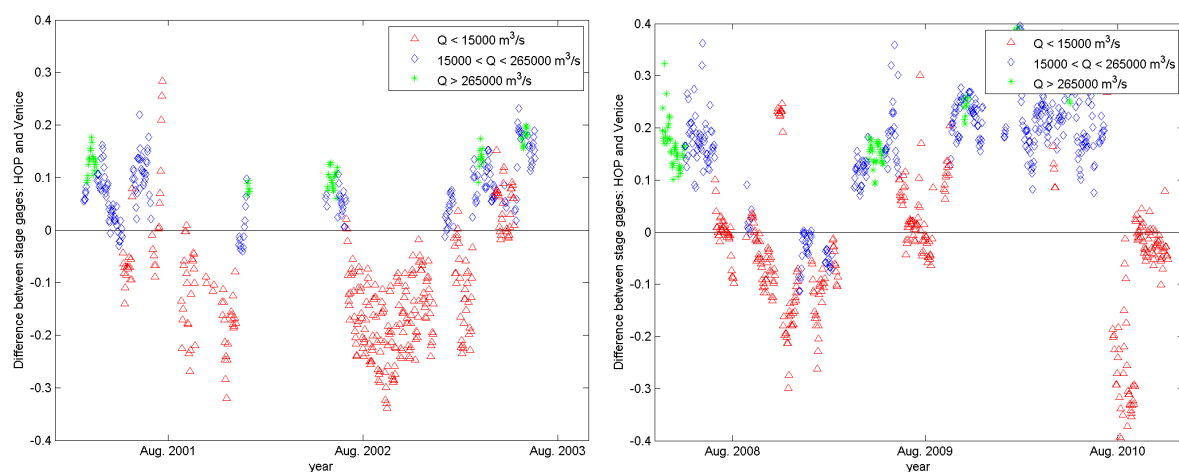


Figure 4.15: Difference between measured stages at Venice and Head of Passes form 2001-2010, for low, intermediate and high flow (red, blue and green).

4.3.3 Conclusions of hydrodynamic calibration

The observed stages with the deviations (black line) and the ideal simulated stages are plotted in figure 4.14. The figure gives a good overview of the model results. The high flow condition (in green) fits fairly well, only there are little data for the Empire gage, the model is slightly under predicting. The intermediate flow (in blue) is only slightly under predicting at the upstream boundary. The simulation of the low flow condition (in red) also gives a satisfactory result. The negative surface slope from Venice to Head of Passes (RK 16 to RK 0) for the observed stages can be seen, but this slope is not reproduced by the model. However the observations are probably not reliable. Therefore the model results are acceptable.

The downstream stage prediction gives a good estimation for the sake of dredging activities. The upstream error for the intermediate flow condition is not critical for navigation and is certainly within the limits. The low flow condition is most critical for the dredging activities.

The loss of energy head is really present in the stage simulation. As from the first bifurcation (RK 19) a change in the surface slope can be seen. This is also due to the bifurcations because the main stem of the river losses flow and therefore energy.

The surface slopes give representative values varying from 0.5 to 3×10^{-5} [Nitttrouer *et al.*, 2008]. The surface slopes could be adjusted by tuning the roughness parameter.

4.4 Method of verification

The discharge data set at Talbert Landing from 2010 are used for verification of the model.

4.4.1 Flow boundary conditions

New upstream boundary conditions for the model have to be determined. The discharge distribution of 2010 is plotted together with the distribution of the calibration data set (2001 to 2009) in figure 4.16. Again the discharge distribution is divided in three levels, high, intermediate and low flow respectively. The curve of the verification data set is slightly moved to the right. This implies that the upstream boundary conditions (discharge levels) for the intermediate and low flow will be higher (the red stars in the figure). The boundary condition for high flow will be lower since the maximum discharge in 2010 was 29,000 m³/s. The discharge levels for the verification data set are 13,500, 22,500 and 27,000 m³/s for low, intermediate and high flow respectively.

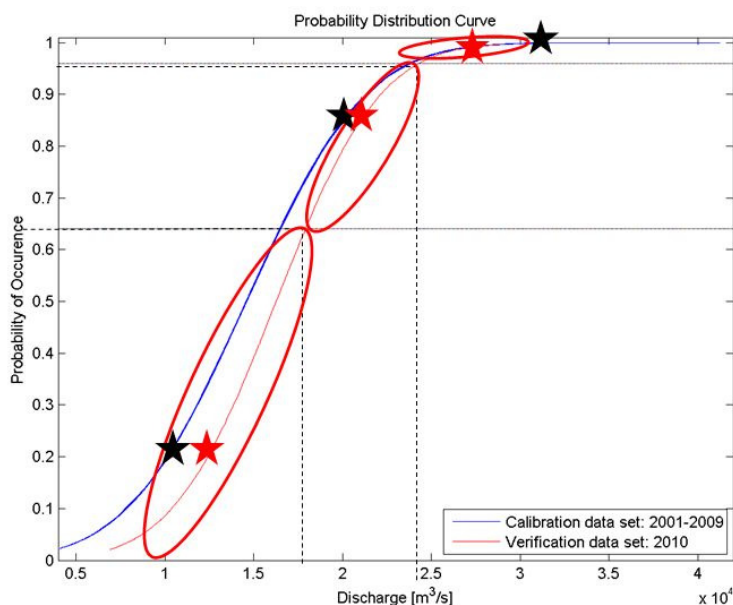


Figure 4.16: Discharge distribution of calibration and verification data set

4.4.2 Results

Simulations were done with these three discharge levels to see how the model responds. The model behavior is checked the same way as during the calibration; i.e. with the stages along the river at four gages. The roughness parameters in the model are kept the same as defined after the final calibration. The stages from 2010 are plotted in relation to the discharge data set of 2010 for the four gages, see figure 4.17. Q-h lines were formulated to describe the relation between the discharge and the stage. This is done for the Point a la Hache, Empire, Venice and Head of Passes gage. The closer the gage is to the Gulf of Mexico the gentler the slope of the Q-h relation is, because of the release of flow through the distributaries and the backwater effect. The Q-h lines in figure 4.17 are formulated as follows:

$$h = \left(\frac{Q}{6000} \right)^a - b \quad (4.2)$$

in which h is the stage, Q is the discharge, a and b are coefficients. For higher value of a the slope of the relation is steeper; the highest value is used for the gage most upstream. The value a decreases for downstream gages, see table 4.4.

Table 4.3: Coefficient for Q-h lines for verification

Gage	a	b
Point a la Hache	0.55	0.47
Empire	0.40	0.50
Venice	0.28	0.54
Head of Passes	0.20	0.60

The bold colored markers in figure 4.17 are the model results for the three discharge levels at the four gages. It can be seen that the model results fit well to the Q-h lines. Only the model is over predicting for the Head of Passes gage.

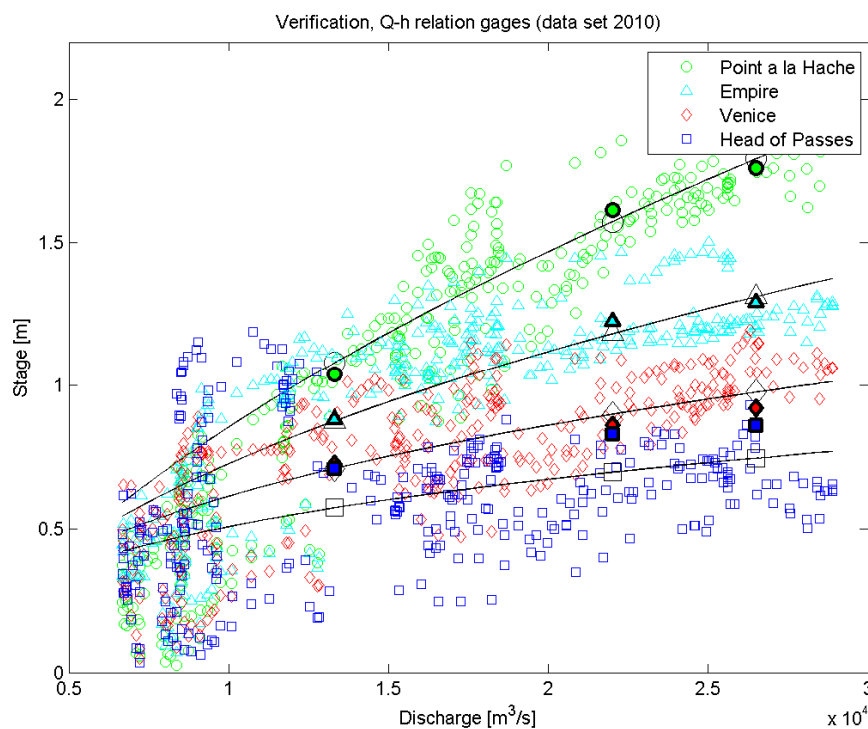


Figure 4.17: Verification of the model

4.5 Conclusions of Hydrodynamic Calibration & Verification

The verification of the model indicates that the hydrodynamic behavior in the model is representative. During verification the downstream boundary condition is kept the same as during calibration at 0.65 m, while the average stage by analyzing the 2010 field at the downstream boundary is -0.17 m. The difference is 0.82 m. The simulated stage at the downstream boundary is kept too high. This explains why the model is over predicting at Head of Passes. Defining a lower downstream boundary would result in lower stages in the model.

Chapter 5. Morphological calibration

5.1 Bed material of the river

The sediment transport in the Mississippi River consists of three sediment fractions: sand, clay and silt respectively, which all have a contributing effect to the sediment transport behavior. The three fractions combined have one median particle grain size (D_{50}), which in general varies over the river bed. The natural behavior of rivers is to sort its sediments, downstream the sediments are often much finer than upstream. The median grain size decreases from Talbert Landing to Head of Passes. In general this decreasing effect coincides with the decreasing bed slope of the river, from upstream to downstream. The bed material of the river consists downstream mainly of fine sand and only little coarse gravel [Parker, 2004; Mossa, 1996].

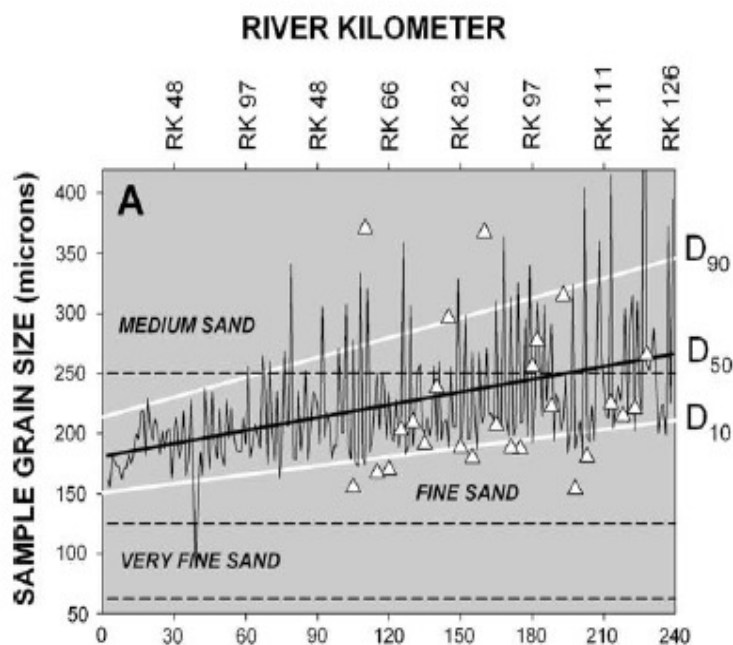


Figure 5.1: Bed material grain size in the Lower Mississippi River from Head of Passes until RK 126, 2003 data (low discharge as a line plot) and 2008 (high discharge as triangles), upper axis is River Kilometer, lower axis is sample number [Allison *et al.*, 2010]

From the data analysis of D_{50} (figure 5.1) it can be seen there are only small differences between the upstream and downstream boundary of the reach from RK 126 to RK 0. From measurement D_{50} is known to be 265 μm at RK 126 near New Orleans (English Turn) and 180 μm at RK 0 at Head of passes. The dataset from figure 5.1 contains 240 samples. The data were collected in 2003 and 2008 by Nittrouer and Allison [Nittrouer *et al.*, 2008].

The model reach of this study starts from RK 78 at Point a la Hache and because there is only a small variation between RK 126 and RK 0 an average D_{50} is chosen to represent the bed material of the model. A D_{50} of 200 μm is defined as upstream model boundary. The D_{50} in suspension is approximately 125 μm [Meselhe *et al.*, 2010]. The wide scatter of the data shown in figure 5.1 also shows the bandwidth of the sediment samples, i.e. there is not only one D_{50} which represents the

bed material of the study area. The morphological calibration will determine the final grain size of the bed material which can be used in the model.

5.2 Sediment transport Boundary conditions

5.2.1 Suspended sediment transport

The suspended sediment load and concentration data have been measured at Talbert Landing and St. Francisville, see figure 5.2 for the locations. Permanent, long-term, suspended sediment sampling stations do not exist below St. Francisville. Some suspended sediment load is measured further downstream at e.g. Belle Chase (RK 122) and Empire (RK 47) during events like the flood of 2008 [Allison *et al.*, 2010].

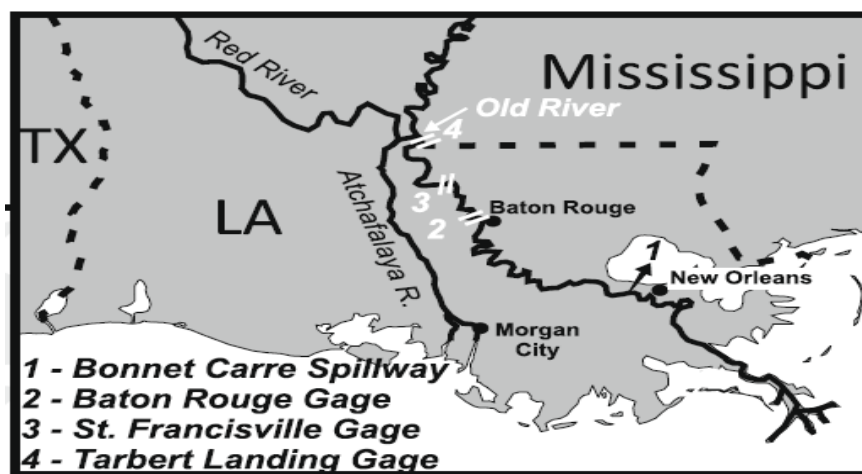


Figure 5.2: Lower Mississippi [Allison & Meselhe, 2010]

Figure 5.3 and 5.4 show the measured suspended sediment load and concentration between 1987 and 2010 at Talbert Landing by USGS. From these data sets the suspended sediment load and concentration can be obtained for the three discharge upstream boundary conditions, which were set in Chapter 4. An overview of the obtained sediment loads and concentrations is given in table 5.1. The annual suspended sediment load is estimated to be 91×10^6 ton/year [Allison *et al.*, 2010].

The suspended sediment load in the Mississippi River is not fully dependent on the flow discharge. The sediment load varies substantially for certain discharges, which include an uncertainty for model schematization when one sediment load value is picked for one flow discharge. From the poly-fitted curves in figure 5.3 and 5.4 it can be seen that the relation between the flow discharge and the sediment load as well as the concentration is non-linear.

Sediment distribution

The total suspended sediment load and concentration consists of three different kinds of sediment: sand, silt and clay respectively. Sand and silt are non-cohesive and clay is cohesive. For modeling purposes silt and clay are considered cohesive, because the silt particles interact with the clay particles. This phenomenon is called flocculation. Another classification states that sand is coarse sediment, silt and clay are fine sediments. The river transports far more fine sediments, only 23% of

the total annual suspended transport is suspended sand, which implies the average suspended transport of fines is 77%. The suspended sand transport is only ~4% for low discharges and ~40% for high discharges. [Barbé *et al.* 2000; Ashurst, 2007; Nittrouer *et al.*, 2008; Allison *et al.*, 2010]. This relation is also shown in figure 5.5.

The cohesive fine sediments together are also called ‘mud’. The substantial amount of mud clarifies why the Mississippi River is known as ‘Big Muddy’. The clay/ silt distribution is, ~65% and ~35% respectively [Galler and Allison, 2008].

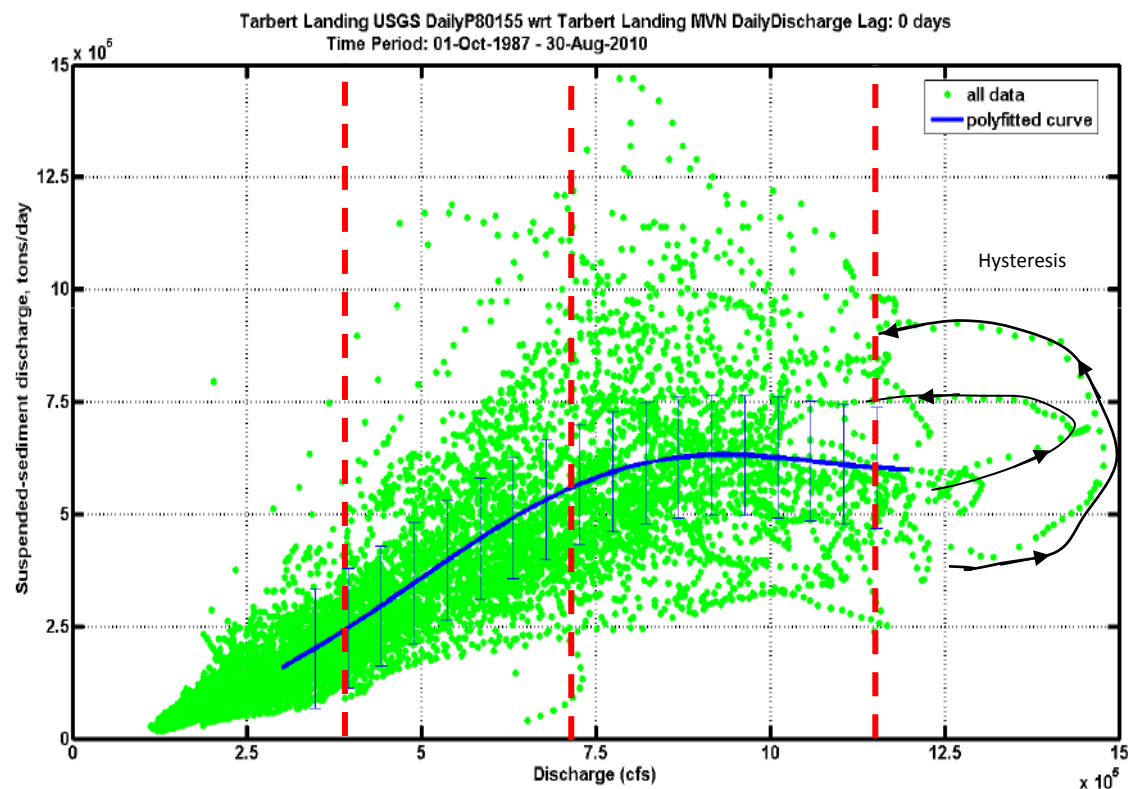


Figure 5.3: Suspended sediment discharge measured at Talbert Landing, 1987-2010 [Karadogan, 2010]

Hysteresis

In figure 5.3 the phenomenon of hysteresis can be observed. Ideally a given discharge is related to a certain sediment discharge (with a certain deviation), according to the discharge- sediment discharge relation (Q/Q_s - relation), see also section 5.5. In figure 5.3 this relation, with its deviation is presented as the poly-fitted curve. Hysteresis in figure 5.3 occurred during the high discharges (see two half circles). The sediment discharge is “lagging behind”. The sediment discharge rises quickly at a relatively small increasing discharge. After a while the sediment discharge is constant for decreasing discharges. In the end the sediment discharge drops again. Hysteresis makes it difficult to predict the sediment discharge in the river.

The reason is that suspended sediment concentration is coupled to the supply from upstream. At the start of the flood season usually sediment-enriched conditions occur (a lot of fines are on the bed in the upstream reaches). After they are flushed in the start of the flood, the

concentration drops again. Another cause is the hysteresis of flood levels/ gradient. During rise the flood, gradients (and flow velocities) are different than at fall of the flood.

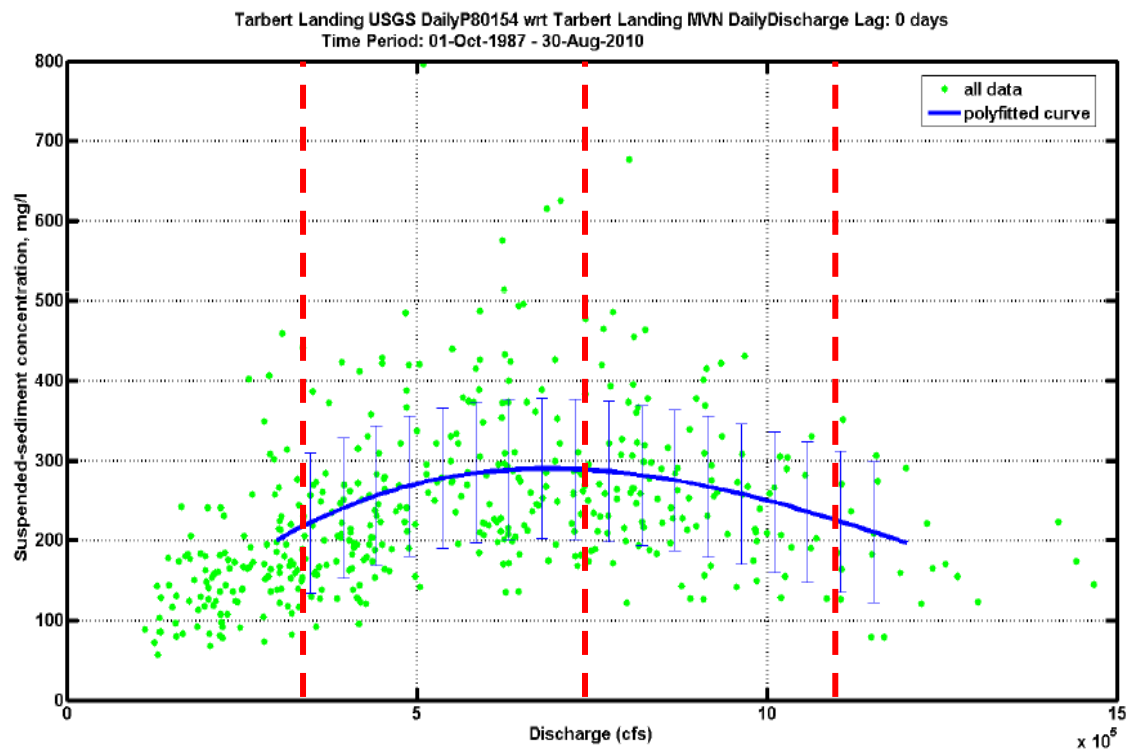


Figure 5.4: Suspended sediment concentration measured at Talbert Landing, 1987-2010 [Karadogan, 2010]

5.2.2 Boundary conditions

The dotted lines at the flow boundary conditions in figure 5.3 and 5.4 indicate how the values in table 5.1 have been obtained; the conversion from English to Metric system is done. For higher discharge more sand is in suspension. Higher discharges result in more uplift force, therefore more sand comes in suspension. Figure 5.5 shows a rough representation of the process described; i.e. the relation between discharge and percentage of sand in the suspended sediment transport for the Mississippi River. During low flow especially clay is in suspension, because silt and sand are heavier, most of these particles are only transported during higher flows.

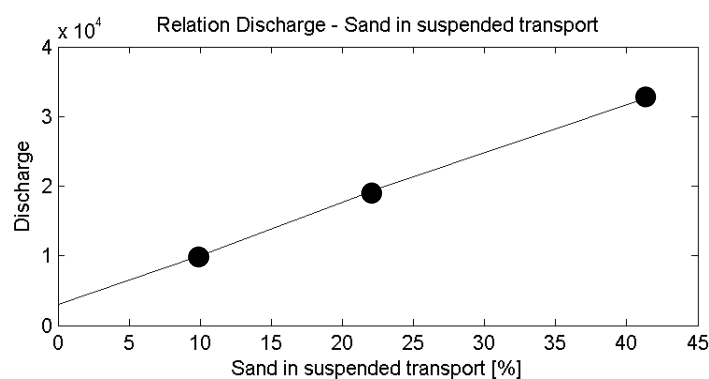


Figure 5.5: Relation between discharge and sand in suspended transport [Barbé *et al.*, 2000; Nittrouer *et al.*, 2008 and Allison *et al.*, 2010]

Table 5.1: Obtained sediment discharges and concentrations for flow boundary conditions

Discharge [m ³ /s]	Discharge x 10 ⁵ [ft/s]	Sed. discharge Qs total x 10 ⁵ [ton/day]	Sed. discharge Qs sand x 10 ⁵ [ton/day]		Total concentration [mg/l]	Clay [mg/l]	Silt [mg/l]	Sand [mg/l]
10000	3.6	2.09	0.05		210	178.5	31.5	5.25
20000	7.2	5.39	1.3		290	133	87	70
33000	11.8	5.96	2.5		210	80	44	86

5.2.3 Bed-load transport

There are not many data available on the annual bed level behavior and bed-load transport in the Lower Mississippi River. The best study so far is done by Nittrouer *et al.* (2008). This study presents the annual bed level changes, bed-load transport and bed form behavior in the river from New Orleans to Venice at three different locations.

Bed level change rates needs to be measured in order to define an annual bed level change. Nittrouer *et al.* (2008) did this at e.g. New Orleans (Audubon Park RK 162-167). The bed level change rates vary from $1.15 \times 10^{-5} \text{ m}^2/\text{s}, \text{m}$ to a maximum of $5.4 \times 10^{-4} \text{ m}^2/\text{s}, \text{m}$ per unit width and at Venice (RK 16) they vary from $0.88 - 3.4 \times 10^{-5} \text{ m}^2/\text{s}, \text{m}$ per unit width for low flow (6,120 m³/s) and high flow (34,300 m³/s) flow conditions respectively [Nittrouer *et al.*, 2008].

The annual cross-sectional averaged bed level changes at New Orleans and Venice are 0.45-21 m/year and 0.35 -1.34 m/year respectively. To refer this rate to the Waal River in the Netherlands, the rate is about 20-700 times higher, since the rate of the Waal is 2 to 3 cm/year [pers. comm. Sloff, 2010].

5.2.4 Boundary conditions

Based on the study of Nittrouer *et al.* (2008) an upstream boundary condition can be defined for the model. The boundary condition of the bedform transport rate is $1.26 \times 10^{-5} \text{ m}^3/\text{s}, \text{m}$ per unit width (0.5 m/year and is cross-sectional averaged).

The average annual bed-load transport is $2.2 \times 10^6 \text{ ton/year}$, which approximately 2.5% of the estimated suspended sediment transport of $91 \times 10^6 \text{ ton/year}$ [Allison *et al.*, 2010].

5.3 Transport formulas

The bed shear stress (τ_{flow}) is the force on the bed due to the flow and is dependent on the flow velocity (u) and the defined bed roughness parameter (from hydrodynamic calibration) according to:

$$\tau_{\text{flow}} = \frac{\rho_l g u^2}{C^2} \quad (5.1)$$

in which ρ_l is the density of the water, g is the gravitational acceleration constant, u is the depth-averaged flow velocity and C is the Chézy roughness parameter.

The critical bed shear stress (τ_{cr}) for sand (100-200 μm) is $\sim 0.15 \text{ N/m}^2$ [Van Rijn, 1993]. The critical Shield parameter (θ_{cr}) describes whether a sand particle (D_{50}) is in motion or not. The formula reads:

$$\tau_{cr} = \rho_l g D_{50} \theta_{cr}, \quad \theta_{cr} = \frac{0.14}{D_*^{0.64}} \quad (5 < D_* < 10), \quad D_* = D_{50} \left(\frac{\Delta g}{\nu^2} \right)^{1/3} \quad (5.2)$$

in which D_* is the dimensionless particle diameter, Δ is the relative density and ν is the viscosity.

5.3.1 Sand transport formula

The sediment transport in this study area consists mainly of suspended sediment transport (S_s) and only for 2.5 % of bed-load transport (S_b), because the river transports fine sediments. In order to represent the suspended sediment in the model, it is important to select a transport formula that is able to calculate the suspended sediment transport very reasonably and takes the fine sediments in account. A different formula is necessary to calculate the very fine sediments (mud).

The Meyer-Peter & Müller transport formula (1948) is an empirical formula and only relates to bed-load transport. The formula is most suitable for coarse sediment transport, therefore the formula has no preference. The Engelund & Hansen transport formula (1967) can be used to calculate the total fine sand transport. Suspended load is included, but without accounting for the advection- diffusion processes (this is a total-load formula). Therefore also unlikely to select for this study. Because of its simplicity it can be used to find orders of magnitude for analytical calculations. The Van Rijn transport formula (2007a,b) takes bed-load and suspended load in account. In addition the formula is also suitable for the fine sand particles, which means by choosing this formula 23% of the total sediment transport can be calculated.

The total sand transport (S) is the sum of suspended- (S_s) and bed-load transport (S_b). The Van Rijn (2007a,b) sediment transport formula is selected for this study and reads:

$$\begin{aligned} S_b &= \alpha_b \cdot 0.1 \sqrt{\Delta g D_{50}} D_*^{-0.3} T^{1.5} \\ S_s &= \alpha_s \cdot f_{cs} u h C_a \\ S &= S_b + S_s \end{aligned} \quad (5.3)$$

in which D_* is the dimensionless particle diameter, T is the dimensionless transport stage parameter, f_{cs} is a shape factor, u is the depth-averaged velocity, h is the water depth and C_a is the near bed concentration. Besides the physical parameters, α_b and α_s are both calibration parameters, ranging from 0 to 1.5, which will be defined during the calibration, see section 5.6.2. The bed shear stresses are taken into account by the transport stage parameter (T) and the shape factor (f_{cs}).

5.3.2 Mud transport formula

For the cohesive mud and the silt fractions a different formulation is needed. Delft3D uses the transport formulation by Partheniades-Krone (1965), (eq. 5.4 and 5.5). For engineering practice silt is assumed that it behaves as cohesive sediment, because it interacts with the clay particles. This way the silt behavior can also be simulated. Basically it describes how when a fine sediment particle is depositing on the river bed or eroding from the river bed. A critical bed shear stress needs to be defined in order to calculate whether a particle will deposit ($\tau_{cr,d}$) or erode ($\tau_{cr,e}$). The force (τ_{flow}), the bed shear stress due to flow, on the sediment particle is the same as for the sand particles.

The critical erosion shear stress ($\tau_{cr,e}$) for mud varies between 0.1-0.5 N/m² [Van Ledden, 2003]. The critical deposition shear stress ($\tau_{cr,d}$) for mud varies between 0.05 and 0.15 N/m² [Winterwerp, 1989; Van Rijn 1993]. It is assumed that the same value can be used for silt and clay. The morphological model calibration will define the most ideal value for both critical shear stresses. The affect of $\tau_{cr,d}$ has been looked at in section 5.5.4, where $\tau_{cr,d}$ has been chosen as 1000. This way the Sink process is only dependent of the fall velocity and the near-bed concentration. The transport formulation by Partheniades-Krone (1965) for source and sink reads:

$$Source = M \left(S \left[\frac{\tau_{cw}}{\tau_{cr,e}} - 1 \right] \right) \quad (5.4)$$

$$Sink = w_m C \left(S \left[1 - \frac{\tau_{cw}}{\tau_{cr,d}} \right] \right) \quad (5.5)$$

in which M is the erosion parameter, S is the erosion and deposition step function, w_m is the fall velocity of the sediment particle and C is the concentration of sediment in the water column.

It is assumed that the Erosion parameter (M) for cohesive sediment is equal to the Erosion parameter for non-cohesive sediment [Van Ledden, 2003]. The Erosion parameter (M) for mud: $M=10^{-3} - 10^{-5} \text{ kg/m}^2/\text{s}$ [Winterwerp, 1989].

The fall velocity (w_m) of the sediment particle is dependent on their grain size. The bigger the grain size the faster will a particle sink to the bed of the river. The following fall velocities are determined for sand, silt and clay, resp. 1 cm/s, 0.1 cm/s and 0.01 cm/s [Parker, 2004].

Deposition & Erosion patterns

According to the suspended sediment concentrations measured in the river during different flow discharges the following can be said; the reach from St Francisville to Head of Passes acts as a sedimentation/ settling zone during low or moderate flow and a resuspension/ erosion zone during high flow. The turning point is around 17,000 m³/s, see figure 5.6 [Mossa, 1996].

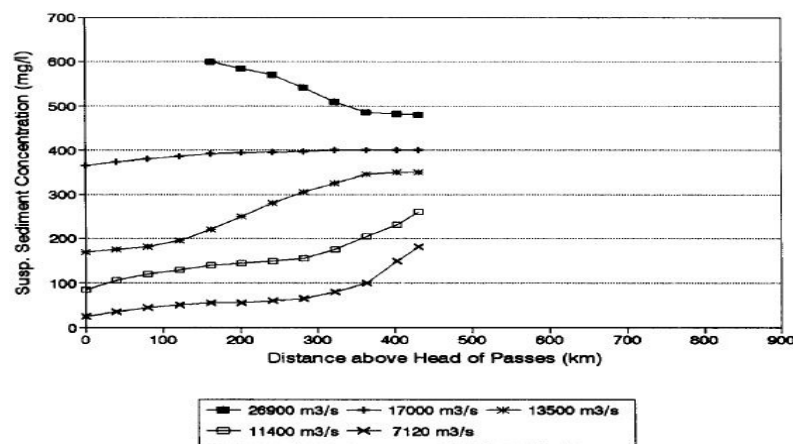


Figure 5.6: Pattern of suspended sediment concentration from St Francisville to Head of Passes [Mossa, 1996]

Figure 5.6 shows the suspended sediment concentration especially drops in the most downstream reach. This effect partly explains the net accretion of the bed level during low flow. Besides that, the river turns shallower downstream near the mouth of the river. In water depths of less than 20 m, from Venice further downstream, mud deposition starts during low flow as a result of a decreasing bed friction, and further reduction of the flow velocities, salt wedge and flow reversals due to the tide [Allison *et al.*, 2010]. The mud deposition really starts during the low flow season (autumn). The mud deposits atop of the sandy bedforms and can remain at the bed for several months. During the winter the mud layer first needs to be flushed away before the bed can erode again, this takes a considerable time [Nittrouer *et al.*, 2008; Galler and Allison, 2008; Allison *et al.*, 2010]. Unfortunately in the model these effect are not taken into account, because of the assumptions that has been made and the model schematization.

5.4 Morphological schematization

In Chapter 4 an analysis is done to schematize the discharge regime of the Lower Mississippi. This schematization determines three discharges levels with certain duration of days. The three levels together with their duration represent a hydrodynamic flow year.

The relationship between sediment transport (Q_s) and discharge (Q) is non-linear. The degree of non-linearity in the Mississippi river is in the order of 1 to 1.3. The formula gives an understanding of the relation between sediment transport and discharge:

$$Q_s = B^{1-n/3} m Q^{n/3} C^{2n/3} i^{n/3} \quad (5.7)$$

in which Q_s is the sediment transport, B is the width of the channel, m is the transport parameter, Q is the discharge, C is the Chézy roughness parameter and i is the slope and n is the degree of non-linearity.

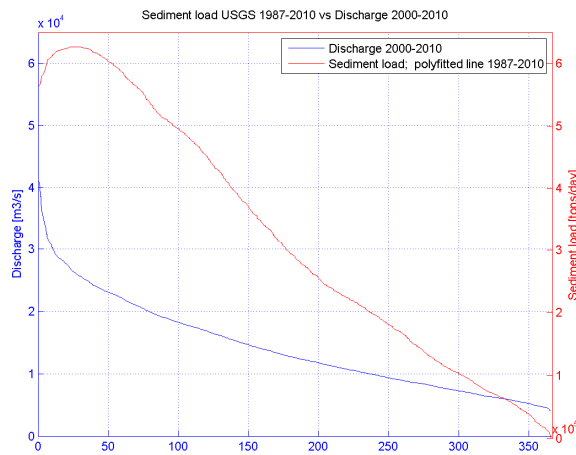


Figure 5.7: Frequency curve (in days) of discharge and sediment load from data set

In Figure 5.7 the discharge and sediment load (poly-fitted line from figure 5.3) are shown. From this plot it can be seen that the relation between the discharge and sediment load is non-linear. For higher discharges the sediment load is much higher than for low discharges. Besides that, also explained in section 5.2.1, the sediment transport rate reaches its maximum at $\sim 27000 \text{ m}^3/\text{s}$ according to the hydrodynamic schematization. This non-linear relation is translated to the schematization of the morphological year. A modification of the flow duration per discharge level is done in order to scale the sediment transport.

The hydrodynamic year is represented as 235, 115 and 15 days for the low, intermediate and high discharge level respectively. The morphological year after scaling is determined as 176, 175 and 15 days for low, intermediate and peak discharge respectively. Much more weight is given to the intermediate discharge period in order to represent a correct yearly sediment transport.

5.5 Method of calibration

The morphological performance of the model can be calibrated according to representative 1D and 2D river behavior. The 1D calibration addresses: the annual suspended and bed-load transport rates, celerity of bed disturbance, and the annual bed level change. First the calibration of the sediment transport rates is done, in order to calibrate the width-averaged annual bed level change. The 2D calibration focuses on the transverse bed-slopes. In addition to the parameters used for 1D- and 2D calibration a calibration is done on the dredging quantities, by adjusting the parameters for several simulations.

Setting and requirements

CFL-condition: The model simulations in Delft3D also have to meet the Courant condition (CFL) for Morphology according to the following relation.

$$CFL = MorFac \frac{\Delta t}{\Delta x, \Delta y} c_b \leq 0.9 \quad (5.8)$$

in which Δt and Δx are described in Chapter 3 and c_b is the celerity of bed disturbances. MorFac is a user defined morphological acceleration factor [Deltares, 2010].

Morphological acceleration factor (MorFAC): The MorFAC is a factor that simply multiplies the erosion and deposition in one computational time step. This means by using for example a factor 50, one hydrodynamic flow day will result in 50 days of morphodynamics. Therefore it is possible to simulate long-term morphological processes for more than decades. A small MorFAC is often used for high discharges, and a large MorFAC is used for low discharges, because of restrictions for numerical stability (expressed by the CFL-condition). Using a MorFac results in a significant reduction of the computation time of a simulation [Deltares, 2010]. Table 5.1 gives an overview of the MorFACs which are used for the model.

Table 5.2: Model MorFACs

Discharge level	MorFAC
10000 m ³ /s	634.5
20000 m ³ /s	400
33000 m ³ /s	90

5.5.1 1D Calibration

Annual transport rates

As described in section 5.3 the model uses the Van Rijn transport formula (2007a,b) to calculate the sand transport in the model. To match the observed sand transport the formula has two important calibration parameters, which need to be defined, α_s and α_b , respectively. When using $\alpha_s = 1$ and $\alpha_b = 1$ the original formula of Van Rijn (2007a,b) is used. Coefficient α_s and α_b can be used as multiplication factor for suspended- and bed-load respectively.

Besides that the grain size diameter of the bed and the sediment in suspension can be tuned. A good definition of these parameters will give the correct yearly sand transport. The calibration of the 'mud' transport can be done by tuning the critical bed shear stresses, the erosion parameter and the fall velocities. The definition of all the calibration parameters is an iterative process. A summary of the calibration parameters is given in table 5.3 and 5.4.

Offline calculations of the sand transport give a first estimate of the calibration parameter α_s and α_b for all three discharge levels; the first estimate of the calibration parameters are for $\alpha_s = [0.33; 0.3; 0.145]$ and $\alpha_b = [0.175; 0.45; 0.29]$ for low, intermediate and high discharge respectively.

Model runs were done with adjusting the calibration parameter in order to optimize the sand transport in the model. The parameters in Delft3D slightly differ from the offline defined parameters. This can be expected due to model behavior and uncertainties. The Delft3D calibration parameter are defined as $\alpha_s = [0.33; 0.3; 0.1]$ and $\alpha_b = [0.42; 1.0; 0.29]$, for low, intermediate and high discharge respectively. These parameters are redefined after the annual bed level change calibration and 2D calibration.

Celerity of bed disturbance

The celerity of bed disturbances (c_b) gives an indication of the wave speed of small disturbances [De Vries, 1965]. The formula of the celerity of bed disturbances reads:

$$c_b = \frac{nS}{h(1 - Fr^2)}, \quad Fr = \frac{u}{\sqrt{gh}} \quad (5.9)$$

in which n is the degree of non-linearity (as in eq. 5.7), S is the sediment transport per unit width, h is the water depth, Fr is the Froude number, u is the flow velocity and g the gravitational acceleration constant.

Annual bed level change

The bed topography of 2010 of the dredging reach from Venice to Gulf of Mexico is known and can be used for the annual bed level change calibration. Figure 5.8 shows that at many locations the bed level of the reach is increased by 5 m. This is even including the dredging activities of 10 to 15 million m^3 a year. Given this fact, the annual bed level change is estimated at approximately 1 m/year.

Simulations were done with a varying bed-load calibration parameter (α_b) of 1.0 and 1.5 for all discharge levels. The suspended transport calibration parameter is kept constant during these simulations at $\alpha_s = 0.3$ for all discharge levels. Only bed level data of the navigation channel is available, the areas outside the navigation channel are excluded from surveys. The green strokes along the navigation channel in figure 5.8 indicate the missing data. No recent bed level data is available.

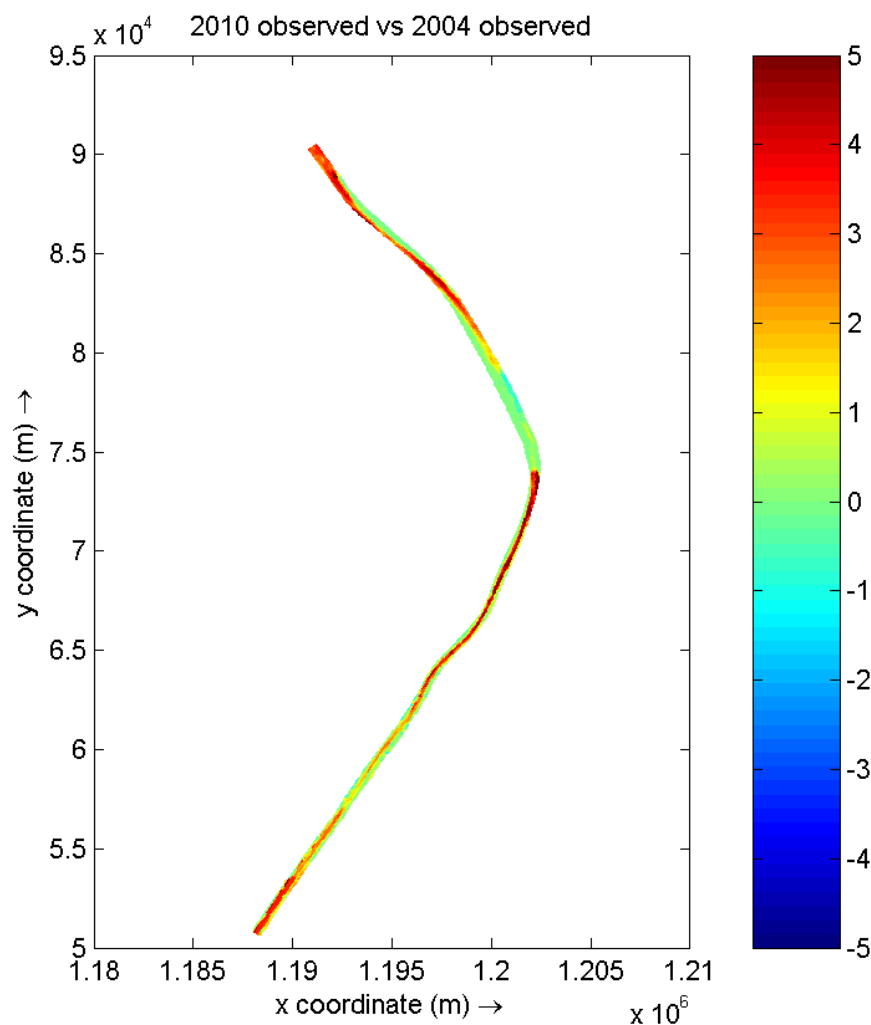


Figure 5.8: Observed increased bed level from 2004 to 2010, from Venice (RK 16) down to the Gulf of Mexico (RK -30). Main stem of the Mississippi River.

The results of the simulated bed topography after eight years can be seen in figure 5.9. From these simulations it becomes clear using $\alpha_b = 1.5$ results in more sedimentation between RK 0 and -30, as shown in figure 5.8 between 2004 and 2010. Therefore $\alpha_b = 1.5$ is chosen as the final calibrated value. The higher value of the bed-load transport parameter is necessary to assure enough accretion

of the bed in the dredging reach. A_{shields} is the 2D calibration parameter, which is treated in the next section. An explanation of the black circle is given below and is shown in figure 5.10.

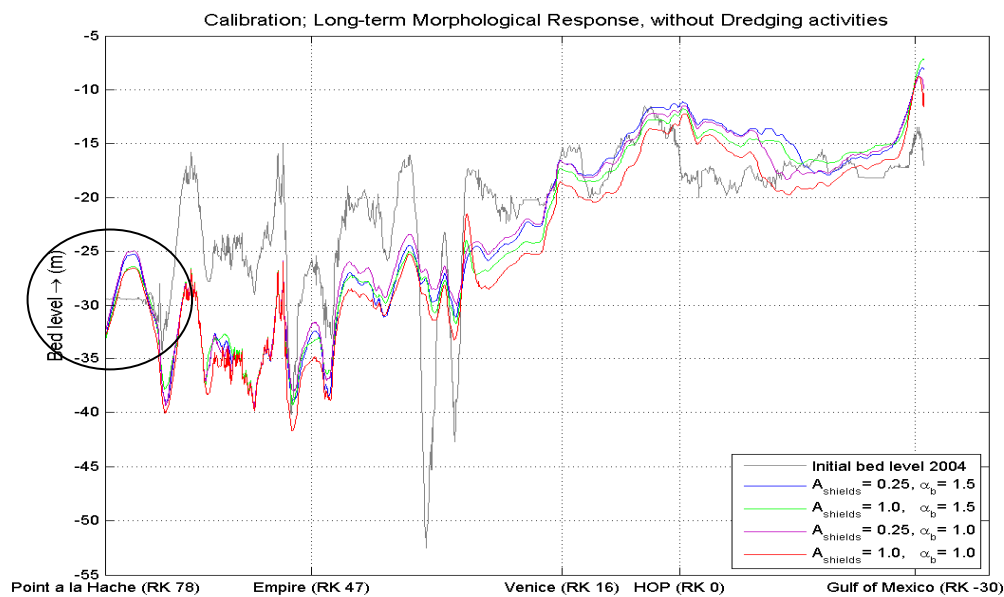


Figure 5.9: Simulation with different calibration parameters, maximum bed level change (8 years), in centreline of the river (black circle is figure 5.10)

At the upstream boundary of the model a remarkable steep bed level gradient is simulated, see figure 5.9 and 5.10 (the red lines). Figure 5.10 shows the simulated steep bed level gradient is independent of the imposed boundary condition, because decreasing this boundary condition does not affect the steep gradient (no significant difference between 0.10 and 0.50 m/year). The steep gradient is only dependent of the local geometry in the river. The river becomes wider as a result the river becomes shallower.

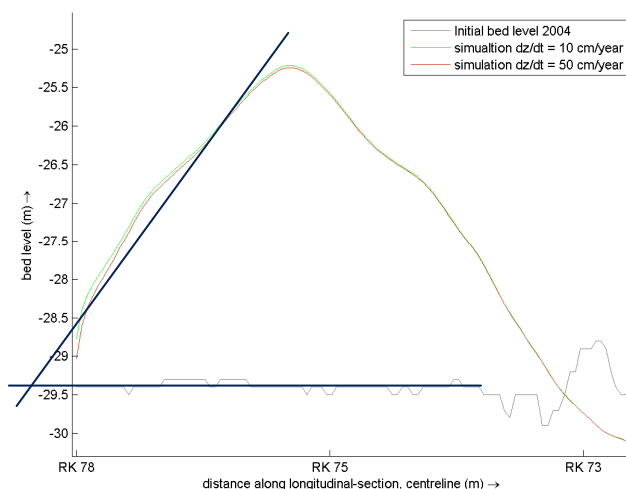


Figure 5.10: Calibration: bed level gradient, difference between imposed upstream boundary condition for bed level change, 0.10 and 0.50 m/year.

An overview of the 1D model results for annual sediment transport are given in table 5.3. These results are cross-section averaged transport rates. The bed-load in the model is larger than observed in the river but is necessary to reproduce the annual bed level change in the river.

Note: The sediment transport in the river highly fluctuates over the years. The estimated observed values of the sediment transport therefore have some uncertainties. This uncertainty in the estimated observed sediment transport needs to be taken into account when modeling the sediment transport.

Table 5.3: Results of sediment transport through model

	Observed	Delft3D	Reference
Total Suspended load Upstream*	91±21	107	Allison <i>et al.</i> , 2010
Sand_Suspended load Upstream*	17.6	15	Nittrouer <i>et al.</i> , 2010
Sand Suspended load Head of Passes*	4-6	3.97	Allison <i>et al.</i> , 2006
Total sediment load through West Bay Diversion*	2.9	3.1	Ashurst., 2007
Sand_Bed-load Upstream	2.2	~3.8	Nittrouer <i>et al.</i> , 2010
Bed level change	0.35-21 m/year	0.3-2.5 m/year	
Propagation of bed disturbances	2.4 km/year**	1-3 km/year	

* Mton/year

** calculated with e.q. 5.9

5.5.2 2D Calibration

This section specifies the transverse slope and the bar-pool pattern (dynamic behavior) in the river. As described in chapter 3 the grid contains 20 cells in lateral direction, perpendicular to the direction of the flow and it is described in section 2.5 the river has bank protection on each side along the inter reach (see also the gray lines along the river banks in Appendix E). These protected banks are translated into the model design. The first five grid cells on both sides get a non-erodible layer, see figure 5.11. This means the model has fixed river banks, which cannot erode. The river bed, which is the 10 grid cells in the middle, can erode. Extending the non-erodible layer does not help to get better results.

Computed bed levels of two simulations of 10 year and the initial condition can be seen in figure 5.12. The red line shows the simulation without the non-erodible layer. Despite the sedimentation which occurs in the cross-section the banks slip away. This is certainly not realistic.

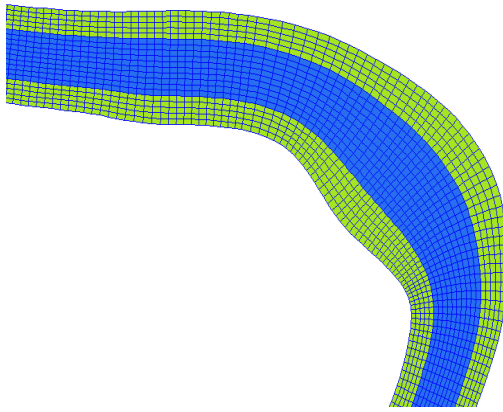


Figure 5.11: River bends in the model, green are the riverbanks with its non-erodible layer. Blue is the river bed

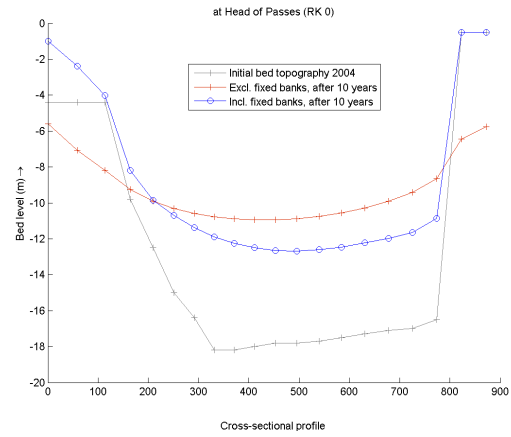


Figure 5.12: Non-erodible layer included into the model

2D Theory

The 2D bar-pool pattern in the river is influenced by the curvature of the channel geometry and the channel width variations. The 2D behavior in the bends of the river is related to the transverse bed-slope. It is described by the following relation for axial-symmetric situation [Struiksma *et al.* 1985]:

$$\sin \beta = A \cdot f(\theta) h / R \quad \text{and} \quad \theta = \frac{\tau_{flow}}{(\rho_s - \rho_l) g D_{50}} = \frac{u^2}{\Delta C^2 D_{50}} = \frac{h i}{\Delta D_{50}} \quad (5.10)$$

in which $\sin \beta$ is the transverse slope, A is the helical flow coefficient, $f(\theta)$ is a function of the Shields parameter, h is the depth and R is the radius of the bend curvature.

The function of the Shields parameter represents the bed shear stress (τ_{flow}), the density of the sediment (ρ_s) and the liquid (ρ_l), the gravitational acceleration constant (g) and the grain size diameter (D_{50}). This can be translated in which θ is described following the depth (h), slope (i), relative density (Δ) and the grain size diameter (D_{50}). The helical flow coefficient (A) reads:

$$(5.11)$$

$$A = 2E_{spir} / \kappa^2 \left(1 - 0.5 \frac{\sqrt{g}}{\kappa C} \right)$$

in which E_{spir} is the calibration parameter for helical flow in Delft3D, κ is the Von Karman constant, g is the gravitational acceleration constant and C the roughness coefficient.

And the function of the Shields parameter is given by:

$$f(\theta) = 9(D_{50} / h)^{0.3} \sqrt{\theta} \text{ and in Delft3D formulated as } f(\theta) = A_{shields} \theta^{B_{shields}}, \quad (5.12)$$

in which D_{50} is the median grain size and h is the depth [Talmon *et al.*, 1995].

Bar behavior of the river

The free dynamic response of bars in the river corresponds to the way the river is able to react to disturbances from upstream and refers to the ratio of the adaptation length for sediment (λ_s) and water motion (λ_w). Rivers with several bars in a cross-section have a high ratio and therefore a relative high adaptation length for sediment motion and vice versa. The free dynamic response of bars in the river is formulated in the following way [Struiksma *et al.*, 1985]:

$$\lambda_s = \frac{f(\theta)}{\pi^2} \left(\frac{B}{h} \right)^2 \cdot h \rightarrow \lambda_s = \frac{A_{shields} \theta^{B_{shields}}}{\pi^2} \left(\frac{B}{h} \right)^2 \cdot h \quad (5.13)$$

$$\lambda_w = \left(\frac{C^2}{2g} \right) \cdot h \quad (5.14)$$

$$IP = \frac{\lambda_s}{\lambda_w} = \frac{A_{shields} \theta^{B_{shields}}}{\pi^2} \frac{2g}{C^2} \left(\frac{B}{h} \right)^2 \quad (5.15)$$

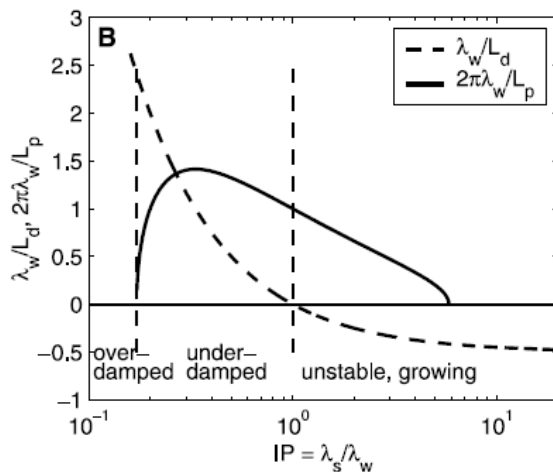


Figure 5.13: Dynamic system in the river [Kleinhans *et al.* 2008]

The interaction parameter (IP) is strongly depended on the width –depth ratio, for varying discharge condition and for different cross-sections. According to Kleinhans *et al.* the Lower Mississippi River is a overdamped system ($IP \ll 0.2$, see figure 5.13). The Lower Mississippi River has a narrow and deep channel as already stated in section 2.1. This implies the small width - depth ratio and consequently the small IP parameter [Kleinhans *et al.* 2008]. In the study area the IP parameter is between 0.01 and 0.15. The interaction parameter increases downstream because the river gets wider and shallower. Because the river bed is overdampening, there is no development of the free dynamic response. The position and length of bars at the banks of the river are not strongly influenced by the dynamic behavior in the river. Their position and length is forced by the fixed banks in the river (fixed by bank protection).

Results 2D calibration; Cross-sectional profiles

In order to calibrate the 2D behavior in the model the following parameters can be tuned:

A_{shields} , B_{shields} and E_{spir} . In Delft3D these parameters can be included by adding the Koch & Flokstra formulation [Koch & Flokstra, 1980]. In Delft3D the parameter B_{shields} is set as 0.5. E_{spir} is chosen as 1.0. E_{spir} is linearly related to the A_{shields} parameter, and also linearly affects the transverse bed slope. Therefore it is chosen to keep E_{spir} constant and to tune A_{shields} during calibration.

The 2D calibration is done with the A_{shields} parameter. Increasing the A_{shields} parameter increases the steepness of the transverse bed slope of the inner bend. Empirically the A_{shields} parameter would be 0.25, which means a very mild slope in the river bends. Simulations were done with $A_{\text{shields}} = 0.25$ and $A_{\text{shields}} = 1.0$. The transverse slope is different for varying A_{shields} in several cross-sections and is presented in figures 5.14 to 5.17. The simulations are including the dredging activities. Cross-sections are presented from RK 10 (Upstream of West Bay Diversion) to RK -20 (Mouth of the River). The simulations start with the initial bed level of 2004 and run for 6 years. Therefore the simulations can be compared with the bed of 2010.

From these cross-sections it can be seen that they respond to the A_{shields} parameter. Changing the α_b parameter not really has influence on the transverse slope. The response to $A_{\text{shields}} = 1.0$ is overdone compared to $A_{\text{shields}} = 0.25$. The simulation with $A_{\text{shields}} = 1.0$ deepens the cross-section, because the bed-slope tends to be steeper. The cross-sections with $A_{\text{shields}} = 0.25$ give the best results.

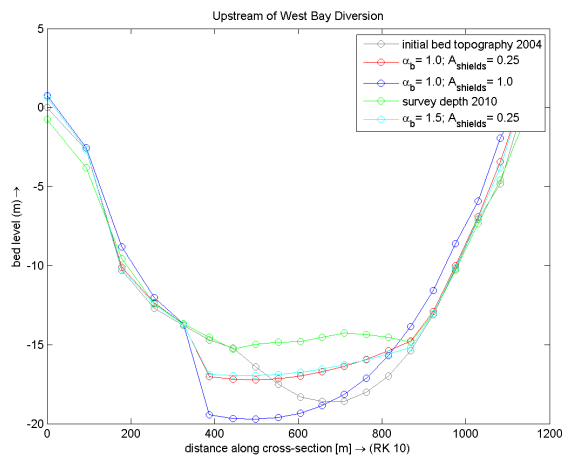


Figure 5.14: Cross-section RK10

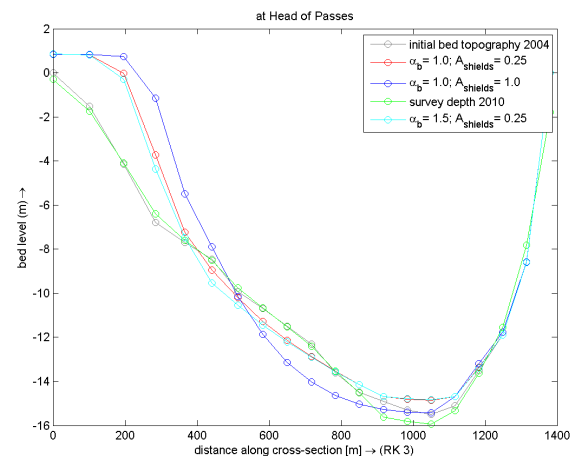


Figure 5.15: Cross-section RK 3

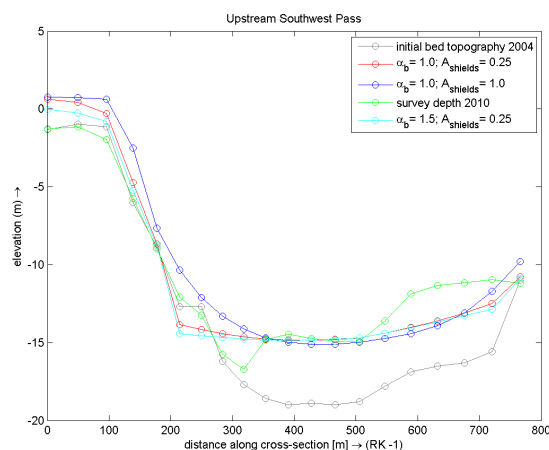


Figure 5.16: Cross-section RK -1

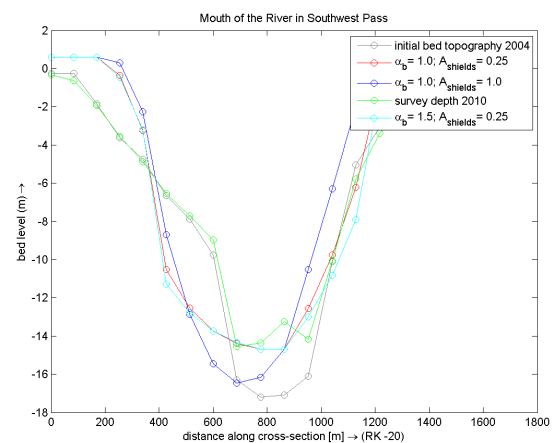


Figure 5.17: Cross-section RK -20

Effect of $A_{shields}$ parameter on transport capacity

The $A_{shields}$ parameter also affects the sediment transport in the river. A lower value for $A_{shields}$ means a lower value for the function of the Shields parameter (eq. 5.12) and therefore a lower value for $A_{shields}$ results in more sediment transport through the river, see figure 5.18. Next to the different $A_{shields}$ values, the figure shows the cumulative sediment transport for simulations with a varying transport calibration parameter (α_b). Increasing α_b results in more sediment transport.

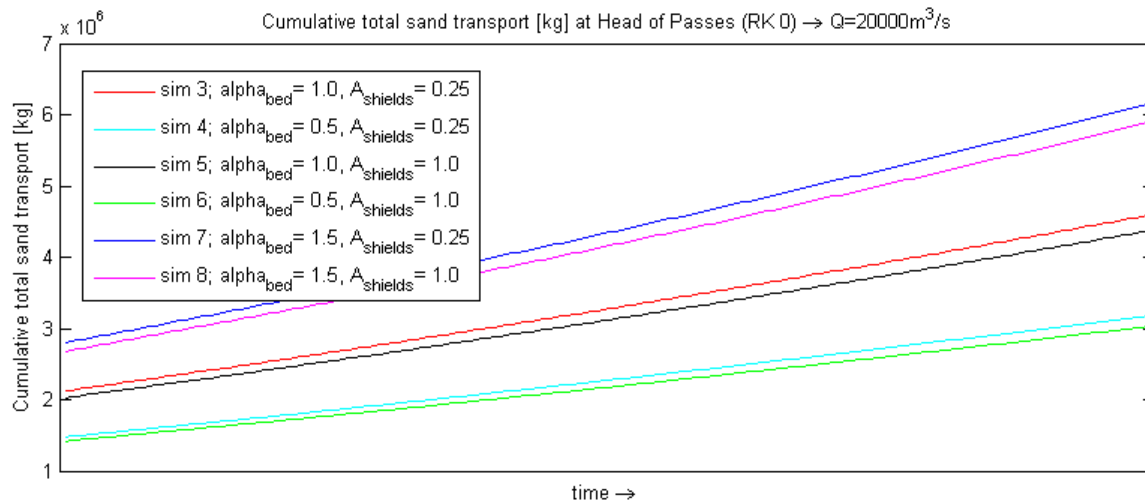


Figure 5.18: Cumulative sediment transport at Head of Passes with varying calibration parameters, during the intermediate discharge level, $Q=20000 \text{ m}^3/\text{s}$

5.5.3 Calibration of the dredging quantities

The Mississippi is maintained by dredging every year. The average annual dredging quantities from 1990 to 2010 are 13.3 million m^3 [Ulm, 2010]. The dredging quantities have significant impact on the morphological response. Therefore simulations were done to find out how well the model represents the dredging activities in the river. The dredging reach in the model corresponds well with the present dredging reach from Head of Passes up to the mouth of the river and is submitted in the model by a dredge polygon. Every grid cell centre that lies within this polygon is included in the dredging calculations.

Simulations:

Six simulations were done and they differ in the transverse slope parameter ($A_{shields}$), the transport capacity parameter (α_b) and the dredge depth. The flow is schematized according to the hydrograph determined in chapter 4. As stated in section 2.5 (and shown in Appendix F) no dredging activities take place in the period from October to January. The simulated dredging activities are present throughout the year. The simulations show that the simulated dredging activities are negligible during the low discharge level [Ulm, 2010; Ulm 2011].

- Intermediate discharge level from January to April: $Q= 20000 \text{ m}^3/\text{s}$
- High discharge level in April: $Q= 33000 \text{ m}^3/\text{s}$
- Intermediate discharge level from April to May: $Q= 20000 \text{ m}^3/\text{s}$
- Low discharge level from May to December: $Q= 10000 \text{ m}^3/\text{s}$

Parameter settings

1. The A_{shields} parameter expresses the steepness of transverse slope of the banks. Increasing the parameter increases the slope. A_{shields} is chosen at 0.25 and 1.0.
2. Simulations were done with two different Transport capacity parameters, $\alpha_b=1.0$ and $\alpha_b=1.5$ respectively. The alternative with $\alpha_b=0.5$ is excluded, since it would not be interesting because of the low transport capacity.
3. Two different dredge depths were simulated, 14.7 and 15.2 m respectively.

Results

Figure 5.19 shows an example of the cumulative dredging quantities after running the simulations; this one is the optimal simulation (#7). The results of all the simulations are enclosed in table 5.4. The figures are enclosed in Appendix G. The simulations start in 2004, which refers to year 1. This because of the fact the initial bed topography of the model is from 2004, see section 3.4. The simulations need 3 to 4 year to get equilibrium dredging quantities.

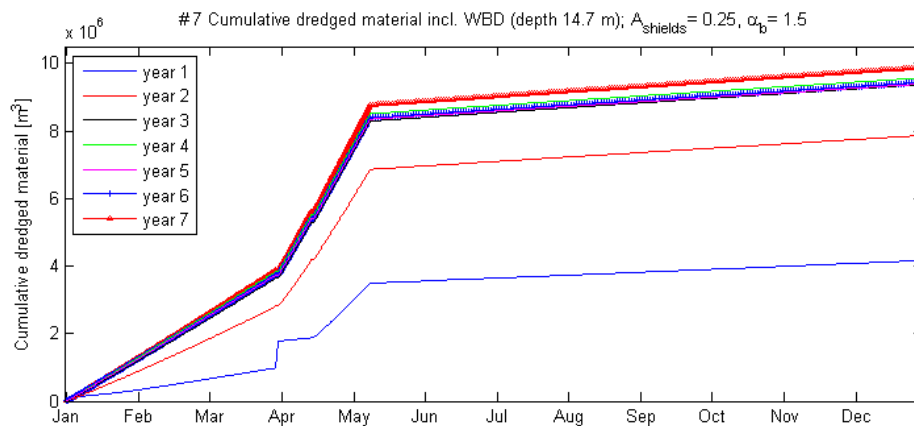


Figure 5.19: Results of Simulation, representation of cumulative dredging quantities

Table 5.4: Results from Dredging Simulations

A_{shields}	α_b	depth (m)	# sim.	Cum dredged material $\times 10^6$ [m ³] Incl. West Bay Diversion
0.25	1.5	14.7	7	9.5
0.25	1.0	15.2	2	8.5
0.25	1.0	14.7	1	7.5
1.0	1.5	14.7	9	7.5
1.0	1.0	15.2	5	6
1.0	1.0	14.7	4	4.5

Dredge option 1: This dredge function includes grid cells, which lie with their cell centres in the dredging reach. This means that some grid cells within the dredging reach could be excluded from this functionality.

Dredge option 2: This dredge function includes grids cells, which lie with at least one corner in the dredging reach. This means all grid cells are included, but also dredges at some locations outside the dredging reach.

The differences between these two functions are clearly shown in figures 5.20 to 5.22. Dredge option 2 also dredges outside the reach as dredge option 1 dredges to little within the reach. The differences between these two options are approximately 10 %. This should be taken in account for the predictions of dredging quantities, in chapter 6.

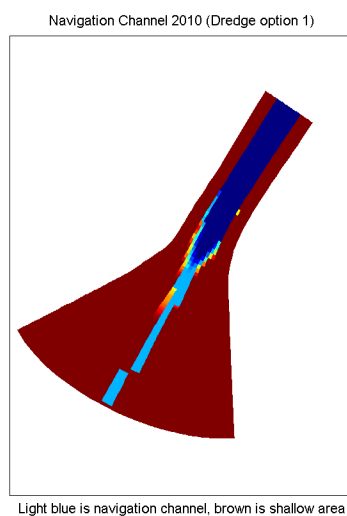


Figure 5.20: Dredges only cell centres

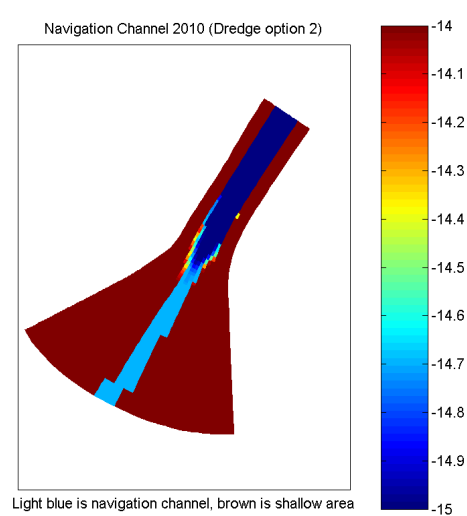


Figure 5.21: Dredges at least one corner

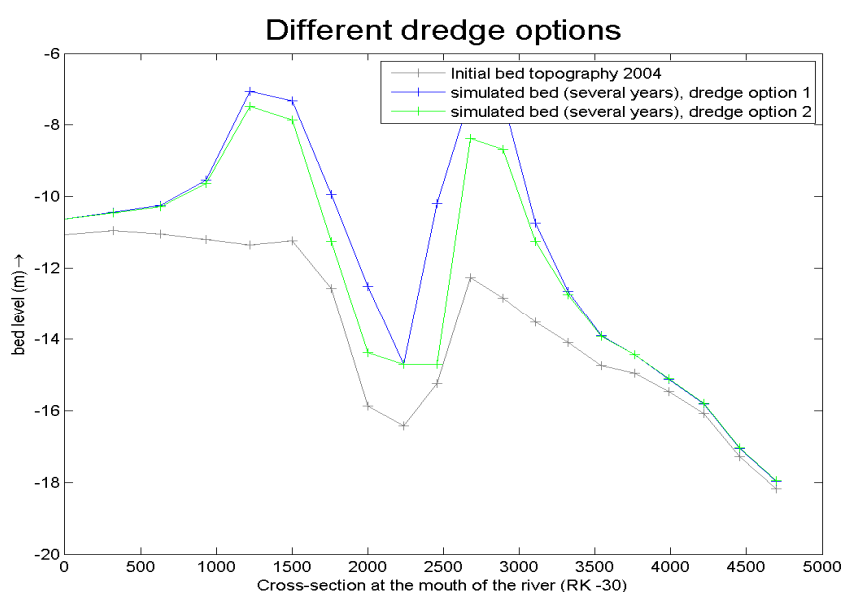


Figure 5.22: Differences between two dredge options

5.5.4 Calibration of the mud deposition processes

In section 5.3.2 the mud transport formula is introduced, this formula is used to calculate the mud erosion and deposition processes during the simulations. The mud transport formula of Partheniades-Krone (1965) consists of two parameters, which can be tuned to obtain the desirable mud erosion and deposition processes and mud transport rates. These parameters are the critical shear stress parameters for erosion ($\tau_{cr,e}$) and deposition ($\tau_{cr,d}$). These two parameters are empirically derived from previous studies [Winterwerp, 1989; Van Ledden, 2003]. In this study the $\tau_{cr,e}$ and $\tau_{cr,d}$ are 0.5 and 0.05 respectively.

More research needs to be conducted, this way appropriate values of these two parameters can be obtained for simulating the mud erosion and deposition processes in the Lower Mississippi River. Unfortunately limited field data is available.

An insight is given of the effect of adjusting the critical shear stress parameters. Two representations of simulations are shown in figure 5.23 and 5.24. Both simulations ran for several years. Figure 5.23 shows the mud fraction in the river bed with the derived parameters i.e. $\tau_{cr,e} = 0.5$ and $\tau_{cr,d} = 0.05$. This simulation indicates no mud deposition takes place on the river bed.

The deposition process in Delft3D can be tricked by choosing a very high value for the critical deposition shear stress e.g. 1000. Defining $\tau_{cr,d} = 1000$ implies the deposition process of mud always takes place independent whether or not erosion takes place. This way the deposition process is continuous and only depends on the fall velocity and near-bed sediment concentration, see formula 5.5. Figure 5.24 shows the results with the adjusted critical shear stress parameters. These are $\tau_{cr,e} = 0.15$ and $\tau_{cr,d} = 1000$. The figure shows that the adjusted deposition parameter (up to $\tau_{cr,d} = 1000$) significantly attributes to the mud deposition process on the river bed. The simulation shows a substantial difference from a negligible mud fraction to order 4% on the river bed.

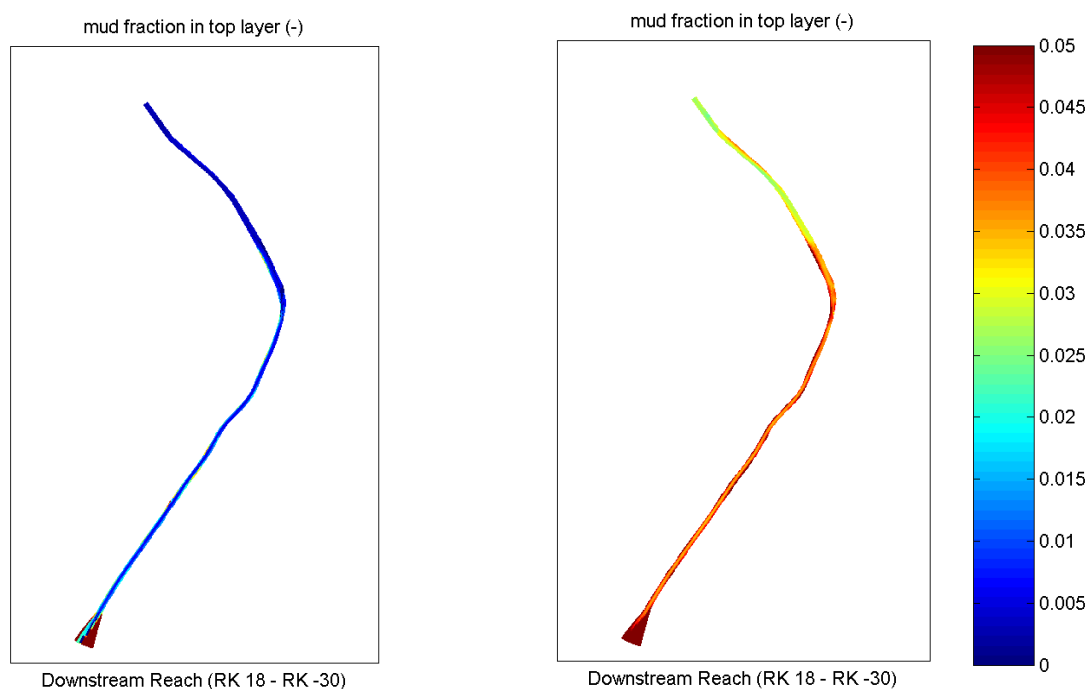


Figure 5.23: Simulation with no mud deposition

Figure 5.24: Simulation with enhanced mud deposition

Due to the adjusted settings the sedimentation process in the downstream part of the river is significantly increased. This fact is shown in figure 5.25. The blue line (enhanced mud deposition) clearly lies atop of the red one (no mud deposition). The simulation with the enhanced mud deposition is better able to fill up Southwest Pass, which is the reach between RK 0 and RK -30.

In addition the increased sedimentation processes in the downstream reach increased the simulated dredged volumes in the dredging reach. The dredged volumes in the simulation with the enhanced mud deposition are about 1.9 times larger, with an equilibrium of 18 million m³/year instead of 9.5 million m³/year simulated dredged material.

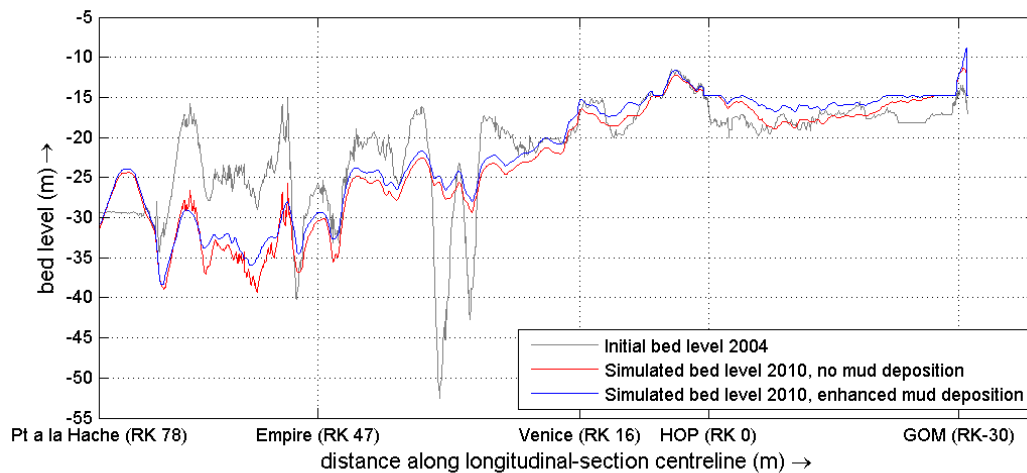


Figure 5.25: Simulated bed levels, no mud deposition vs. enhanced mud deposition

5.5.5 Results

The morphology in the model depends on many parameters and they are all included in the model. An overview of all these calibrated parameters is given in table 5.5 and 5.6

Note: previously is shown adjusting critical shear stress parameters significantly influences the simulated mud erosion and deposition processes. Despite of this enhanced sedimentation effect, further study and simulations are conducted with the derived parameters after empirical analysis and calibration of the sediment transport rates, because too little is known about the real mud deposition processes, see table 5.5. The underprediction of the simulated sedimentation processes are taken in account.

Table 5.5: Summary of morphological parameters

	Observed	Delft3D	Reference
D₅₀	200 μm	194 μm	[Pereira <i>et al.</i> , 2009]
D₅₀ in suspension	125 μm	116 μm	[Meselhe <i>et al.</i> , 2010]
$\tau_{cr, sand}$	0.15 N/m^2	0.16 N/m^2	[Van Rijn, 1993]
$\tau_{cr, e Mud}$	0.1-0.5 N/m^2	0.5 N/m^2	[Van Ledden, 2003]
$\tau_{cr, d Mud}$	0.05 and 0.15 N/m^2	0.05 N/m^2	[Winterwerp, 1989; Van Rijn, 1993]
M	$10^{-3} - 10^{-5} \text{ kg/m}^2/\text{s}$	$10^{-5} \text{ kg/m}^2/\text{s}$	[Winterwerp, 1989]
w_{sand}	1 cm/s	1 cm/s	[Parker, 2004]
w_{silt}	0.1 cm/s	0.1 cm/s	[Parker, 2004]
w_{clay}	0.01 cm/s	0.01 cm/s	[Parker, 2004]
D_*	5.0		
θ_{cr}	0.05		
Porosity	60-75%		[Galler and Allison, 2008]
Δ	1.60		
u	$1.0 \times 10^{-6} \text{ m}^2/\text{s}$		Default Delft3D

Table 5.6: Summary of calibration parameters

Calibration parameter	[-]
α_b	1.5
α_s	0.3
E_{spir}	1.0
A_{shields}	0.25
B_{shields}	0.5

A Long-term simulation with the derived parameters was run for 7 years. The simulation starts with the initial bed level of 2004. Figure 5.26 shows the simulation achieved to represent the observed bed level of December 2010 at Head of Passes fairly well. At the beginning of the dredge reach and in the middle of the Southwest Pass the simulation is under predicting the sedimentation (see red marks). The underprediction is in the order of 2 to 3 m. At the mouth of the river the results are representative again.

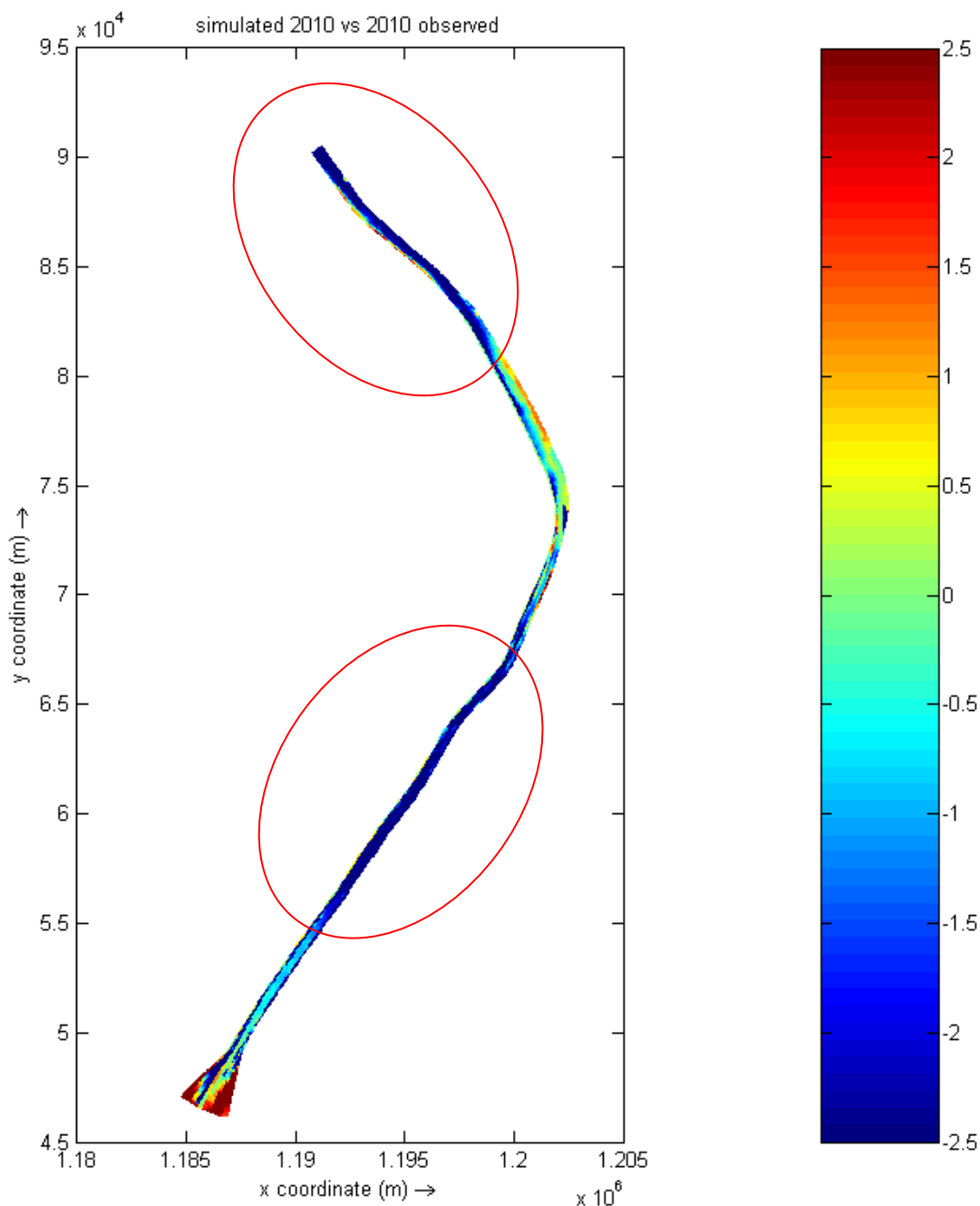


Figure 5.26: Simulated vs. Observed bed level dredging reach

5.6 Conclusions of Morphodynamic calibration

The following conclusion can be drawn from the 1D and 2D morphological calibration as well as the calibration of the dredging quantities and mud deposition processes. No bed topography data of the entire study area more recent than 2004 is available. Therefore it is not possible to execute a morphological verification.

1D calibration

1. From the long-term simulation can be learnt the model slightly underpredicts the sedimentation processes in the Southwest Pass.
2. Most sedimentation problems are at Head of Passes and at the mouth of the river. The model is able to give insight in this phenomena.
3. The simulated bed-load is larger than observed one to reproduce the bed level change in the model.

2D calibration

4. A_{shields} is chosen relatively small and corresponds with the empirically calculated value.
5. Adding the fixed banks to the model is a substantial improvement. The modeled river stays at a fixed position after running long-term simulations.

Calibration of dredging quantities

6. the increased bed-load has significant influence on the dredging quantities. However the dredging quantities in the model fairly reproduce the observed quantities.
7. Increasing the steepness calibration parameter (A_{shields}) decreases the dredging quantities.
8. Increasing the dredge depth negatively influences the dredging quantities. It enhances the dredging volume and therefore the costs, which is undesirable. An increase from 14.7 to 15.2 m results in additional dredging volume of + 13% for $A_{\text{shields}} = 0.25$ and + 27% for $A_{\text{shields}} = 1.0$. This can be explained because the model calculates steeper slopes and therefore simulates bigger cross-sections which needs to be dredged.
9. The average dredging quantities from 1990 to 2010 is 13.3 million m³; simulation #7 suits most to this average. Many uncertainties, as the precise position of the dredge reach as well as the dredge depth should be considered. The dredge function 1 (dredges grid cells which are > 50% in the dredge reach), therefore not 100% of dredge reach is dredged during simulations. This explains the underprediction of the model results.
10. Analysis shows using dredge function 2 (dredges every grid cell in the dredge reach) simulates substantial higher dredging quantities. Its approximately 10% more. The best predictions for simulating the dredging quantities lies within these two (1 and 2) dredge options.

Calibration of mud deposition processes

11. Adjusting the mud deposition parameters ($\tau_{cr,e}$ and $\tau_{cr,d}$) have significant influence on the mud sedimentation processes. The new simulation ($\tau_{cr,d}=1000$ instead of $\tau_{cr,d}=0.05$) results in a multiplication factor of 1.9 for the dredging quantities.

In general

12. The Morphological calibration can be further optimized. The calibration is a iterative process. Continuous research and applications of the model will verify the best model calibration settings.
13. The calibrated model can be used to run several scenarios to see what the influences are on the system and to make predictions for river management purposes.

Chapter 6. Assessment of sediment diversion strategies

6.1 Introduction

As stated before the Lower Mississippi River is one of the most regulated rivers in the world. The river has been regulated because of different interests the river has to coop with, such as: navigability, sediment, water and flood management. There is a need for good understanding of all these interests. Furthermore these regulations need to be maintained properly. Integrated river management focuses on these aspects and issues. The aspects are listed below:

- Navigability of the river, accompanied with maintenance dredging
- Sediment management, along with delta building
- Water management, which environments prefer freshwater and which salt water?
- Flood management, to what extent do the wetlands contribute to decreasing flood risk?

Navigability and sediment management are the topics which are addressed in this thesis. The developed numerical model is used to assess several strategies. These strategies treat the implementation of new sediment diversions and closing off of existing ones. Critical is how these interventions influence the dredging quantities. Therefore first the need of dredging is demonstrated.

6.2 The need of dredging, maintain navigability

The Lower Mississippi River has been intensively dredged over the past 20 years to keep the river navigable as became clear from section 2.5. The reach from Venice (RK 16) until Gulf of Mexico (RK -30) is the dredging reach. Long-term simulations were done with the optimized settings from calibration to see what would happen to the lower reach of the Lower Mississippi River, with and without dredging activities. The intention of the simulations is to clarify the need of dredging. Therefore the long-term simulations were done over 20 years, see figure 6.2 and 6.3. These figure represent the longitudinal section over the centreline of the river, see figure 6.1.

The analysis of the simulations reveals trends for the river bed; around RK 3 (at Head of Passes) the river bed is practically in equilibrium. More upstream the bed is subjected to erosion and degrading. Downstream of this point, the sediment deposits and the bed aggregates. The dredging activities do not really affect the upstream bed topography. The simulations show pretty similar results for the upstream part. Between RK 3 and 5 the centreline slightly deviates from the dredging reach. This is noticeable in figures 6.2 and 6.3 within the red circles.

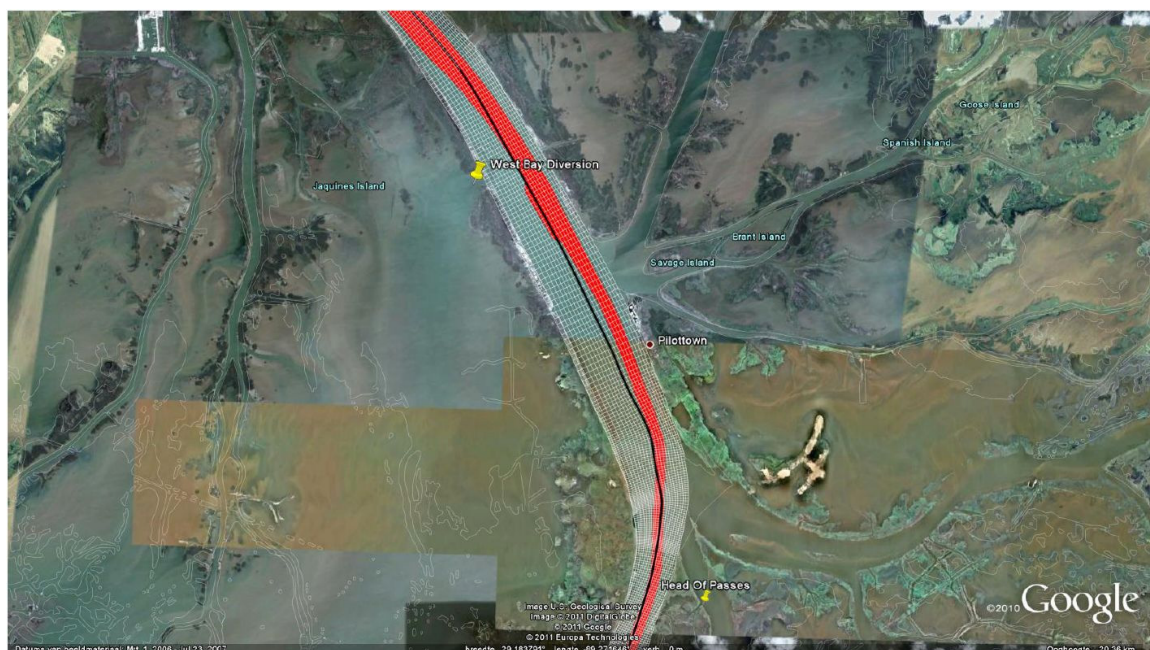


Figure 6.1: Centreline and Dredge reach, within grid design [Google Earth, 2011; OET, 2011]

Without Dredging Activities: the simulations show the morphological response propagates through the shallow reach (from RK 3 to RK -30). The simulation without dredging activities shows a lot of sedimentation in this reach. The reach becomes pretty shallow. After 20 years the reach is completely filled up with sediment and is not navigable anymore. In figure 6.2 this is represented with the red dotted line.

Including dredging activities: the simulation with dredging activities shows the river stays open and remains navigable. The deep parts are starting to fill up to 14.7 m depth. The average modeled dredging quantities are shown in section 6.4 and are approximately 9.5 million m³ a year. The high rate of the morphological response through the dredging reach clarifies the necessity of the yearly dredging activities.

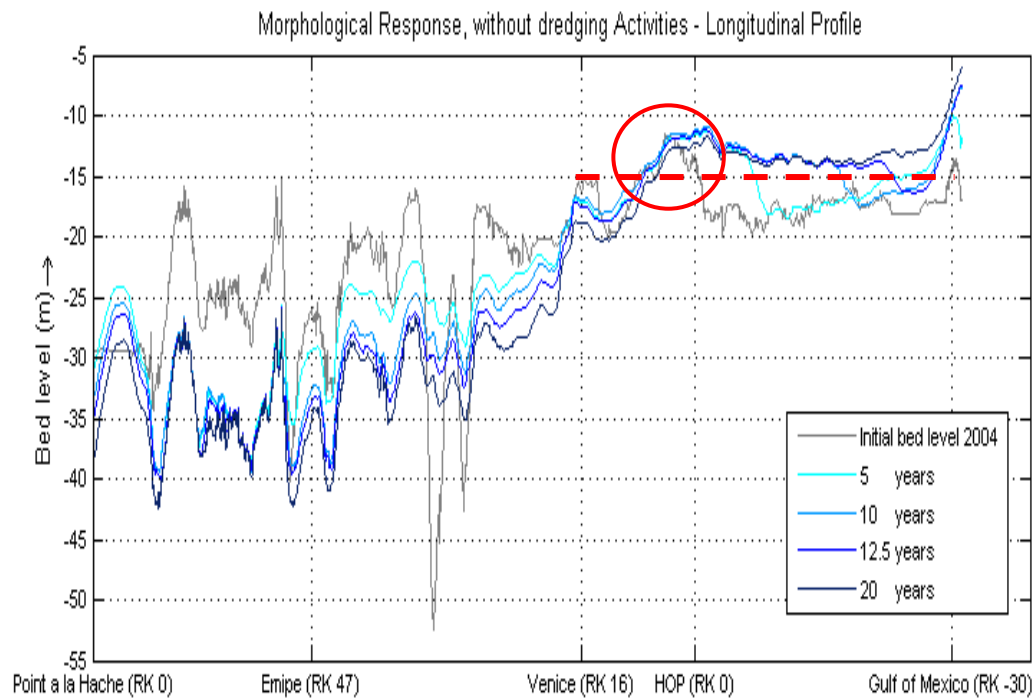


Figure 6.2: Simulated long-term Morphological Response, without dredging activities

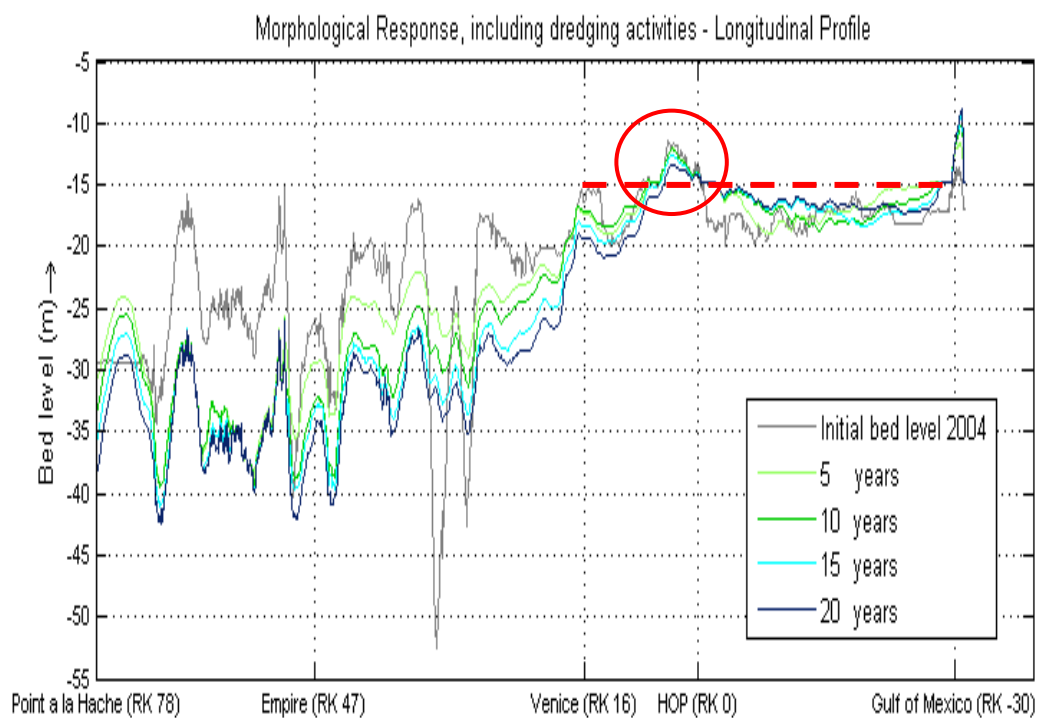


Figure 6.3: Simulated long-term Morphological Response, including dredging activities

Cause of sedimentation

Figure 6.5 helps to understand the following analysis (For $Q = 20000 \text{ m}^3/\text{s}$):

Analysis on the river geometry at the turning point between degradation and aggregation of the river bed at RK 0 leads to plausible explanations of this effect. At RK 0 the channel geometry suddenly becomes wider. Additionally the contribution factor is the distribution of flow over the distributaries. These two things result in a tremendous decrease of the flow velocities. The sediments are able to deposit because of the decreasing flow velocity and the related transport capacity.

This phenomenon propagates through the Southwest Pass, down to the Gulf of Mexico. At the mouth of the river in the Gulf of Mexico the same deposition process happens because of the widening of the river channel. The sediment is captured at this location by jetties and breakwaters. These structures were built for navigation purposes to secure the ships from exposure to waves and currents.

Flow velocities (m/s) in the lower reach of the river
From RK 18 to RK -30

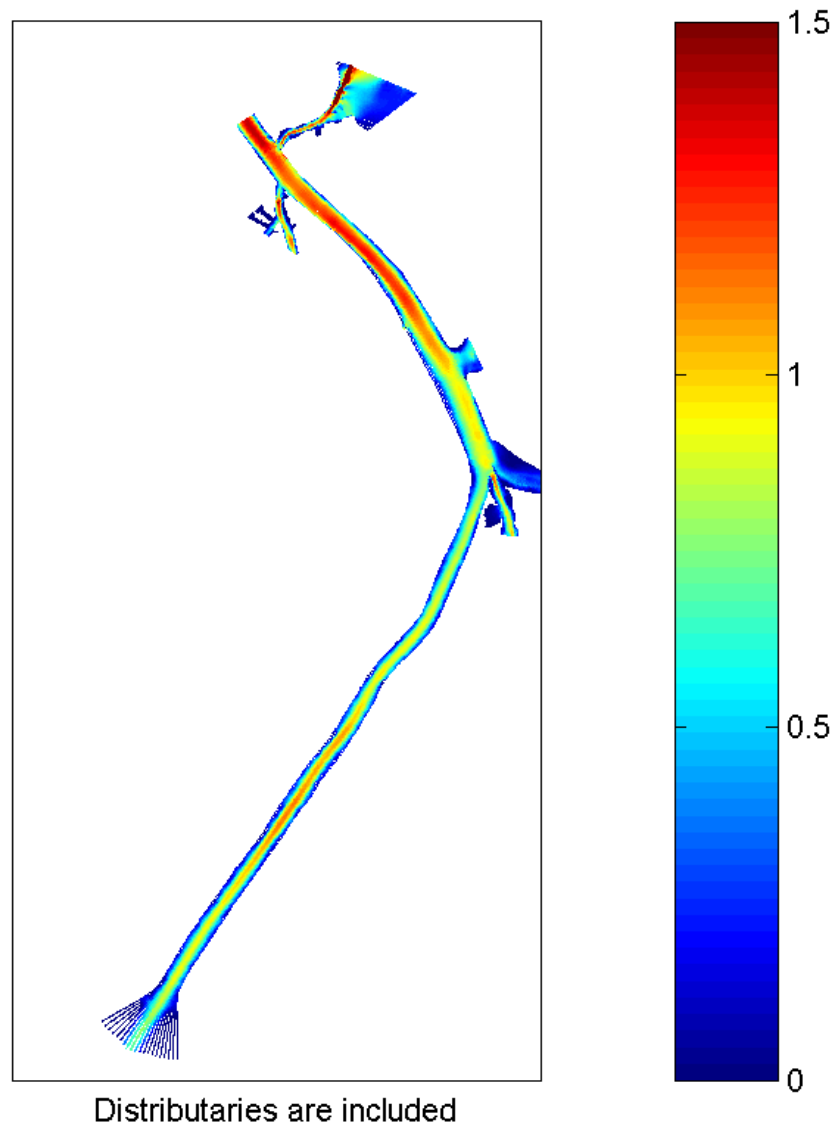


Figure 6.4: Velocities in the lower reach RK 18 – RK -30; understanding the sedimentation process

Navigation channel

The top views of the navigation channel are given (figure 6.5 and 6.6). At Head of Passes it shows that the navigation channel is pretty narrow. During the simulation the bed of the navigation channel is intensively dredged. It shows that maintenance dredging is very important. The depth in the channel is critical.

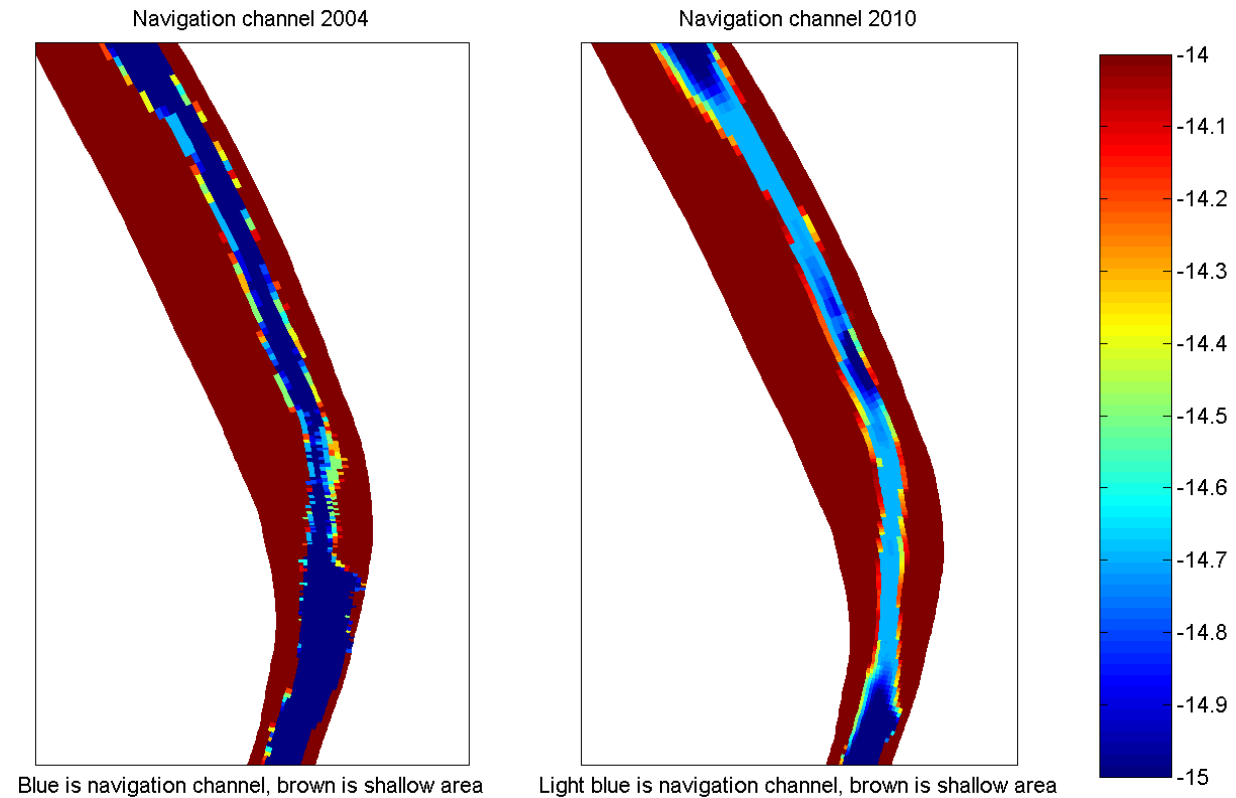


Figure 6.5: Initial navigation channel of 2004 vs. simulated navigation channel in 2010 at Head of Passes

The same representation is given at the mouth of the river. Also the for this area the navigation depth is critical and is maintenance dredging very important.

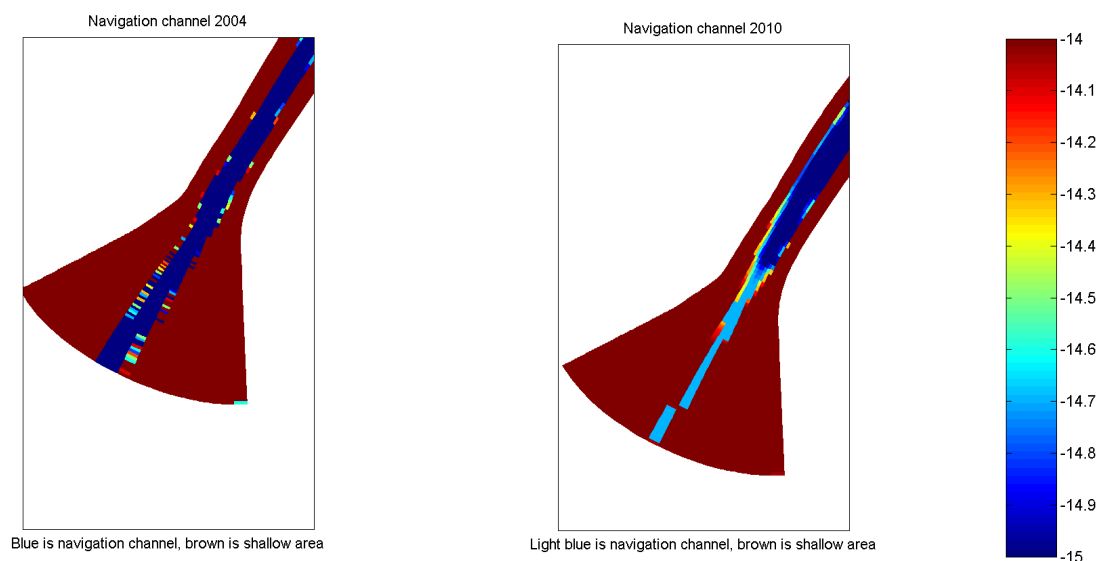


Figure 6.6: Initial navigation channel of 2004 vs. simulated navigation channel in 2010 at the mouth of the river

6.3 Closing off West Bay diversion

The model is applied to simulate the scenario of closing off the West Bay diversion. The closing off of the West Bay Diversion changes the hydro- and morphodynamic behavior in the river. It is interesting to see how the model response to this intervention. Simulations were done with an open and closed off West Bay diversion. Dredging is included, the differences in the dredging quantities are treated in detail in section 6.5. An overview of the changes and the most likely explanation behind the changes are given. The consequences for the system are also described, these are represented with several simulations.

Changes in flow velocity pattern

Figure 6.7 and 6.8 show the flow velocities near the West Bay diversion for the open and closed scenario, during the intermediate discharge level ($Q=20000 \text{ m}^3/\text{s}$). Figure 6.9 shows the differences in flow velocity pattern between these two scenarios. The closing off of the diversion highly influences the flow pattern. The flow pattern influences the sedimentation processes. A quick comparison between figure 6.7 and 6.8 reveals the flow with a closed off diversion is more concentrated in the main channel. The flow pattern with the open diversion is more equally distributed over the width of the river. Figure 6.9 gives more insight in the differences between the two scenarios.

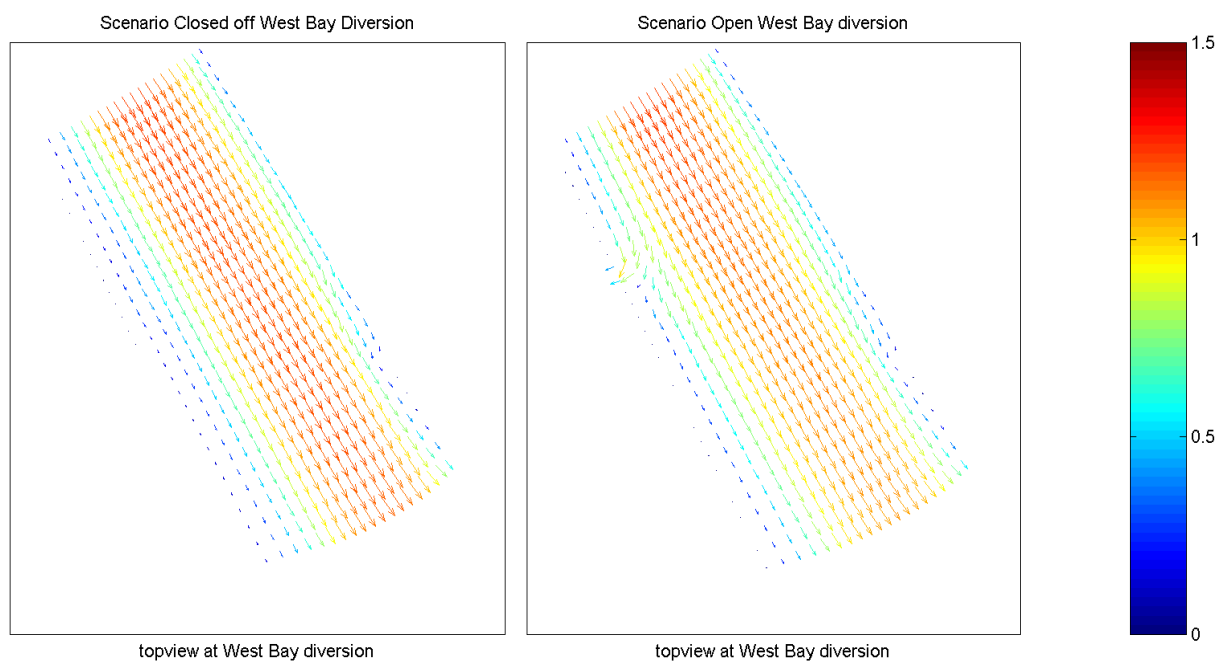


Figure 6.7: Flow velocity pattern [m/s]
Scenario Closed off West Bay diversion

Figure 6.8: Flow velocity pattern [m/s]
Scenario Closed off West Bay diversion

Figure 6.9 shows the closing off of the diversion results in lower flow velocities in the shallow area near the West bank of the river. The reduction is about 15%. Subsequently the flow velocities in the centre of the river increases. The effect is indicated with the upward direction of the arrows (upward means higher flow velocities compared to open diversion).

The increased flow velocities in the main channel of the river induces more sediment transport. This effect is shown in figure 6.10, also the effect is indicated with the upward direction of the arrows (upward means higher sediment transport rates compared to open diversion). The effect of increased sediment transport rates in the main channel is favorable, especially regarding to unwanted sedimentation processes at Head of Passes and in the anchorage area (see section 2.4.2). The sediment transport rates in the main channel for the closed off scenario are 10% higher compared to the open scenario. The effect of the changed flow pattern and sediment transport rates regarding to the changing bed levels is explained below.

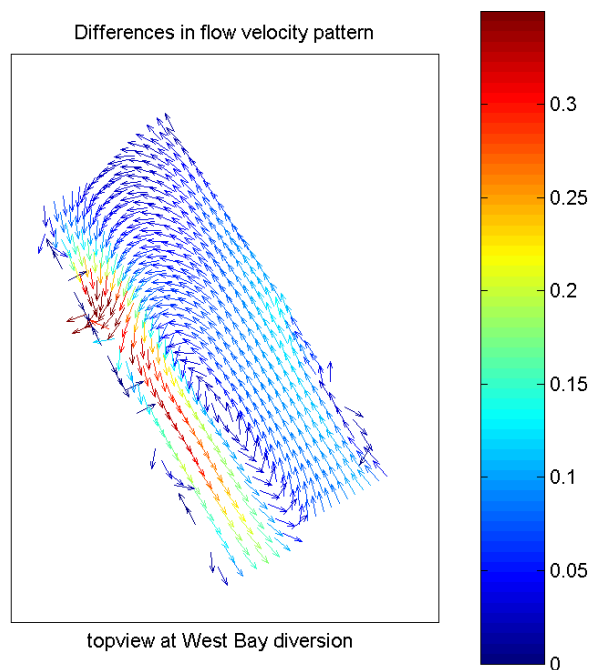


Figure 6.9: Differences in flow velocities for two scenarios [m/s], the direction implies which scenario has relatively higher values. The downward direction of the arrows refers to the open- and upward to the closed scenario.

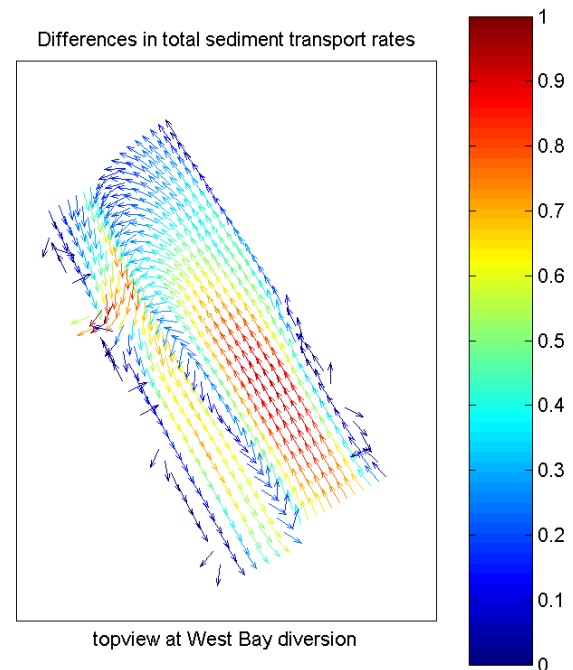


Figure 6.10: Differences in sediment transport rates for two scenarios [kg/ms], the direction implies which scenario has relatively higher values. The downward direction of the arrows refers to the open- and upward to the closed scenario.

Differences in bed levels

Cross-sections of the simulated bed levels are presented in figure 6.11 and 6.12 at Head of Passes, near the West Bay diversion. These cross-sections make it possible to analyze the simulated bed level at various locations near Head of Passes. Also the simulation without dredging is used for this analysis. The simulations ran for several years.

The simulations show differences in the bed levels. The representation of the bed levels for the open en closed off scenario confirm that the change in flow velocity pattern and sediment transport rate substantially affects the bed level. The simulation show a persistent lower bed for the closed off scenario.

The simulation without dredging is included to show the bed level at Head of Passes and within the Southwest Pass will get to an equilibrium depth of 12 -13 m. Unfortunately the depth of the navigable channel needs to be 14.7 m. This implies dredging activities are necessary at all times.

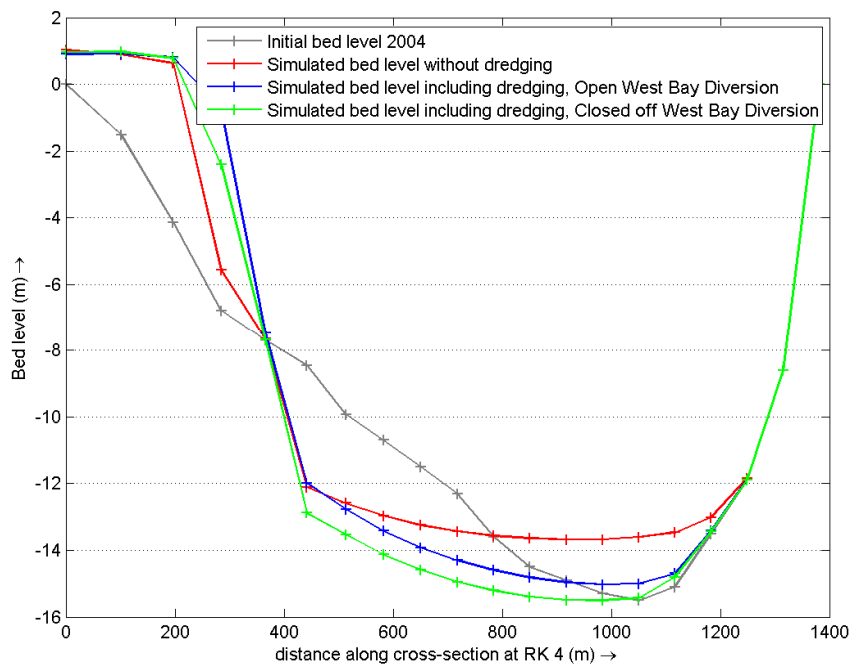


Figure 6.11: RK 4, Simulated bed levels for Open, Closed off West Bay diversion and without dredging

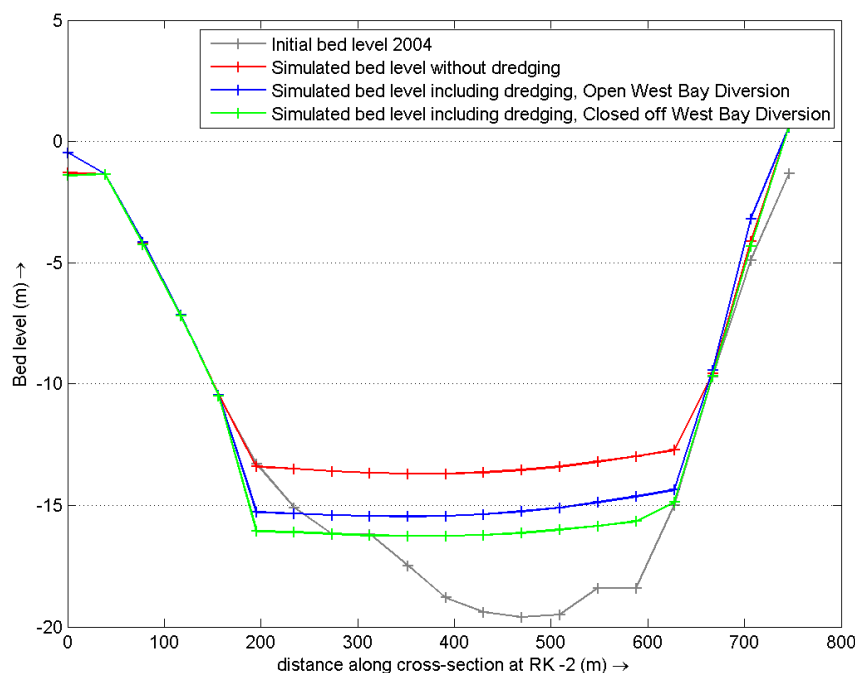


Figure 6.12: RK -2, Simulated bed levels for Open, Closed off West Bay diversion and without dredging

6.4 Implementation of a sediment diversion

A study is done how these sedimentation problems in the lower reach of the river can be limited. The idea is to strategically place a sediment diversion in the river, which extracts sediment from the river. The extracted sediment can be used for delta formation purposes. The location of the diversion is very important, because its location could also negatively influence the sedimentation processes. Insight in this effect is explained in the next section (6.4).

Basically there are three ways to divert sediment from the river in a controlled manner; i.e. a siphon, a gated diversion and a controlled subdelta, see figure 6.13. The implementation of a controlled structure or subdelta is considered. The assumption is a large flow is required to divert the sediments from the river, because the sediments need to be lifted from the river bed and have to be extracted in a direction perpendicular to the flow. This lessons is learned from the Caernearvon Diversion at RK 120, which is a relative small diversion with little ability to divert sediment [Dijkman, 2007].

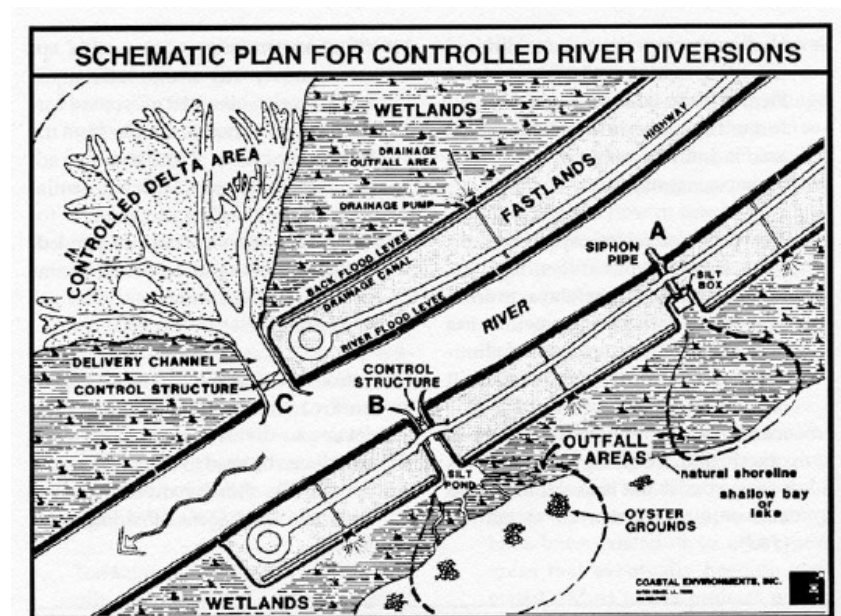


Figure 6.13: Schematization of three basic types of controlled river diversions: A. Siphon; B. Gated diversion; and C. Controlled subdelta. [Wilson, 2008]

Allocation of a sediment diversion site

The study intends to find out what is the most suitable location (diversion site) and size to implement a new sediment diversion. The study is used to get the optimal settings to run several simulations with different management strategies, see section 6.5. According to Meselhe meandering bends in the Lower Mississippi are ideal for sediment diversion sites [Meselhe *et al.*, 2011].

Four locations in the model reach of the Lower Mississippi are examined according to three criteria; the sediment diversion capacity compared to the diverting flow, share of sand that is diverted and the impact on dredging quantities. The simulation were done with the calibration parameters determined in chapter 5, which are $A_{\text{shields}} = 0.25$ and $\alpha_b = 1.5$.

The diversion sites are situated in the inner- and outer bends around the Empire gage (RK 47), see figure 6.14. The share of sand being transported through the diversion is interesting, because sand is the best qualitative sediment to create new land.

Diversion sites 1 and 4 are situated in the shallow inner bends, therefore the water depth in the diversion is also rather shallow and only 3 m deep. Diversion sites 2 and 3 are situated in the deep outer bends; the depth of the diversions is therefore 8.5 m to be able to convey all the sediment from the river, because the highest sediment concentrations are at the bottom of the river, near the river bed.



Figure 6.14: Location of diversion sites 1 to 4, Modified [Google maps, 2011]

Creating diversion in the model

The diversions in the model are created by releasing flow through two grid cells at the grid boundary. The diversion sites in the model extract an imposed flow of $1000 \text{ m}^3/\text{s}$ for the intermediate discharge level, through a 120 m wide diversion. The extracted flow is 5% of $20000 \text{ m}^3/\text{s}$ and is similar to the flow through the West Bay Diversion, further downstream. The model calculates the corresponding sediment transport that goes through the cross-section of the diversion, see figure 6.15. This way the efficiency of the diversion sites can be compared with an existing diversion. Note that the model separately calculates the suspended- and bed-load transport. Therefore it can be independently analyzed.

The sediment transport that goes through the diversion depends on its location and the best conditions. The sediment transport through the diversions therefore varies for the different diversion

sites. Also the share of the three sediment fractions, clay, silt and sand respectively, which goes through the diversions, varies. Figure 6.15 shows the sediment transport capacity for the optimal diversion site; the other three diversion sites are enclosed in Appendix G.

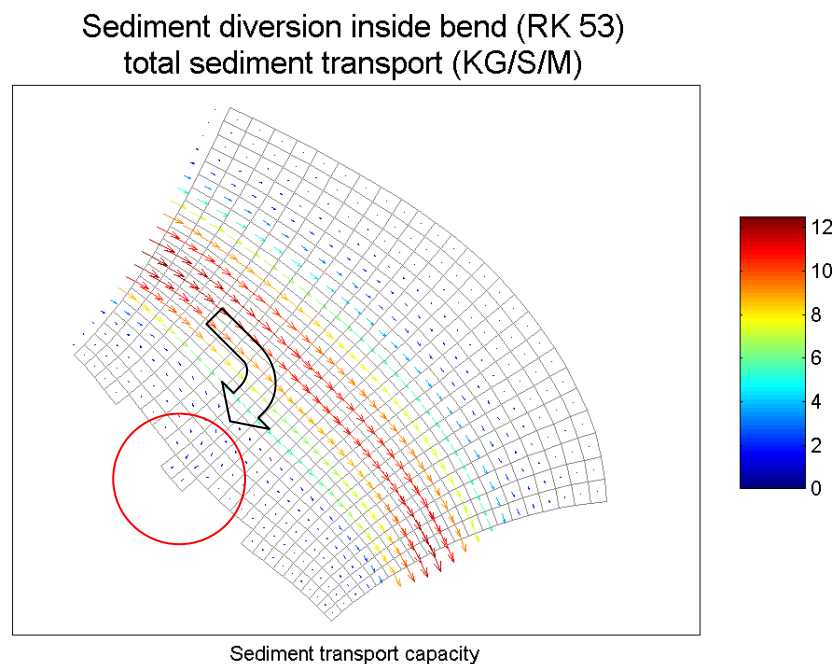


Figure 6.15: top view of the model at diversion site 1 (RK 53), the arrows in the direction perpendicular to the flow represent the released suspended sediment (in the red circle).

Figure 6.15 shows despite the presence of a sediment diversion the majority of the sediment transport still goes through the main channel of the river (see the red arrows).

Furthermore the diversion size is studied; for the optimal location the size of the diversion is doubled (240 m wide) to see what that impact is. This is simply done by releasing flow through four grid cells at the grid boundary instead of two. The effect of doubling the diversion size achieves lower flow velocities through the diversion, see figure 6.16 and 6.17. The average flow velocity through the cross-section is contrarily split in half. This has led to more reliable results.

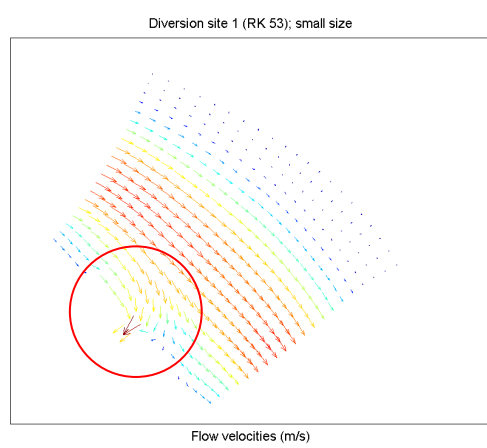


Figure 6.16: Diversion site 1 (RK 53); small size

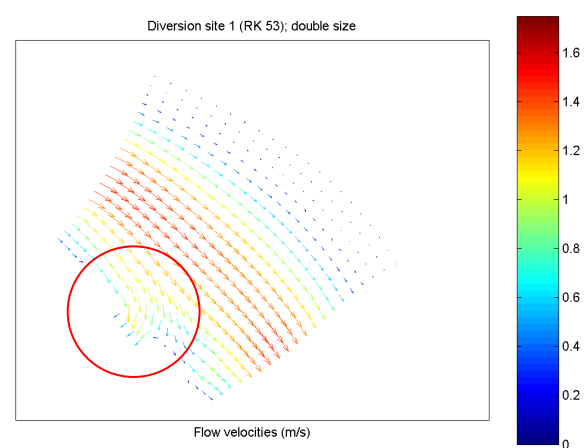


Figure 6.17: Diversion site 1 (RK 53); doubled size

Results

The results of the effectiveness of the four diversion sites and the doubled one are summarized in table 6.1. it includes the suspended transport through the diversion. The effectiveness is expressed as a percentage of the released sediment compared to the released flow. The released flow is 5%, which implies a percentage higher than 5% indicates an efficient diversion site, and the contrary an inefficient site.

Moreover the ratio of sand which is released is shown. At the upstream boundary the sediment ratio for clay, silt and clay is 54, 35 and 11 % respectively. This means when the diversion succeeds in diverting a higher ratio of sand, the diversion would also be more effective. Sand is assumed more appropriate for delta building purposes, because it is coarser material.

Table 6.1: Results for diversion sites

Diversion site	Sediment released (Q_s) [%]	Sand released (Q_{sand}) [%]
West Bay	4.63	11.0
1	5.12	17.3 ⁴
2	4.42	7.5
3	4.33	5.7
4	5.02	18.8
Doubled 1	5.12	17.3

The simulations show the contribution of bed-load transport through the diversion is negligible (bed-load transport = 0.01 kg/s with respect to suspended transport = 250 kg/s).

Conclusions

The performance of the doubled diversion at diversion site 1 seems to be the best. The diversions at site 1 only differ in their width, which results for the doubled diversion in more representative velocities that flow through the diversion. Therefore this diversion is used for simulations with different scenarios, which is treated in section 6.5. The study on the ideal location also shows the diversions in the inner bend have more ability of extracting the sediment than the ones in the outer bend. On the contrary, Nittrouer *et al.* states the outer bends downriver of a straight reach are most suitable of diverting sediments to the wetlands [Nittrouer *et al.*, 2008].

From the study of Pereira it can be learned that increasing the size of the diversion even further and additionally increase the extracted flow, would result in negative impact on the Lower Mississippi River. The extraction of too much flow leads to too little transport capacity of the flow, which results in extra sedimentation problems [Pereira, In Press]. Therefore this variant is not applied in this study.

⁴ Ratio clay, silt and sand is; 50.0, 32.7 and 17.3 % respectively

6.5 Impact of sediment diversions

Long-term simulations were done to evaluate the impact of diversions on the dredging activities. Four scenarios were simulated, see figures 6.18 and 6.19. The first simulations use the settings derived from hydrodynamic and morphodynamic calibration. The second simulations use the settings with the increasing mud deposition settings. The simulations give insight into the effect of implementing new sediment diversions or closing off existing ones and the effect on the dredging quantities. One simulation is done with a control structure, so no flow is released from the river during low flow and one simulation is done without a control structure. Water and sediment can be diverted from the river all year round.

1. Base case scenarios, all settings remain the same as during the calibration.
2. Closing off West Bay Diversion, many discussions are going on about this diversion. It would be interesting to study what would be the response of this model, as already introduced in section 6.3.
3. An open diversion, which extracts flow throughout the year.
4. Controlled diversion, the diversion is closed during low flow.

The new flow distribution over the distributaries after implementing a diversion is assumed according to the existing distribution from Davis (In Press). The 1D model of Davis should be consulted in order to get a proper distribution, therefore it should be taken in mind [Davis, In Press].

Results

Figures 6.18 and 6.19 show the simulated dredging activities for the scenarios (with two different settings) and the results are summarized in table 6.2. The figures demonstrate the dredging activities for the base case scenario are the highest. Closing off the West Bay diversion has influence on the dredging quantities. A controlled diversion seems favorable with respect to the open diversion.

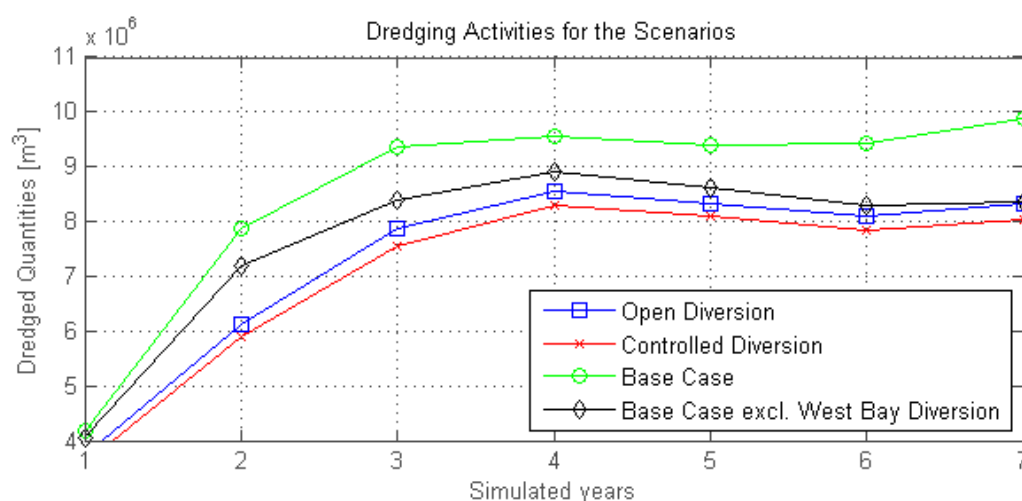


Figure 6.18: First simulated Dredging Activities for the scenarios (according calibration settings)

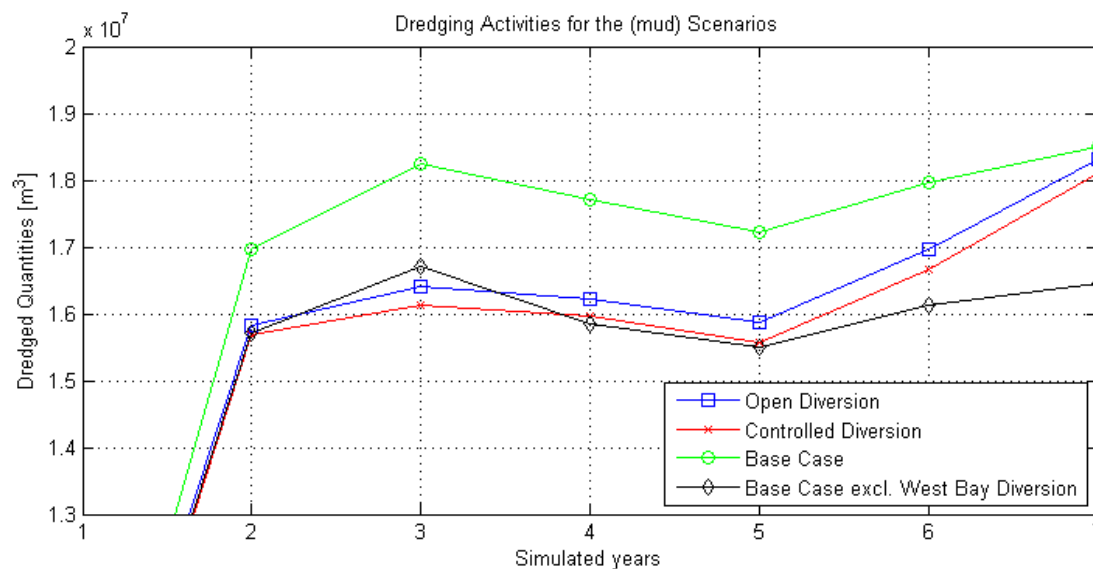


Figure 6.19: Second simulated Dredging Activities for the scenarios (according to mud sensitivity scenario)

Table 6.2: Results from Dredging Simulations

Scenario	# sim.	Calibrated settings		Mud sensitivity scenario	
		$M^* \times 10^6 [m^3]$	$E^{**} \times 10^6 [m^3]$	$M^* \times 10^6 [m^3]$	$E^{**} \times 10^6 [m^3]$
Base Case, incl. West Bay Diversion	7	8.53	9.53	16.40	17.93
Excl. West Bay Diversion	8	7.69	8.52	14.91	16.13
Open Diversion	ED1	7.29	8.24	15.40	16.76
Controlled Diversion	ED2	7.05	7.97	15.13	16.48

*) M = mean over 7 years

**) E = mean after equilibrium is reached

Conclusions

The relative difference between the simulations for the different settings is comparable. This verifies that the morphological calibration parameters have relative influence on the model results. Roughly the multiplication factor is 1.9. Even though closing off West Bay Diversion is even more effective for the second simulation settings.

In general these model results (simulations) show the location substantially affects the dredging activities. The following statements about the model performance are with respect to the base case scenario:

Having a diversion in the dredging reach negatively influences the activities. Therefore closing off the West Bay diversion has a positive effect on the dredging quantities. Less material needs to be dredged from the river. According to these simulations closing off the West Bay Diversion would have a significant effect of 10%.

The simulations with a new diversion endorse the method of using a control structure for the sediment diversion. As a result of the simulations it can be assumed the control structure positively influences the dredging activities. By closing off the diversion during low flow more navigable depth

remains, therefore less dredging activities are necessary to maintain the fairway. Namely during the low flow season all the available flow is needed to maintain a navigable depth in the river. The flow is already enormously decreased for the most downstream river kilometers by all the distributaries and the water depth in this region is already critical. Additional diversion of flow by adding new sediment diversion during the low flow season is therefore undesirable.

The method of using a control structure to only divert flow from the river during intermediate and high flow goes well with the fact that there is only little sediment transport during low flow. During these flow seasons the water depth in the river is less critical.

Diverting sediment during low flow would not have much effect, because of the low sediment transport rates. Therefore it seems unlikely to implement a new sediment diversion without a control structure.

6.6 Optimizing the sediment diversion in the inner bend of river

The previous section suggested that the optimal location for the sediment diversion is in the inner bend of the river. The shallow water depth is ideal to divert sediment from the river. An important physical phenomenon is the basis for the effectiveness of this process i.e. helical flow.

Basic phenomenon in river bends

Helical flow as represented in figure 6.20 is a phenomenon that occurs in river bends. As a result of a positive pressure gradient, because the water level in the outer bend is slightly lifted and the presence of centrifugal forces, because of the curvature of the bend, a helical flow is present in river bend.

This phenomenon has the effect the river bed in the outer bend is subjected to erosion. The outer bends in the Mississippi River are protected and therefore the tendency to further grow and migrate is blocked as explained in section 2.1. The consequence is that the depth in the bends further increases. This also explains the occurrence of 50 m deep bends.

The flow in the cross-sectional direction of the river bend lifts up the sediment from the outer bend and deposits them in the inner bend. The sediments in the bends are spatially segregated, due to gravity; usually the coarse material is in the outer bend and the fines are in the inner bend.

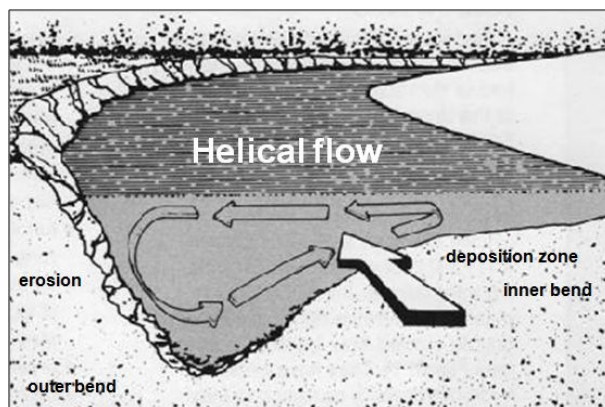


Figure 6.20: Helical flow in river bends, Modified [Odgaard, 2009]



Figure 1-6. Submerged vanes (early version) in East Nishnabotna River, Iowa, protecting stream bank against erosion. View is downstream at extreme low flow, showing vane-induced sediment deposition along right bank. The sediment deposits provide natural toe protection at the bank.

Figure 6.21: Submerged vanes in the river [Odgaard, 2009]

Submerged Vanes

According to Odgaard submerged vanes can be applied to prevent sediment from entering (water) intakes in the river. The application of these vanes the other way around might also work. The vanes guide the sediments to flow in the desired direction. Figure 6.21 shows an example of the application of submerged vanes in order to protect stream bank erosion. When the vanes are directed to the diversion they might influence the effectiveness of the diversion. Therefore the vanes could contribute to divert more sediment from the river. [Odgaard, 2009]. Additional research is necessary.

Structures

The simulations imply that a use of a controlled structure is favorable. Many options for control structures to divert sediment from the river exist; two examples of designs are given. Further investigation, for instance with 3D-modeling, could reveal what would be an optimal structure. The sector gated structure (figure 6.23) is in favor because research in Mississippi has shown the sediment concentrations in the water column are evenly distributed. Therefore it is more effective to extract the entire flow. It also would be most cost effective [Dijkman, 2007; Meselhe *et al.*, In Press].

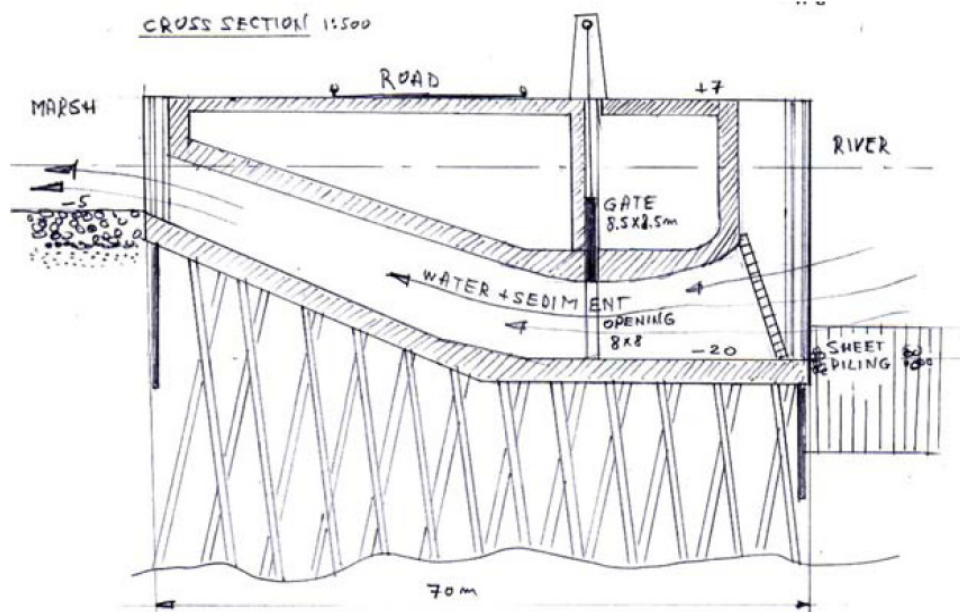


Figure 6.22: Preliminary design a sediment of diversion [Dijkman, 2007]

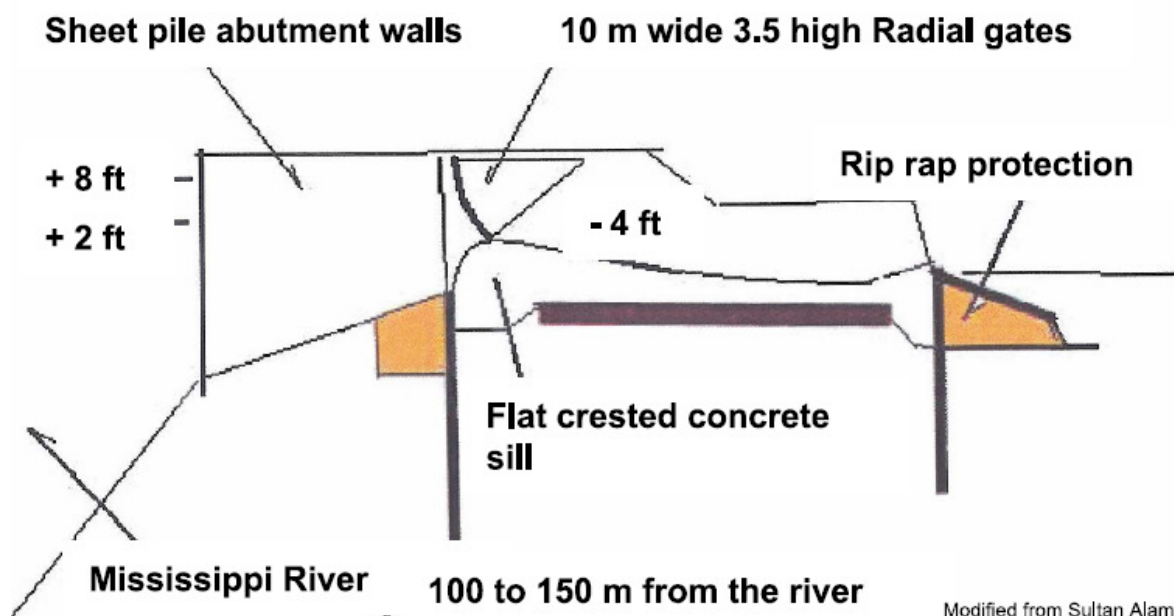


Figure 6.23: Control structure [Harrison *et al.*, 2009]

Chapter 7. Conclusions & Recommendations

7.1 Conclusions

The study shows a 2DH-numerical is appropriate to investigate the behavior and problems of the Lower Mississippi River. The hydrodynamic behavior in the model has been calibrated with a data set from 2001 to 2009 and verified with an independent data from 2010. The model can contribute to analyzing implementations of river engineering interventions in the river and subsequently the effects and impacts of them. For instance to what extent the interventions influence the dredging activities in the river.

The objective was to study sediment diversions in the Mississippi River and to assess the amount of sediment that can be diverted from the river, for delta building purposes, while minimizing the impact on navigability of the river (i.e. no significant increase in maintenance dredging efforts). The questions are addressed and conclusions can be drawn:

What would be the impact of the implementation of diversions to the river system?

Additional diversions: strategically place additional diversion have different effect on the morphological response. The study shows extracting flow and sediment further upstream has beneficial effects compared to extracting flow and sediment right above Head of Passes (at the mouth of the river) like the West Bay diversion does. The beneficial effects are: no disturbance of the flow pattern at the mouth of the river. Flow is optimally used to transport sediment transport instead of depositing it and unwanted locations. Convey sediments upstream, that way a part of the sediments could not reach the problematic areas and the sediment could be used for delta building purposes.

West Bay diversion: simulations show that closing off West Bay diversion has a positive effect on the dredging quantities. This implies the location of a sediment diversion is pretty determining. The location of the West Bay diversion is not ideal. The flow pattern near the diversion stimulates the sedimentation process downstream of the entrance. The flow pattern with a closed diversion is more concentrated in the main channel, which enhances sediment transport rate. Therefore more erosion of the bed is present, which implies a lower bed level.

What would be the best location for the implementation of river diversions for delta building purposes, with minimum impacts?

Optimal diversion site: the best diversion site for this study area is found in the inner bend of the river upstream of Empire at RK 53. This site shows the best performance and efficiency. The site has the ability to convey large quantities of sand through the diversion. Sand is the most interesting for land building purposes.

Delta building capabilities: the simulated new diversion shows higher values for sediment transport through the diversion. This concludes the delta building capability would be also more than for the West Bay diversion. USACE designed its capability at 2 km² a year (9831 acres in 20 years) [USACE,

2004]. Barras expects a land loss rate of approximately 77 km² a year [Barras, 2003]. This means ~38 small equivalent diversions would be necessary. This is not possible with respect to the available resources and the demand of navigability on the river.

Contrarily the diversions positively help the delta building process, but only have a small contribution. It should be placed in perspective. Creating a sustainable delta is therefore of a multidisciplinary matter.

Is it possible to sustain a navigable fairway in the Mississippi River with limited dredging cost?

Analysis of the river bed response: the river bed in the study area can be divided into three categories. Upstream of RK 4 the bed is subjected to erosion, around RK 4 the bed is practically in equilibrium as a result of the dredging activities and downstream of RK 4 the bed is heavily subjected to sedimentation. The reach downstream of RK 4 is also the dredging reach; after analyzing the long-term simulation of 20 years with and without dredging activities it can be concluded the navigability in the river is under great pressure. The simulations and the observed trend of the dredging activities show it is not expected the dredging quantities and costs will suddenly decrease in the future.

7.2 Recommendations

Several recommendation are given for further research.

Redistribution of flow: further cooperation with a 1D hydrodynamic model is recommended, which is capable of redistributing the flow when diversions are implemented.

Dredging strategies: River managers should come up with new management strategies to maintain a sustainable navigable fairway. Further research (for example with the existing model) with various dredging strategies would help to give more insight.

West Bay diversion: closing off West Bay diversion seems desirable from the model results in terms of minimizing the dredging activities. It could be that adequate sediment management strategy with the implementation of extra diversions upstream results in optimal conditions for the dredging activities downstream. Further research with the model could verify this statement.

Optimization of diversion site: The ideal diversion site can be further optimized. A study can be done to the optimal flow release angle. Lessons can be learned from the West Bay Diversion, which has a reverse angle to the flow.

Implementation of vanes: 3D-modeling with the gained boundary conditions from this research could be done, to see what the detailed impact of the diversion is and to investigate what is the best way to build a diversion. For instance how can bottom vanes help in designing and implementing

sediment diversion with high efficiency? Therefore the study of Odgaard could be taken into account [Odgaard, 2009].

Mud sedimentation processes: the morphological calibration reveals corresponding mud transport rates. The sedimentation process has been tried to be simulated, but this is hard and there are little or no calibration data available. Therefore it would be interesting to get more into detail with the mud transport and especially the sedimentation processes of the mud in the lower reach of the study area. The recommendation is to gather more data. Also the influences of salt wedges in the lower reach of the river should be taken in account. Therefore salinity has to be added to the model, which is an option in Delft3D.

Reveal best morphological settings

The morphological calibration of a numerical model is difficult. Many parameters have an influence on the model behavior. The way the model responses is not really straight forward. Continuous research and applications of the model would help to understand the morphological behavior in the Lower Mississippi River. Next to adding more features to the model it would be wise to reconsider and verify all defined morphological settings.

More detail in discharge schematization

For future research it is worthwhile to introduce more detail in the discharge distribution, for example by definition of eight discharge levels to get a more accurate behavior of the river. The three levels described above seem most reasonable within the capabilities and timeframe of this study, because for every discharge level calibration and verification of the model has to be carried out (see section 4.3 en 4.4).

Navigable depth and channel width: Research is recommended in the field of navigability of the river and the demand from the industry. For instance changing the navigable depth to a lower draught would decrease the dredging quantities because the depth in the river would reach more its equilibrium. Therefore simulations can be done with widening the navigation channel and increasing or decreasing its dredge depth and see what the impact is on the dredging quantities. It should be considered if this is desirable and realistic.

Hydro-graphic Survey: a new single beam hydro-graphic survey of the entire Lower Mississippi is desirable to be able to calibrate the bed topography of the entire reach instead of only dredging reach. Even more worthwhile and stronger recommended would be a multi beam survey of the entire Lower Mississippi River, like figure 7.1. The bed topography can be studied in great detail. This is very useful with studying bed composition and the development of sand dunes on the river bed. It would also contribute the mud sedimentation research.

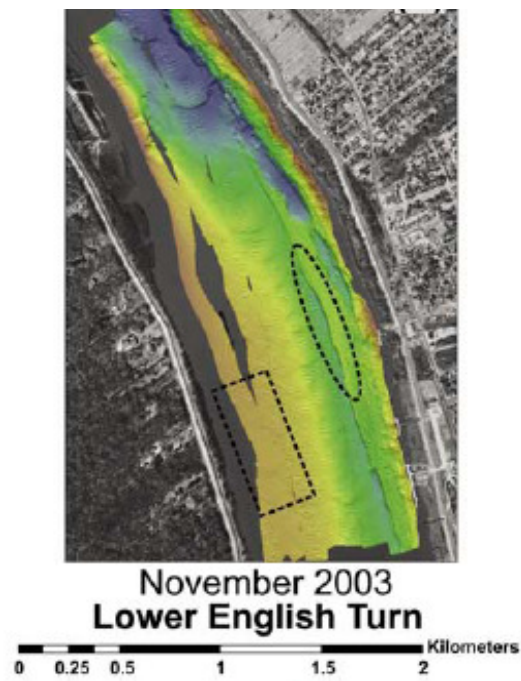


Figure 7.1: Topography obtained from a multibeam survey in the Mississippi River at Lower English turn (RK 132-137). Modified [Nittroer *et al.*, 2008]

Extra features in Delft3D: River training projects will be very interesting to investigate and to implement in the model. This additional implementation will positively influence the morphological behavior in the dredging reach, which eventually leads to less dredging activities. Figure 7.2 shows the river training structure in the developed model. Eventually no calibration with the added structures has been done, therefore no conclusions can be drawn from this extra feature.

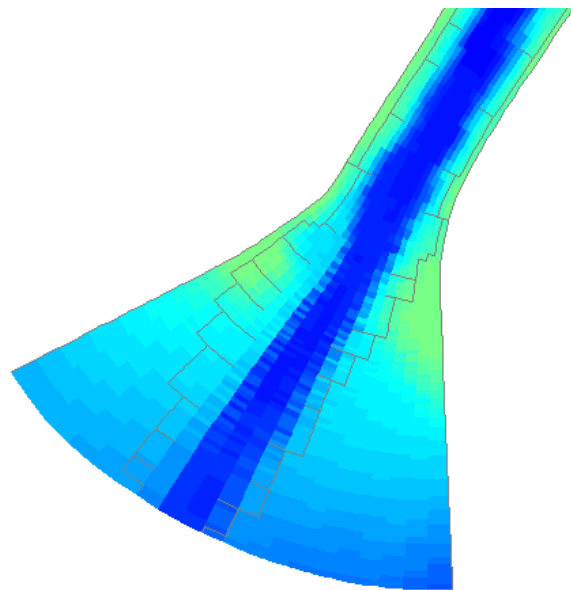


Figure 7.2: River training structures in the developed model

Chapter 8. References

America's Resource Center, Schematized Mississippi River /Percentages of flow to Atchafalaya River.

http://www.americaswetlandresources.com/background_facts/detailedstory/LouisianaRiverControl.html, Accessed January 2011

Allison M.A., E.A. Meselhe (2010) - The use of large water and sediment diversions in the lower Mississippi River (Louisiana) for coastal restoration, *Journal of Hydrology* 387, pp.346–360

Ashurst, T.M. (2007) – Sediment Flux and fate in the Mississippi River Diversion at West Bay: Observation study, MS thesis, LSU

Barbé, D.E., K. Fagot and J.A. McCorquodale (2000) – Effects on dredging due to diversions from the Lower Mississippi River. *Journal of Waterway, Port, Coastal, and Ocean Engineering*, May/ June 2000, UNO, New Orleans, LA

Barras, J., S. Beville, D. Britsch, S. Hartley, S. Hawes, J. Johnston, P. Kemp, Q. Kinler, A. Martucci, J. Porthouse, D. Reed, K. Roy, S. Sapkota, and J. Suhayda (2003) - Historical and Projected Coastal Louisiana Land Changes: 1978-2050, USGS, US Department of Interior, Open File Report 03-334, 39 p. (Revised January 2004)

Bourne (2004) – Gone with the water. *National Geographic Magazine*,
<http://ngm.nationalgeographic.com/ngm/0410/feature5/text2.html>, Accessed: January 2011

Brantley, C. (2010) – Personal Communication, Manager Bonnet Carre Spillway, site visit, November 24, 2010

Bryant (2011) – Mississippi sediment and fresh water flow, <http://web.bryant.edu/~dml1/sc366/deltas/deltas.htm>, Accessed: March 2011

Bunya, S., J.C. Dietrich, J.J. Westerink, B.A. Ebersole, J.M. Smith, J.H. Atkinson, R. Jensen, D.T. Resio, R.A. Luettich, C. Dawson, V.J. Cardone, A.T. Cox, M.D. Powell, H.J. Westerink, H.J. Roberts (2010) – A High-Resolution Coupled Riverine Flow, Tide, Wind, Wind Wave, and Storm Surge Model for Southern Louisiana and Mississippi. Part I: Model Development and Validation, American Meteorological Society

Davis (In Press) - Numerical Simulation of Unsteady Hydrodynamics in the Lower Mississippi River, A MSc-Thesis, May 2010

Day, J.W., Donald F. Boesch, Ellis J. Clairain, G. Paul Kemp, Shirley B. Laska, William J. Mitsch, Kenneth Orth, Hassan Mashriqui, Denise J. Reed, Leonard Shabman, Charles A. Simenstad, Bill J. Streever, Robert R. Twilley, Chester C. Watson, John T. Wells, Dennis F. Whigham (2007) - Restoration of the Mississippi Delta: Lessons from Hurricanes Katrina and Rita, *SCIENCE VOL 315* (www.sciencemag.org) pp.1679-1684

Dean, C. (2006) - Time to move the Mississippi, Experts Say, *The New York Times*.
<http://www.nytimes.com/2006/09/19/science/19rive.html>, Accessed: September 2010

Deltares (2010) - Delft3D-FLOW User Manual, version 3.14

Deltares, Delft3D software: <http://delftsoftware.wldelft.nl/index.php>, Accessed: February 2011

De Vries, M. (1965) – ‘Considerations about non-steady bed-level transport in open channels’. *Proc., 11th Congress IAHR*, Leningrad, pp. 3.8.1-3.8.8

De Vriend, H., H. Havinga, P.J. Visser, Z.B. Wang (2010) – Lecture notes River Engineering, Delft University of Technology

Dijkman (editor) (2007) - A DUTCH PERSPECTIVE ON COASTAL LOUISIANA FLOOD RISK REDUCTION AND LANDSCAPE STABILIZATION, London, Netherlands Water Partnership (NWP), Appendix D Hydraulics and Morphology

Eaglespeak (2010) - Mississippi Drainage Basin, <http://www.eaglespeak.us/2010/02/waterways.html>, Accessed: January 2011

Easley, H. (2000), http://www.daleeasley.com/resources/Essays/FLD_TRIP.html, UNO to Old River, Accessed: January 2011

Galappatti, R. and Vreugdenhil, C.B. (1985) - A *depth-integrated model for suspended sediment transport*. *J. Hydr. Res.*, 23(4): 359-377.

- Galler, J.J., M.A. Allison (2008) – Estuarine controls on fine-grained sediment storage in the lower Mississippi and Atchafalaya Rivers. *Geological Society of America Bulletin* 120, 386-398
- Galloway (1992) – Delta classification, from lecture notes Coastal Dynamics I: Bosboom, J., M. Stive (Delft University of Technology)
- Georgiou, I.Y. (2011) – Personal Communication, Venice gage station, uncertainty for low flow, December 2010
- Google Earth (2011) – Visualization of Study Area, <http://www.google.com/intl/nl/earth/index.html>
- Google maps, <http://www.maps.google.com>, maps of Mississippi Delta, Accessed: December 2010
- Harrison, P., A. Freeman, M. Wood (2009) – Myrtle Grove Sediment Diversion plan, <http://www.mvd.usace.army.mil/lcast/pdfs/09mar/Harrison%20and%20Freeman%20-%20Myrtle%20Grove%20Land%20Building%20Diversion.pdf>, Accessed: January 2011
- Hudson, P.F., R.H. Kesel (2000) – Channel migration and meander-bend curvature in the lower Mississippi River prior to major modification. *Geology* 28, 531-534.
- HydroQual, Inc. (2002) - A primer for ECOMSED. Users Manual, Ver. 1.3, HydroQual, Inc., Mahwah, New Jersey, pp. 188.
- IPCC (2007) - Summary for Policymakers. In: *Climate Change 2007: The Physical Science basis. Contribution of working group I to the Fourth Assessment Report of the Intergovernmental Panel on Climate Change*. Cambridge University Press, Cambridge, United Kingdom and New York, NY, USA.
- Jansen, P.Ph., L. van Bendegom, J. van den Berg, M. de Vries en A. Zanen (1979) - *Principles of River Engineering*. Pitman, Londen, 509 pp.
- Karadogan, E., C.S. Wilson, C.R. Berger (2009) - Numerical Modeling of the Lower Mississippi River—Influence of Forcings on Flow Distribution and Impact of Sea Level Rise on the System, Louisiana State University, Baton rouge, LA
- Karadogan (2010) – Personal Communication and presentation; Hydro- and Morphodynamic Finite Element Model; Overview of his research , December 2010
- Kemp, P. (2010) – Mississippi/ Atchafalaya River and Delta management for the Future, National Audubon Society, McNeese University, August 19, 2010
- Kesel, R.H., E. Yodis, D. McCraw (1992) – An approximation of the sediment budget of the lower Mississippi River prior to major human modification. *Earth Surface Processes and Landforms* 17, 711-722
- Kesel, R.H (2003) – Human modifications to the sediment regime of the Lower Mississippi flood plain, *Geomorphology* 56 (2003) 325-334, Baton Rouge, LA
- Kim, W., D. Mohrig, R. Twilley, C. Paola, and G. Parker. (2008) - Land Building in the Delta of the Mississippi River: Is it Feasible?, Chapter 10. In, R.R. Twilley (ed.), *Coastal Louisiana Ecosystem Assessment & Restoration (CLEAR) Program: A tool to support coastal restoration. Volume IV. Final Report to Department of Natural Resources, Coastal Restoration Division, Baton Rouge, LA. Contract No. 2512-06-02.*
- Kleinhans, M. G., H. R. A. Jagers, E. Mosselman, and C. J. Sloff (2008) - Bifurcation dynamics and avulsion duration in meandering rivers by one-dimensional and three-dimensional models, *Water Resour. Res.*, 44, W08454, doi:10.1029/2007WR005912.
- Koch, F. G. and C. Flokstra (1980) – “Bed level computations for curved alluvial channels.” in proceedings of the XIXth congress of the International Association for Hydraulic Research, 2-7 feb. 1981, New Delhi, India, vol. 2, pages 357-364. 352
- Meselhe, E.A., J.F. Pereira, I.Y. Georgiou, M.A. Allison, J.A. McCorquodale and M.A. Davis (2010) - Numerical modelling of mobile-bed hydromatics of the Lower Mississippi, University of Louisiana at Lafayette, Lafayette, LA, not in press
- Meselhe, E.A., I.Y. Georgiou, M.A. Allison and J.A. McCorquodale (2011) – Abstract, Myrtle Grove Delta Building Project, http://gsa.confex.com/gsa/2011SC/finalprogram/abstract_186999.htm , Accessed: March 2011

- Meselhe, E.A., I.Y. Georgiou, M.A. Allison and J.A. McCorquodale (In Press) – Personal communication, Results of numerical modeling study, summarized in presentation, April 2011
- Mossa, J. (1996) – Sediment dynamics in the lowermost Mississippi River. University of Florida, FL, Engineering Geology 45 (1996), 457-479
- Mosselman, E., C.J. Sloff, H.R.A. Jagers (2005) – *Voorspelinstrument duurzame vaarweg. Voorbereiding. Rapport Q3963*, in Dutch, WL|Delft Hydraulics
- National Research Council (NRC) (2009) - Final Report from the NRC Committee on the Review of the Louisiana Coastal Protection and Restoration (LACPR) Program, THE NATIONAL ACADEMIES PRESS 500 Fifth Street, N.W. Washington, DC 20001, <http://www.nap.edu/catalog/12708.html>
- NGS, National Geodetic Survey (1999a) The method that describes the conversion of the Vertical datum http://www.ngs.noaa.gov/TOOLS/Vertcon/vert_method.html, Accessed: November 2010
- NGS, National Geodetic Survey (1999b) The converter, http://www.ngs.noaa.gov/cgi-bin/VERTCON/vert_con.prl, Accessed: November 2010
- Nittrouer, J.A., M.A. Allison, R. Campanella (2008) – Evaluation of bed-load transport in the lower Mississippi River: implications for sand transport to the Gulf of Mexico, JOURNAL OF GEOPHYSICAL RESEARCH-Earth Surface Processes, VOL. 113, F03004, doi:10.1029/2007JF000795, University of Texas, TX
- Notre Dame (2010) Riverine Flows, Tides and Surge in the Lower Mississippi River and Delta and Atchafalaya River and Delta <http://nd.edu/~coast/projects.html>, Accessed: September 2010
- Odgaard (2009) – River training and sediment management with submerged vanes, ASCE, ISBN 978-0-7844-0981-7
- Open Earth Tools (OET) (2011) – Used as visualization tool together with Google Earth, <http://public.deltares.nl/display/OET/OpenEarth>
- Ottevanger, W., M.F.M. Yossef (2006) – Voorspelinstrument duurzame vaarweg: rooster uitbreiding met Beneden Merwede en Nieuwe Merwede, in Dutch, WL|Delft Hydraulics
- Parker, G. (2004) – E Book & Excel sheets; 1D Sediment transport Morphodynamics with applications to rivers and turbidity currents, Chapter 2 & 4 http://vtchl.uiuc.edu/people/parkerg/morphodynamics_e-book.htm, Accessed: January 2011
- Parker, G., O. Sequeiros (2006) - Large Scale River Morphodynamics: Application to the Mississippi Delta, River Flow 2006 Conference, Lisbon, Portugal, Sept, 6 – 8, 2006 (Balkema), ISBN 0-415-40815-6
- Parker, G. (2009) – Modeling the Morphodynamics of the Lower Mississippi River as a Quasi-Bedrock Stream, <http://www.wun.ac.uk/sites/default/files/mississippimodelbedrockwun-09.pdf>, Accessed April 2011
- Partheniades, E., (1965) – “Erosion and Deposition of Cohesive Soils.” Journal of the Hydraulics, Division, ASCE 91 (HY 1): 105-139. 82, 336, 560
- Pereira, J.F., J.A. McCorquodale, E.A. Meselhe, I.Y. Georgiou, M.A. Allison (2009) - Numerical Simulation of Bed Material Transport in Lower Mississippi River, Journal of Coastal Research, Portugal, SI 56, pp. 1449-1453, ISSN 0749-0258
- Pereira (2010) - Personal communication, use of 1D model of Davis 2010 for determining discharge distribution over the distributaries & calibration of hydrodynamic model.
- Pereira (In Press) - Numerical Modeling of River Diversions in the Lower Mississippi River, A Dissertation, May 2011
- Port of New Orleans (2011) - facts and numbers, http://www.portno.com/pno_pages/about_overview.htm, Accessed: January 2011
- Reed, D.J. (2009) - A New Approach to River Management: Action for a Sustainable Coastal Landscape, *Journal of Contemporary Water Research & Education*, Universities Council on Water Resources (UCOWR), New Orleans, LA, Issue 141, Pages 35-38
- Schleifstein, M. (2010) – West Bay Diversion project on Mississippi River to end, JAN 2010, Times Picayune, http://www.nola.com/politics/index.ssf/2010/01/west_bay_diversion_project_on.html, Accessed: September 2010

- Sloff, C.J. (2010) - Personal Communication. Bedform rates in the 'Waal' river, December 2010
- Struiksmas, N., K. Olesen, C. Flokstra, H.D. Vriend (1985) – Bed deformation in curved alluvial channels, *J. Hydraul. Res.*, 23(1). 57-79
- Talmon A.M., M.C.K.M. Van Mierlo, N. Struiksmas (1995) – Laboratory measurements of the direction of sediment transport on tranverse alluvial-bed slopes. *Journal of Hydraulic Research* 33(4), pp. 495-517
- Thorne, C., O. Harman, C. Watson, N. Clifford, D. Biedenharn, R. Measures (2008) - Current and Historical sediment loads in the Lower Mississippi River, European Research Office of the US Army, London, England, University of Nottingham
- USACE (2009) – LACPR program, plans and strategies, http://lacpr.usace.army.mil/default.aspx?p=LACPR_Final_Technical_Report, Accessed: September 2010
- Ulm (2010) - Personal Communication, Operational Manager of dredging activities and river maintenance, Data and explanation of Dredging Cost and Strategy of Mississippi River (Baton Rouge to Gulf of Mexico), December 2010
- Ulm (2011) – Dredging schedule Lower Mississippi, FY 2011, March 2011
- USACE (2004) – Fact sheet, <http://lacoast.gov/new/Projects/Info.aspx?num=mr-03>, Accessed: October 2010
- USACE (2007) - Survey maps, <http://www.mvd.usace.army.mil/navbook/riverMain.aspx#imgmap0>; Accessed: December 2010
- USACE (2009a) – LACPR report, <http://www.lacpr.usace.army.mil/default.aspx?p=report>, Accessed: October 2010
- USACE (2009b) - Presentation; Keith Martin, Gary Brown, and Phu Luong - MR-03 Special Technical Committee Meeting Dec. 1 2009 - Presentations - 6 of 6 Multi-Dimensional Modeling (2009); <http://lacoast.gov/new/Projects/Info.aspx?num=mr-03>, Accessed: September 2010
- USACE (2010) – Dredging strategies, <http://www.mvn.usace.army.mil/od/FY11MississippiRiverSouthwestPass.pdf>, Accessed: December 2010
- USACE (2011) - River gages, <http://www2.mvr.usace.army.mil/WaterControl/new/layout.cfm>, Accessed: January 2011
- USACE (2011) USACE water control website. <http://www.mvn.usace.army.mil/eng/edhd/tar.gif>, Observed discharge, Army Corps of Engineers, Accessed: February 2011., May 2011
- USACE (2011) - Stage and discharge dataset, <http://www.mvn.usace.army.mil/eng/edhd/wcontrol/miss.asp>, Accessed: October 2010, January 2011
- USACE (2011) – Medium diversion at Myrtle Grove with dedicated dredging, stakeholders update meeting, February 2011 (LCA).
- USGS (2003), 100+ Years of Land Change for Southeast Coastal Louisiana, <http://www.nwrc.usgs.gov/upload/landloss8X11.pdf>, Accessed September 2010
- USGS Press release (2006), Latest land change estimates, http://www.nwrc.usgs.gov/releases/pr06_002.htm, Accessed: September 2010
- Van Rijn, L.C. (1993) – Principles of sediment transport in rivers, estuaries and coastal seas. Amsterdam: Aqua Publisher
- Van Rijn, L.C. (2007a) - Unified View of Sediment Transport by Currents and Waves. I: Initiation of Motion, Bed Roughness, and Bed-Load Transport, *Journal of Hydraulic Engineering*, Vol. 133, No. 6, June 1, 2007. ©ASCE, ISSN 0733-9429/2007/6-649–667
- Van Rijn, L.C. (2007b) - Unified View of Sediment Transport by Currents and Waves. II: Suspended Transport, *Journal of Hydraulic Engineering*, Vol. 133, No. 6, June 1, 2007. ©ASCE, ISSN 0733-9429/2007/6-668–689
- Van Ledden (2003) – Sand-mud segregation in estuaries and tidal basins, dissertation Delft University of Technology, ISBN 90-9016786-2

Wilson (2008) - Small scale Physical model of the Lower Mississippi,

http://www.lwrri.lsu.edu/downloads/2008%20Louisiana%20Coastal%20Engineering%20Conference/Presentations/Wilson_TheMississippiRiveranditsRoleinRestorationEfforts.pdf, Accessed: December 2010

Winterwerp (1989) – Flow induces erosion of cohesive beds. A literature survey. In Cohesive Sediments (Rep. 25). Delft:

WL|Delft Hydraulics and Rijkswaterstaat

Yossef, M. C. Stolker, S. Giri, A. Hauschild and S. van Vuren (2008) – '*Voorspelinstrument duurzame vaarweg*', in Dutch, WL | Delft Hydraulics (Q4357.20)

Appendices

Appendix A: Port of New Orleans

Figure A.1 shows the location of the Port of New Orleans in red at RM 96 (RK 154), the yellow line represents the navigation deep channel fairway of the Mississippi river. Further upstream there are also two other ports; Port of South Louisiana and the Port of Baton Rouge. The red line is also the stretch that is noted in table 2, which represents the dredging cost to maintain the 45 ft (15 m) for mooring of the vessel at the quay.



Figure A.1: Map of Port entrance and Port strip; Port of New Orleans [Google Earth, 2011]

Facilities and numbers of the Port of new Orleans

The Port can accommodate an average of 2,300 vessel calls a year. The port has 4 gantry cranes which have an annual capacity of 366,000 TUE. (2010 Rotterdam 11.1 million TUE) There are contracts awarded for two addition gantry cranes (planned to be built in 2010). In the next ten years the port will do an investment of \$500 million and wants to triple the size to get a capacity of more than 1.3 million TUE. The quay has a length of 3.2 km and can handle 15 vessels simultaneously. Besides that the port has an unlimited turning basin.

The port has a good access to the inner land by an interstate highway and all six Class 1 rail lines. The port claims to be the most intermodal Port in America. The location of the port is ideal on the 14,500-mile (23,200 km) Mid-America inland waterway system. On annual bases more than 6,000 ocean vessels move through New Orleans on the Mississippi River. The cargo they issue is; rubber, steel, coffee, containers and manufactured goods [Port NO, 2010].

Appendix B: Lower Mississippi River control structures

Old River Structure

The course of the river is man-made; the Mississippi river tried to shift back to the Atchafalaya River, first early 1800 and later in the mid 1900. In 1831 the engineers prevent that from happening and cut-off the river, this was done by supervision of Capt. Henry M. Shreve, see figure B.1. Therefore the river chose the Mississippi River again as the main track.

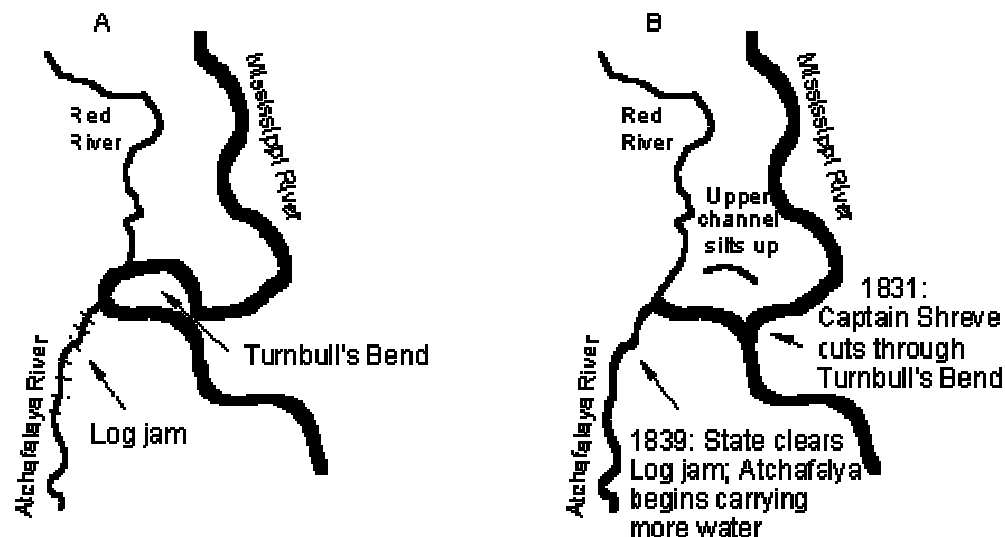


Figure B.1: Cut-off the Mississippi River [Easley, 2000]

But the cut-off only helped for 100 years, because the river again wanted to switch to the Atchafalaya River. If the river would change in the other direct, the problem would be drastic for Southern Louisiana. Probably the Mississippi delta would turn into a salt water estuary and the Port of New Orleans would be abandoned. This would mean no drinking water or a navigable fairway for New Orleans and Baton Rouge. Therefore the Old River structure was built in 1951 at that diverting point. Today this structure diverts 30% to the Atchafalaya River and 70% to the lower Mississippi River at all times.

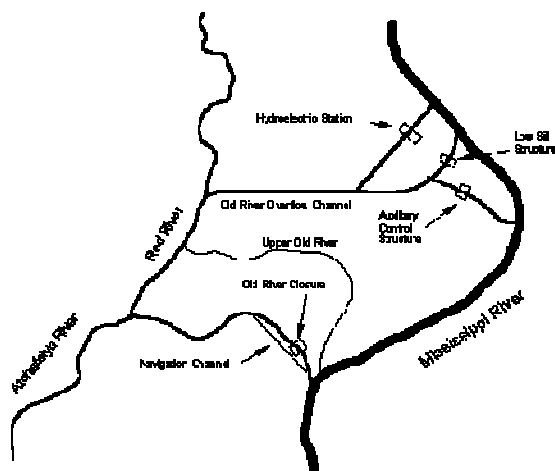


Figure B.2: Overview of control structures built by USACE [Easley,2000]

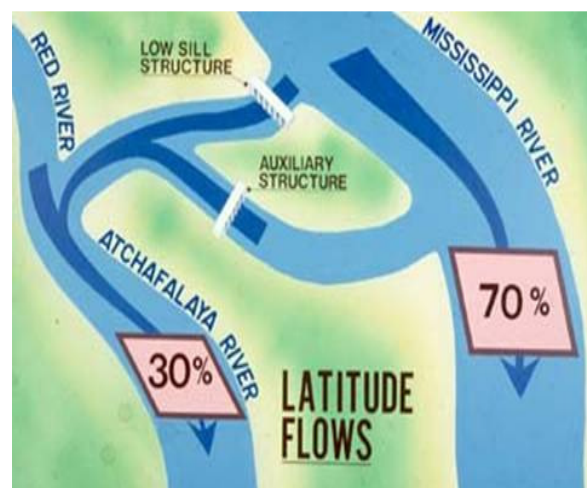


Figure B.3: Schematization of river flow distribution [America's Wetland Resources Center, 2011]

Table A.1: Overview of percentages flow to Atchafalaya River [America's Wetland Resources Center, 2011]

Year	Percentage
1850	<10.0
1900	13.0
1920	18.1
1940	23.3
1950	30.0
1973	34.6
1974	34.7
1975	34.9
1976	31.8 (Partial control restored)
1977-1985	30.0 (Full control)

Directly downstream of the Old River Structure is Talbert Landing (RM 306), a gauging station of the USACE operating at that location since 1963, see Figure B.5 [Allison *et al.*, 2010]. The station measures flow discharges, stages and sediment concentrations that enter the lower Mississippi River. The figure also gives a clear overview of the area [Brochure Old River Structure USACE].

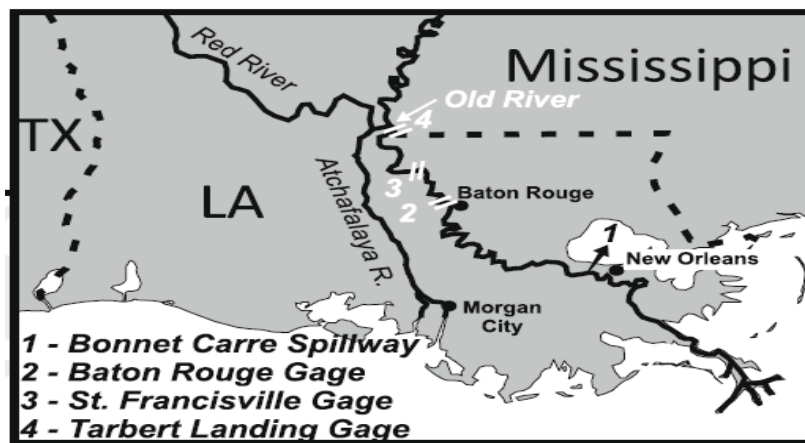


Figure B.5: Lower Mississippi [Allison & Meselhe, 2010]

Bonnet Carre Spillway

The Bonnet Carre Spillway was constructed in 1932 direct after the flood of 1927 that flooded most parts of Louisiana. The spillway was used for the first time in 1937 and opened eight times thereafter. It was designed for one in ten years operations to lower the stages at New Orleans and further downstream, to protect the city from flooding. The spillway can divert the water as the flow discharge reaches a maximum of 1,250,000 cfs (42,000 m³/s) to Lake Pontchartrain. Most of the times the spillway will operate for two weeks until the stages upstream in the river are lower again. [Brantley, 2010].

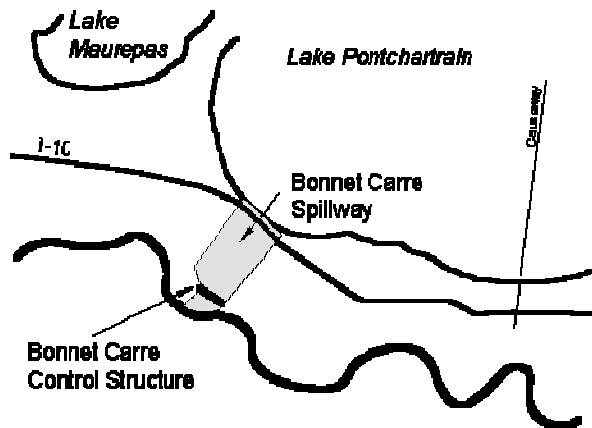


Figure B.6: Bonnet Carre Spillway overview [Easley, 2000].



Figure B.7: Bonnet Carre Spillway (photograph Bos)

Appendix C: Dredging Strategy

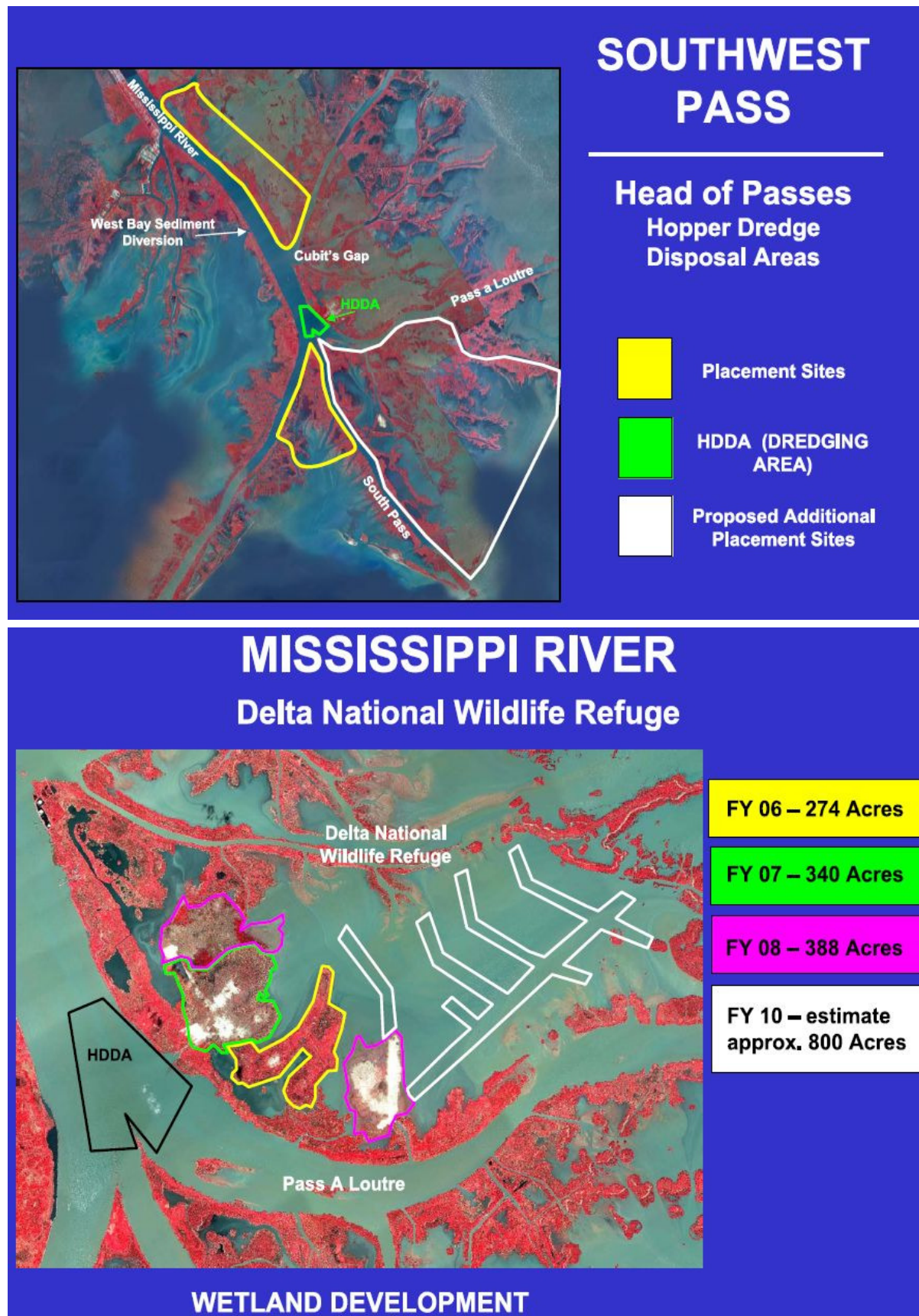


Figure C.1: Dredging strategy at Head of Passes in the Mississippi River, year 2006, 2007, 2008 and 2010 [USACE, 2010]



Figure C.1: Dredging strategy in the Southwest Pass at the mouth of the Mississippi River, from RM 0 to -17, Areas in yellow are Cutter dredger placement sites [USACE, 2010]

Appendix D: Fundamental 2D equations used by Delft3D

The fundamental flow equations for 2D model which are used by delft-3D will be discussed in this appendix. Also the numerical grid which is used will be explained. Besides that the underlying equations will be explained.

2D flow equations

The 2D equations follow logically from 3D equations by integrating over the depth. The 2D continuity equation is as follows:

$$\frac{\partial \zeta}{\partial t} + \frac{\partial(HU)}{\partial x} + \frac{\partial(HV)}{\partial y} = 0$$

The 2D momentum equation in x and y direction:

$$\frac{\partial U}{\partial t} + U \frac{\partial U}{\partial x} + V \frac{\partial U}{\partial y} + g \frac{\partial \zeta}{\partial x} + \frac{\partial \tau_{xx}^*}{\partial x} + \frac{\partial \tau_{xy}^*}{\partial x} + \frac{\tau_{bx}}{H} = fV$$

$$\frac{\partial V}{\partial t} + U \frac{\partial V}{\partial x} + V \frac{\partial V}{\partial y} + g \frac{\partial \zeta}{\partial y} + \frac{\partial \tau_{yx}^*}{\partial x} + \frac{\partial \tau_{yy}^*}{\partial x} + \frac{\tau_{by}}{H} = -fU$$

Explanation of the terms in x direction:

The first term is the local flow acceleration in the x direction, the second and third terms are the advection terms in 2 directions. The fourth term is the external forcing cause by pressure gradients. The fifth and sixth terms are the Reynolds normal and shear stress. The seventh term is the bottom friction stress and the eight and last term is the Coriolis force reduced with the f-plane approximation.

The bottom friction is described by:

$$\tau_{bx} = c_f U \sqrt{U^2 + V^2}, \quad \tau_{by} = c_f V \sqrt{U^2 + V^2}$$

$$c_f = \frac{g}{C^2}$$

The non dimensional c_f can be rewritten as a Chezy constant which is used regularly to define the bottom friction in a Delft-3D flow model

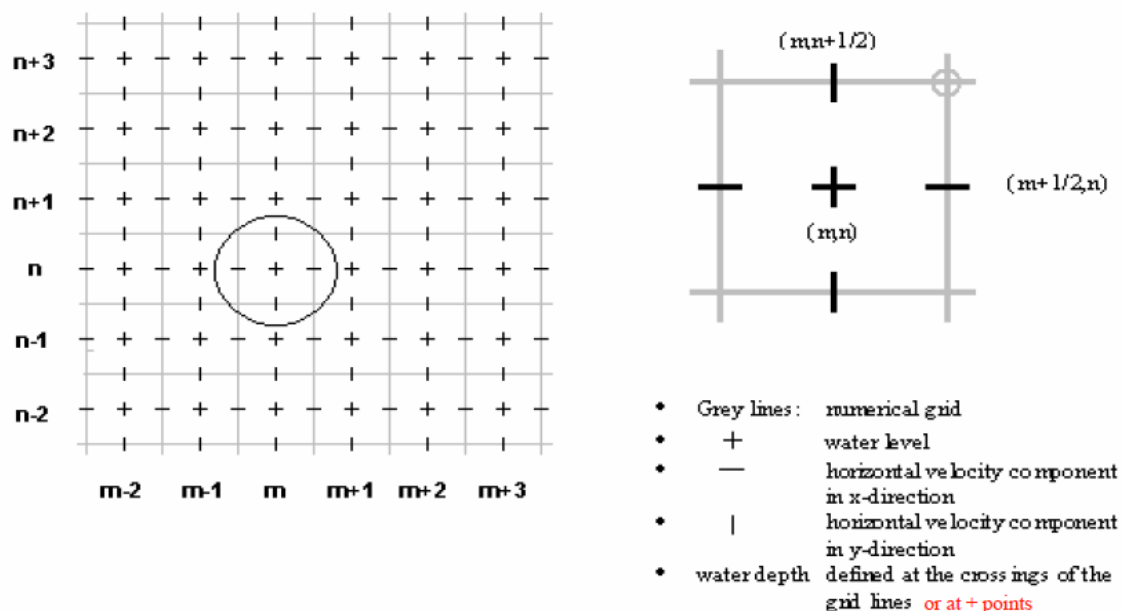
Boundary conditions and initial conditions

The 2D equations are discretized using numerical integration methods like ADI/AOI and are used in a numerical grid. ADI is semi implicit so it does not need to fulfil the CFL condition but is more computational efficient than an implicit method. To be able to solve the equations the model needs boundary conditions at each boundary and initial conditions for all grid points.

The numerical grid

Delft-3D uses a staggered grid (see picture) where it specifies water levels at the (m,n) locations and defines the velocities on the $(m+1/2,n)$, $(m-1/2,n)$, $(m, n+1/2)$ and the $(m, n-1/2)$ locations which are the surrounding numerical grid points. So the depth and velocity aren't specified at the same location. For numerical purposes the depths and velocities can be interpolated at various locations.

2D grid



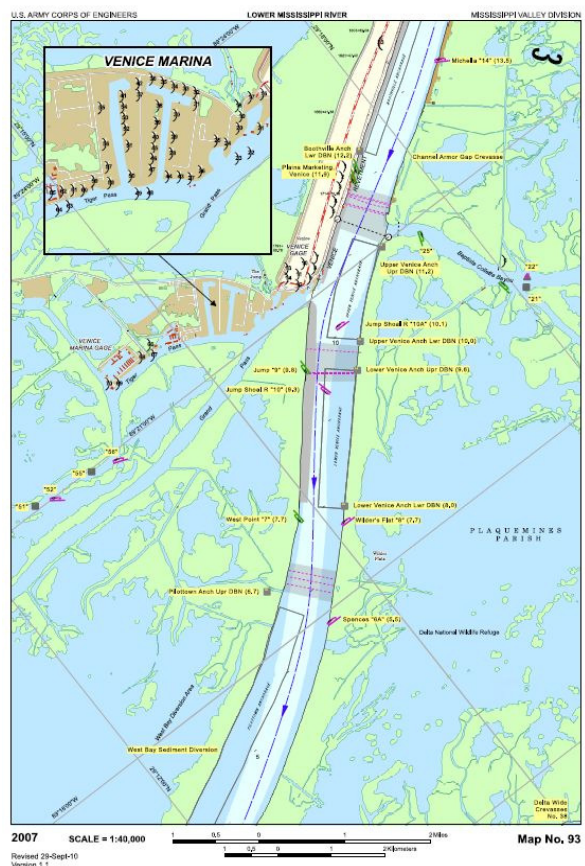
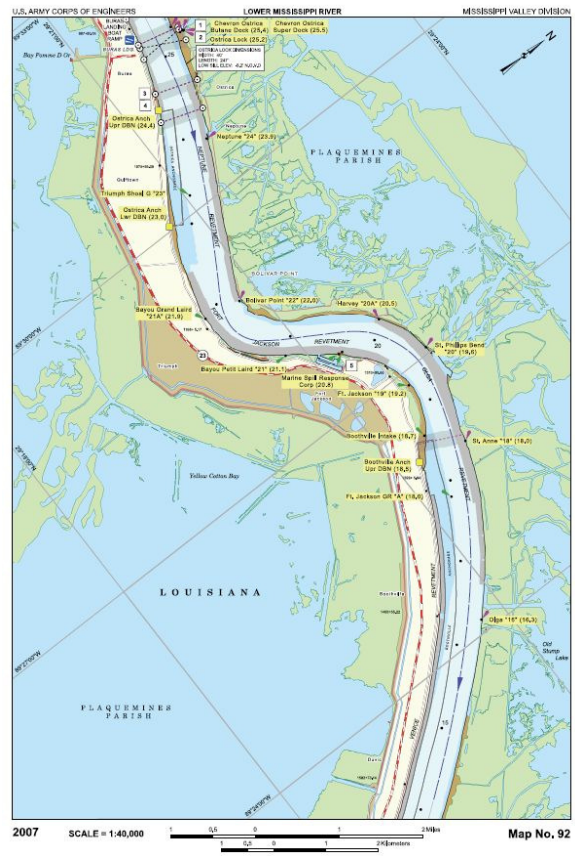
Appendix E: River Navigation Maps

These maps represent the study area. In these maps especially the bank protections (revetments) are well presented. Also the navigation channel is marked. Besides the river training works in the Southwest Pass can be seen [USACE, 2007].

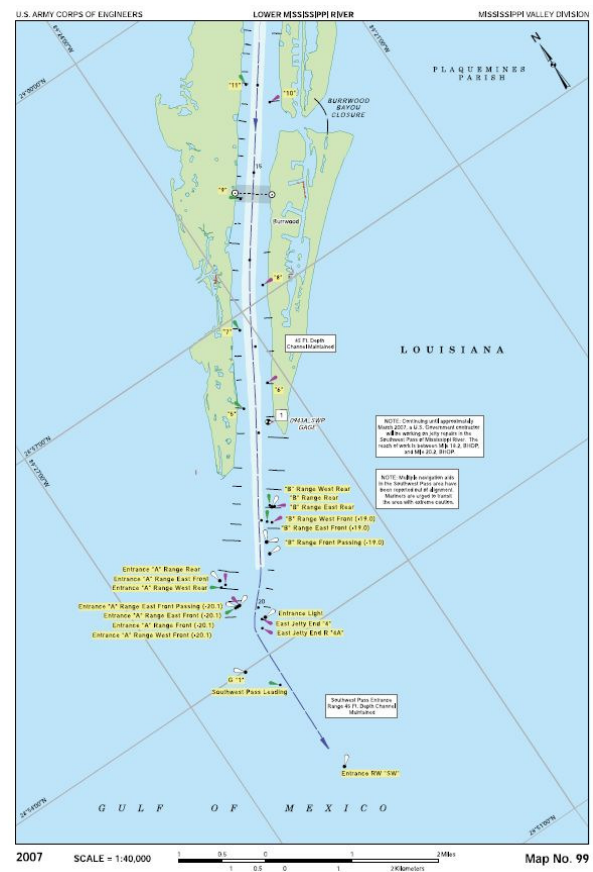
Point a la Hache to Empire



Empire to Head of Passes



Southwest Pass to Mouth of the River



Appendix F: Topography/ Bathymetry data set

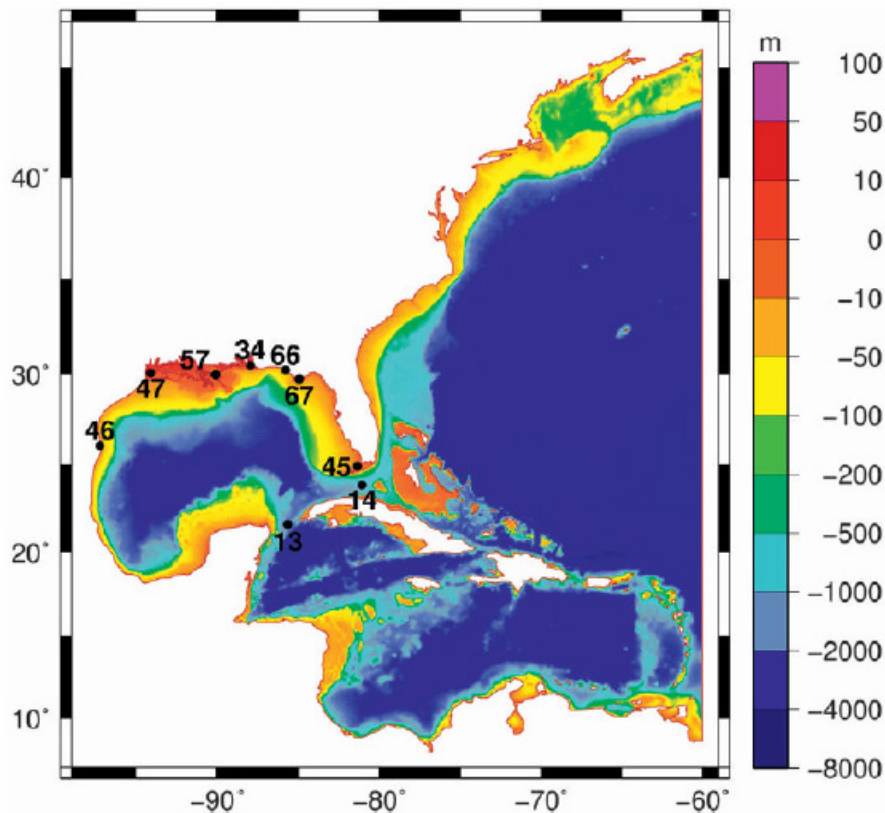


Figure F.1: Gulf of Mexico and Atlantic Ocean, ADCIRC model domain, including the Bathymetry and topography [Bunya *et al.*, 2010]

SL16 v18c3 : Bathymetry and Topography

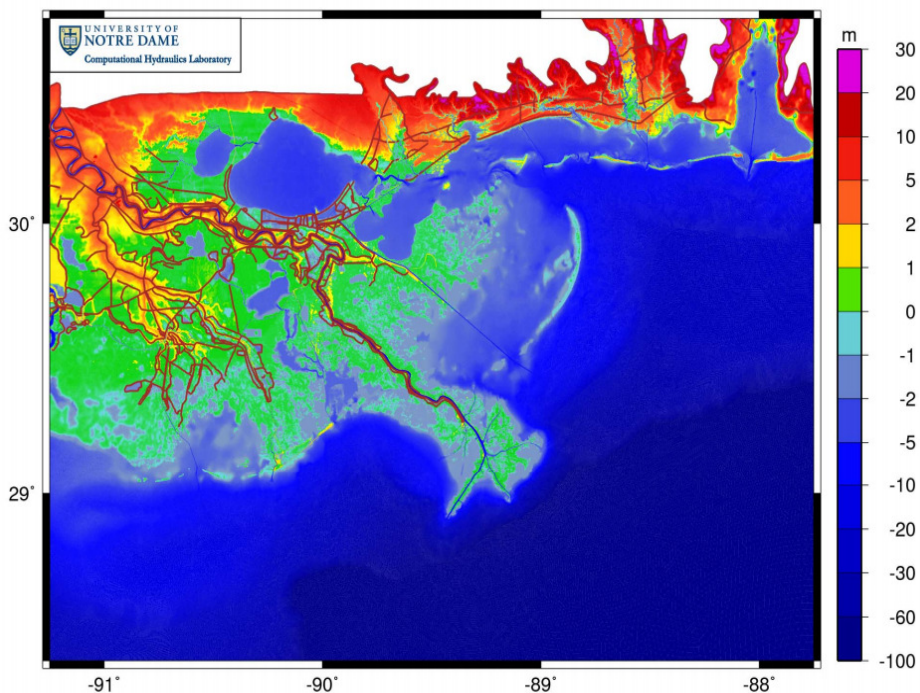


Figure F.2: Mississippi delta in the Gulf of Mexico, zoomed ADCIRC model of the delta, including the bathymetry and topography [Notre Dame, 2010]

Appendix G: Dredging schedule

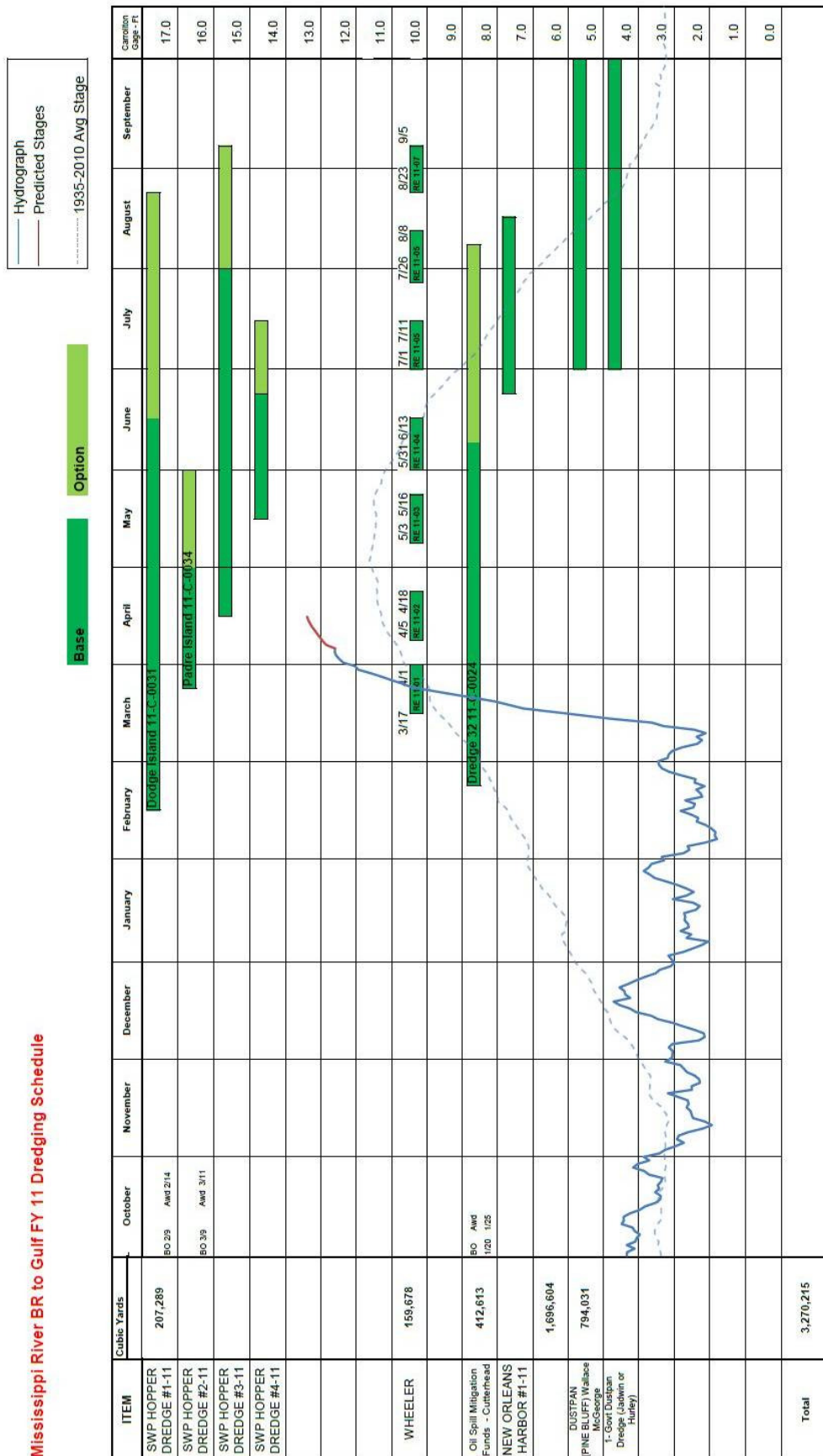
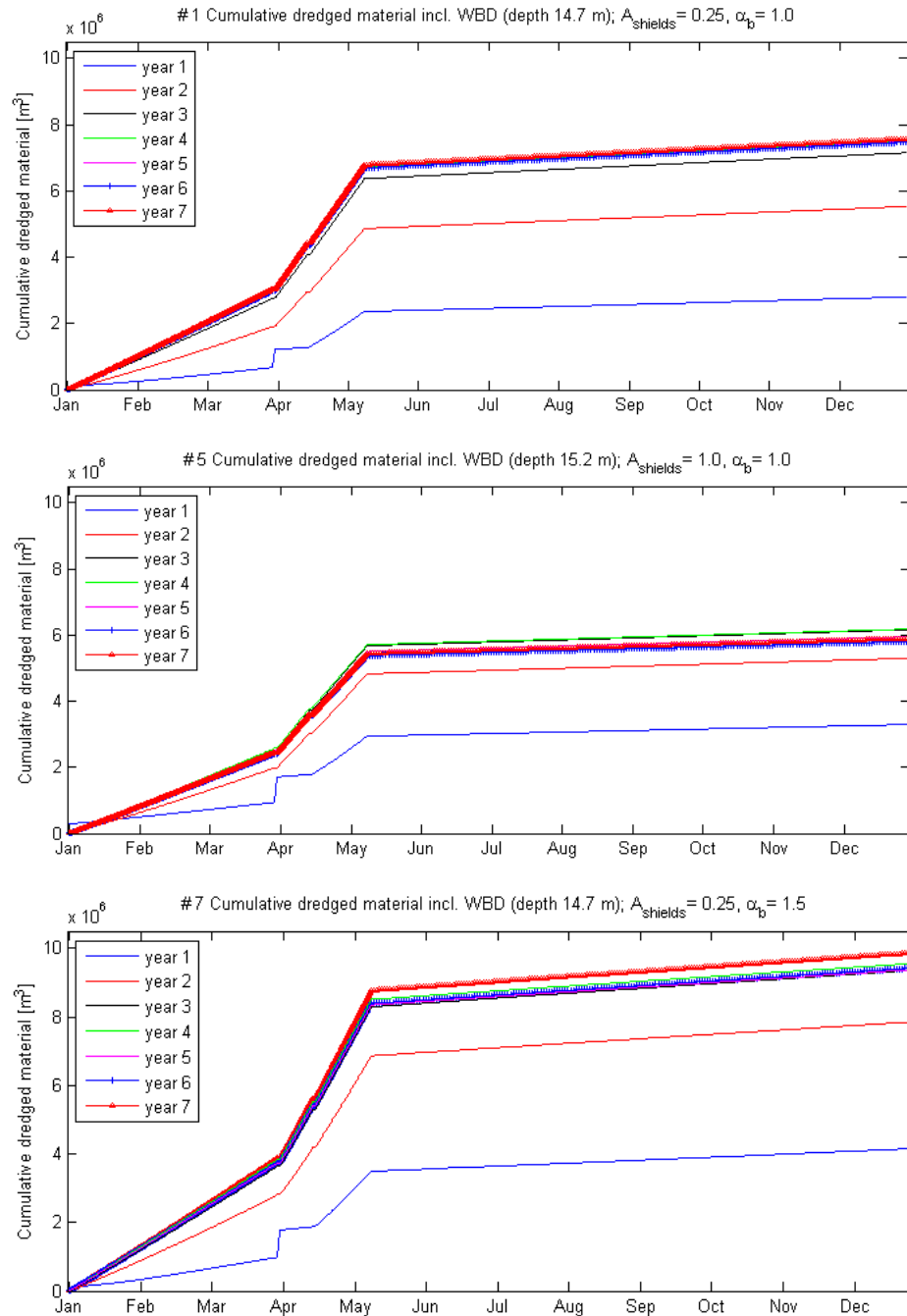


Figure G.1: Dredging schedule of the Lower Mississippi [UIm, 2011]

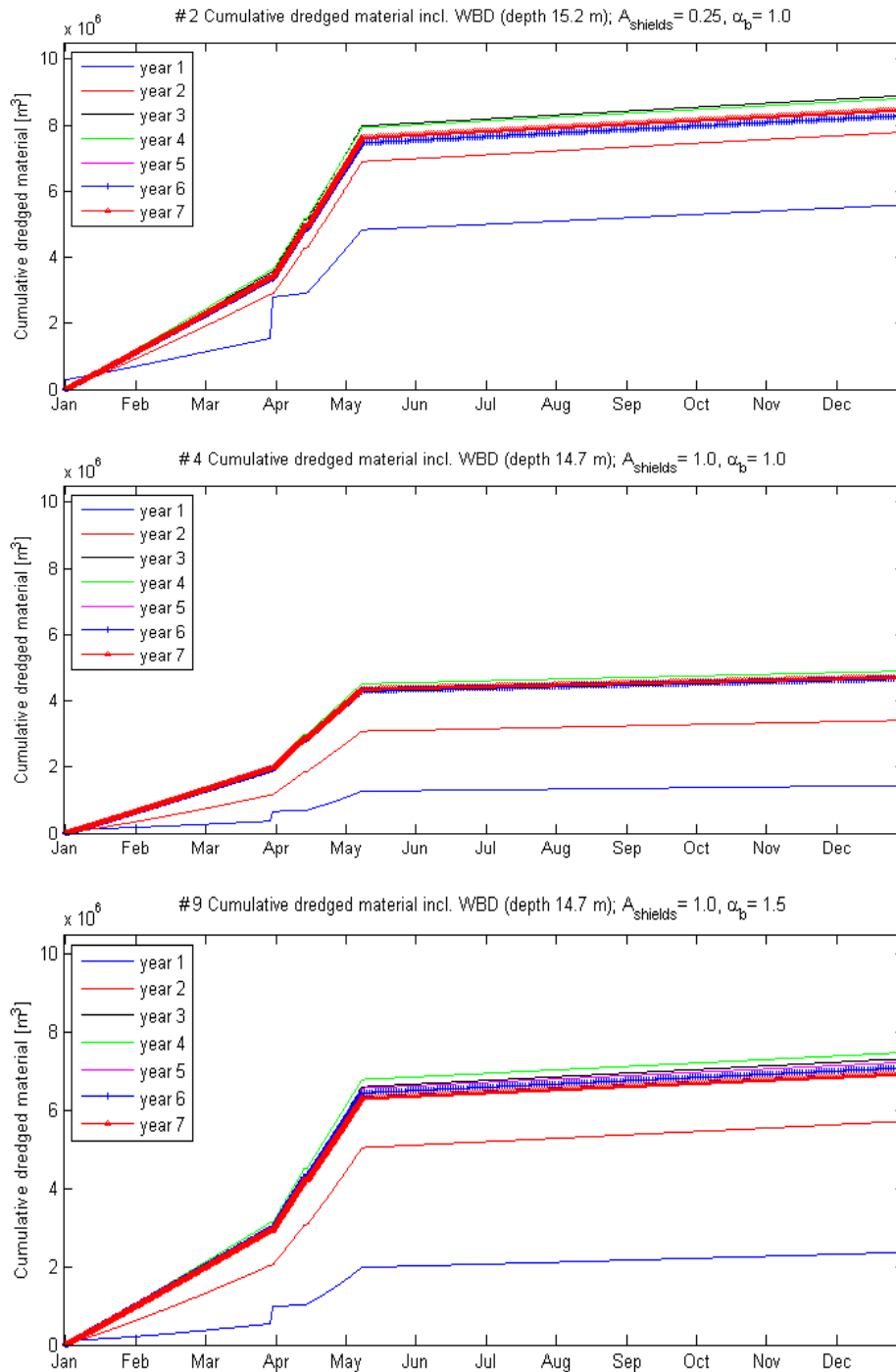
Appendix H: Results of Dredging Simulations

Varying the A_{shields} and α_b parameters influences the dredging quantities. Simulation #7 is the optimal simulation, because the quantities come close to the average dredged quantities in the river. The settings of simulation #7 are used to simulated different scenarios in chapter 6.



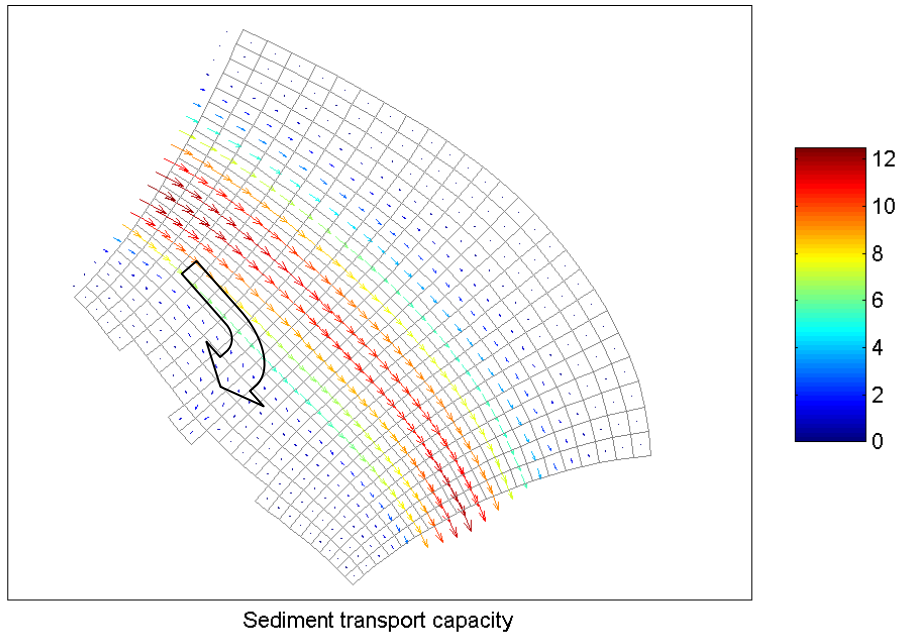
Varying the dredging depth

The dredge depth is increased from 14.7 m to 15.2 m. This has negative effect on the dredging quantities. The negative effect is 13 and 27 % for simulations 2 and 4 respectively. The difference between simulation 2 and 4 is about a factor 2.

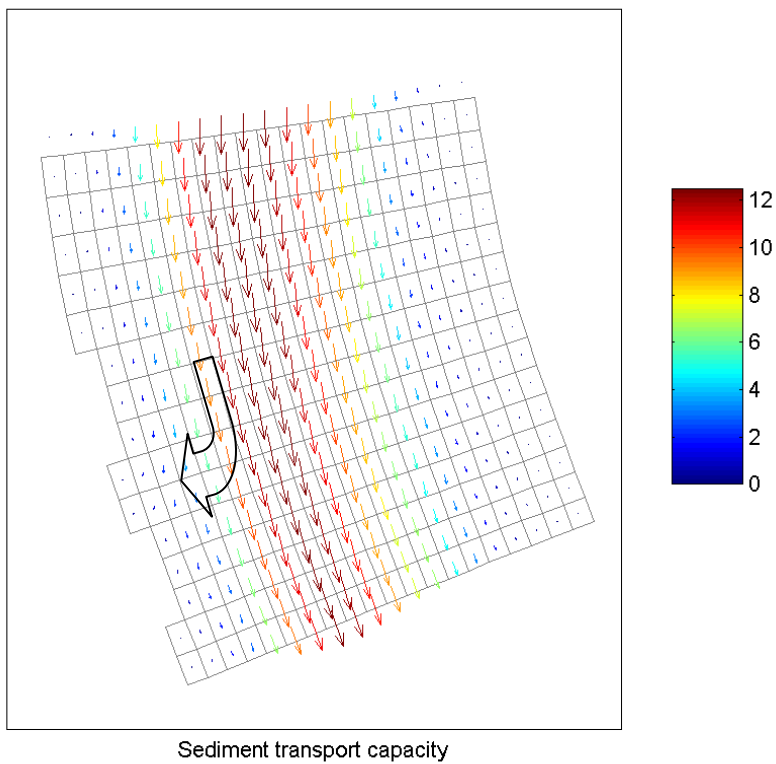


Appendix I: Suspended Transport at Diversion Sites

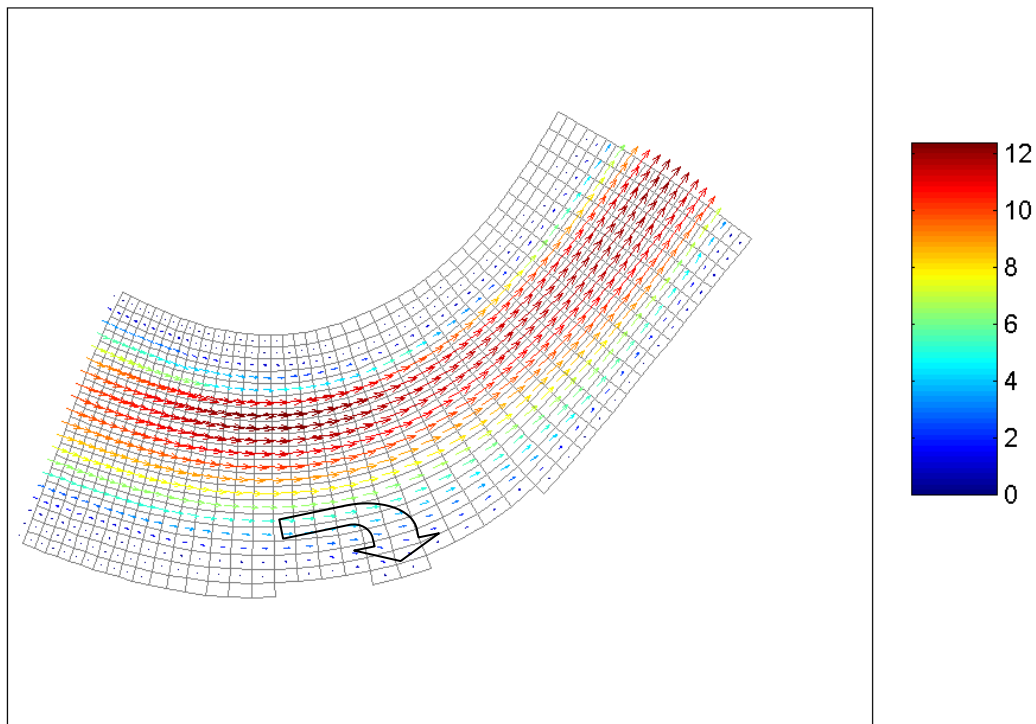
Sediment diversion inside bend (RK 53)
total sediment transport (KG/S/M)



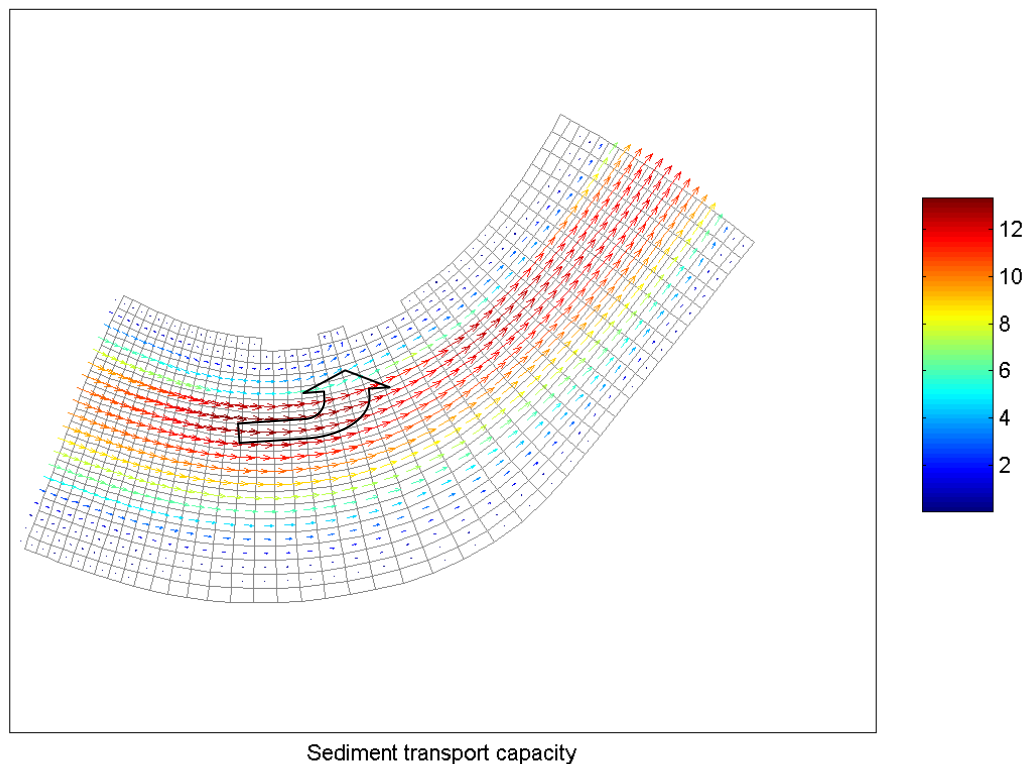
Sediment diversion inside bend (RK 48)
total sediment transport (KG/S/M)



Sediment diversion outside bend (RK 35)
total sediment transport (KG/S/M)



Sediment diversion inside bend (RK 35)
total sediment transport (KG/S/M)



Appendix J: Nedeco Blog

Stay in New Orleans from November 2010 to January 2011

<http://www.nedeco.nl/trainees/matthijs-bos>

Week 1: November 01 - 07

Today I start my blog about my stay in New Orleans, USA. I am Matthijs Bos (25) and I will be here for 12 weeks to further work on my MSc-thesis for Civil Engineering, Delft University of Technology. The thesis has the title "*The morphological effects of River Diversions on the Lower Mississippi River*". I started last September and planned to finish it the end of April. The project is committed by Royal Haskoning, they also invited me to come over to New Orleans, where they have an office Haskoning Inc. since the Hurricane Katrina in August 2005. Besides that Deltares is also advising me, because I am using their computational modeling program 'Delft3D'.

There was some delay in my plan, but finally I made it to New Orleans in Louisiana State last week. I am here to see what is going on in this field of research, speak to several researchers and look to different computational models.

In the Netherlands I read a lot of articles about the Mississippi River and noticed that a small group of researchers is studying the Lower Mississippi River for quite some time. Haskoning and Deltares brought me into contact with these researchers. So I will discuss the diversion projects with them and seeing if they can help me further on my research, and see how I can contribute to them.

All the basic needs are set, I got introduced to all my colleagues; I have a nice apartment in Uptown New Orleans, a car and an office with a panoramic view over Lake Pontchartrain in Metairie. The Haskoning Inc. office has six fulltime employees; next to I am here with another MSc student also writing here MSc-thesis. This week I joined the strategy meeting, so now I really know what they are doing here and which project are going on.

Also my own project is taking off; the first month September I was reading articles, looking for references and writing my proposal. October I was setting up my Mississippi River model and learn how to work with Delf3D, because that's not as easy as it looks like. Besides that I was arranging my trip to New Orleans. Now I am at the point to get deeper into my own model. Next week I can tell you more about it. My first simulations ran and I got my first results from the model, so that's a good start.

Let's say, I have enough plans to do over here, so I will keep you informed every week. And I have to say, the football games are great, definitely when the New Orleans Saints and the Tigers from LSU are also winning. Maybe I will go to one of them!

Week 2: November 08- 14

In the beginning of the week I had brief contact with my supervisors in Holland, I was discussing the model and how to go further with it. There are many different phases when building a model like this. Many phases are now left behind, but there surprisingly enough to go through.

Haskoning has connections with the University of New Orleans (UNO), this week I was introduced to them. I presented my project and they gave me some things to think about. The researchers at UNO have a 1D calibrated flow model of the Mississippi and all her distributaries, and they gave me data from their model that I can use as boundary condition for my model.

It is nice to be around with people who are working on the same project and it is interesting how they all contribute in a different way. They also gave me confidence that I am on the right way which is always pleasant to know. From this week on I also have my workplace at UNO, it will make it easy

to be in contact with other students and researchers.

Besides working on my computer model I also take the opportunities to go out on fieldtrips to interesting Hydraulic Engineering related places. This time I went to the Port of New Orleans with my colleagues and fellow student. It is nice to see the differences between the ports over the world. After seeing the Port of Rotterdam, Antwerp, Marseille, Le Harve and Zeebrugge I can make up some comparisons. The Port is really unique by his location, meanders along the river and is in the middle of the city. The site is very narrow and relatively small; although there was much land unused what is ready for new development. At night time we had a nice Haskoning dinner and of course until midnight some drinks on Bourbon Street.

Later on in the week I was preparing my model calibration and verification. The following two/three weeks I will be busy with that. Besides that I started to understand the basics of computational modeling of morphology and determining the boundary condition. The theory behind it is familiar, only I never made the computations.

Next week I am going to Louisiana State University, do a fieldtrip to the West Closure Complex and the Bonnet Carre Spillway. Besides that it will be Thanksgiving next Thursday, it will be interesting to see why that is such a big day in the US. You will hear about it.

Week 3: November 15 - 21

Unfortunately the trip to LSU was postponed; I will get back on that. Either way it was quite a busy chaotic week, with many different activities and fieldtrips. I could not spend much time on my thesis, next I will focus on that again!

A MSc student from Delft was here for the week. He came over from Houston where he is doing his project and because he was around he liked it to visit New Orleans. Together we went to see a couple of interesting hydraulic projects; all related to the Flood Risk Reduction System of New Orleans. We have seen the West Closure Complex who is still under construction and the Bonnet Carre Spillway. The Spillway is built in 1932 after the 1927 Mississippi flood. Besides that we had a tour through East New Orleans, the part of New Orleans that was heavily damaged by hurricane Katrina in 2005. Pretty impressive to see, because there are still parts of that area's that not have been rebuilt.

Just to give an idea; it is 25 degree Celsius, what makes live easy over here. I think I choose a nice time of the year to be here, especially because it started snowing in The Netherlands, sorry for that.

Week 4: November 22 – 28

This week it was Thanksgiving; they made me believe it is tradition to run the Turkey Trot in the early morning (8:30 am) and we did. Last few weeks I practiced a couple of times. Luckily I did so I could run the 5 miles straight in a respectable time (44:30 min). I know, the professionals ran it in 26:18 min, but I can live with that. The Saints game was also on Thanksgiving and is part of the tradition to watch it too and they won again. Since I have been around the won all games!

I also went to the New Orleans Zoo where they have quite a complete collection of animals. Nice to see and it was fun to hang out! The LSU team did not really well this week, hopefully next week the will win. Last but not least; this week I enjoyed the live Jazz music, I have been to two performances and I have to say it is great!

Week 5: November 29 – December 05

Like I wrote last week, that week was pretty busy with a lot of activities besides my actual study. Of course that is OK, but that also reminds you there is enough to work on. That is why this week the

focus was completely on my thesis again. I started writing, and started to summarize what I am doing. As from now I will also write the things down, the beginning of the thesis is made.

Besides that I started on the hydrodynamic flow calibration of my model. I already noticed it is not as easy as it seems, because there are so many factors and parameters that can be different. Every time I change one thing and one problem is solved, another thing pops up.

Through the weekend I worked on an update for Holland, since I have been in New Orleans already for one month. I tried to give an overview of my preliminary results; the model set up and the start of the flow calibration. This way my supervisors are able to give feedback on my project and I can seriously involve them. Next to I will use their expertise. Last couple of months I kept them informed and they were looking over my shoulder, but mostly I did the things on my own. After a while you are at a point you start asking again, because you can go either one or the other way. Also choices have to be made for the further development of the model, and I have to assume certain elements. Together we discuss the assumption, so that those can be implemented to the model.

Luckily in the weekend there is always time for some fun, this time I went to a real American home Party. I really enjoyed it☺, I met some nice people and had a good time.

Week 6: December 06 - 12

This week I went on another fieldtrip, this time with the Civil students from University of New Orleans. We went to Seabrook Floodgate and the IHNC barrier. Both structures are still under construction and are part of the Hurricane protection system. It was very interesting to see, especially to what phases it goes through. They build the structures in a really short time. The barrier will be built in less than two years. That is incredibly fast. We also walked over the barrier, I think that is a special experience, but probably it is because I am a hydraulic Engineer.

I also spoke to some interesting people of the Army Corps about the Maintenance Dredging in the river and the Restoration Project in the Wetlands. They both also gave me some data which I can use for my analysis.

Next to that I tried to go in more detail with my model at some places. But after two days I recognized that it didn't make any differences. Sometime you have to try and fail in order to get to a next step. This means that for this study I will keep to the same model which I finished a few weeks ago. Now it is time to calibrate the hydrodynamics of model so I can add the morphology to the model

Before I forget to mention the social parts of my trip; I was one of the lucky guys who went to the Saints American Football Game! It was amazing; it is really a nice experience to be at the game with 80,000 other people. And again we won; it is going to be exciting to next couple of weeks.

Week 7: December 13 - 19

Another week went by and again a lot happened. I went to LSU, department of Civil Engineering, which is the Louisiana State University. At LSU they put much effort in research of the Mississippi. The PhD student I met has been modeling the lower Mississippi for four years. At this time he has quite a good representative 2D numerical model, but he is still working to get the morphology right in the river. He showed me his result so far and gave me data he used to set up his model. Besides that they also built a physical model of the lower Mississippi in 2003. They are still doing research on it, and are looking to future improvement of the model.

Next to I had some review on my work until this time with my supervisors. We looked at my table of content for my report, since I really have to start writing. This way I have a clear overview where I am

and what still needs to be done. I am already half way through my research; this means first results need to be presented.

Like I wrote last week, I am working on the calibration of my hydrodynamic model. Together with one of my supervisors in New Orleans we made a plan how to analyze the model and to present the results. During the weekend I did the simulation runs and at the end of the weekend I sent my analysis to Holland for review and approve. After that we will see what changes needs to be made and if I can go further to the next step.

Next week also will be the last week before Christmas, you already can notice everyone is in a holiday mood. I also joined the Christmas lunch of our group of the Army Corps, it was a nice lunch at one of the local restaurants. I was a nice chance to speak some of the people from the Corps.

The Saints lost unfortunately, but they are still in the race for the play offs.

Week 8: December 20 - 26

The Army Corps of Engineers took my on a fieldtrip this week. I went on a boat survey on the lower Mississippi from Venice down to the mouth of the river. I had to put some effort into this trip since I had to be in Venice at 7 am and it was a two hour drive. At 7.30 am we were already on the river and luckily I choose a very good day to go out, in the morning it was 15 Celsius degrees and it went up to 20 Celsius degree. When we were at the mouth of the river I had the chance to see a group of dolphins playing along the Vessels entering the navigation channel to sail up the river. I was very nice to experience the river and to see how big it is. The river is what I expected from it, and it is off course really different if you compare it to having a look at Google earth. Now I had the chance to see the river in its perspective. I also could see all the traffic on the river, to see how busy it is and to clarify that the Mississippi is a very important.

At work it was noticeable it was the week before Christmas. It was very quiet, most people were gone off for the holidays, and I could finish my work in all rest. It was convenient my supervisors in Holland were still working, so I could discuss my progress on the calibration with them. My flow calibration is almost done now, maybe after New Year some minor changes and a verification run; then I finally can start to add morphology to my Delft3D model.

The end of the week my girlfriend came over. She is spending the holidays in New Orleans with me and I really enjoy my time with her.

Week 8 & 9: December 20 – January 02

It though it is time for a holiday to celebrate Christmas and New Years Eve, also my girlfriend came over from Holland. It was a very relaxing week. We did not do too much, just being the tourist in New Orleans. Since I had seen already quite some things of New Orleans I could take my girlfriend on trips to show her where I have been telling all about. We also been to the Mall, it was not that big as I thought it would be, but always nice to shop with many discount. And off course everyone who is coming to New Orleans has to see the Saints playing, so I we watched the game in one of the bars which was crowded. The Saints won from Atlanta Falcons, this means the will go to the play-offs. The can revive their last year's Championship.

New Years Eve was also great, we went to an all inclusive party downtown at the river levee. It was a nice party, which was not too busy. At 12 pm the fireworks started in front of us at barges on the river. It was great, because we were at this party, nice and warm at the balcony, over 3000 people were outside at the levee.

Sometimes weeks go by too fast I think, it happens all the time. The break is over again, next week a lot of work needs to be done. I can start counting down, I have 4 weeks left to finish my work over here.

Week 10: January 03 - 09

Holidays are over and it's a pity but my girlfriend left the country already. It's time to work! This week I had to finish the write up of my first two chapters of my report.

In the end of the week I had some time left to start adding the morphology to the model. I wrote it down in almost every blog, but now I really have to start with the morphology. There is no way back! I think I will have to struggle new difficulties where I am at this point not aware of, we'll see what it brings.

Since I have done the calibration I've also got an overview of the available verification dataset, now I have to define some time series where I can validate my model with, and see if my model behaves well. I hope so!?

In the weekend we had a nice New Year Party with all the Haskoning colleagues and families. Unfortunately the Saints lost in the Wildcard game before the Play-offs, it is the end of the season for the Saint. In August 2011 the can start over again.

Week 11: January 10 - 16

The clock is ticking, only two weeks left and then I already return to Holland. Time to wrap it up and see where I am at the moment.

I showed my preliminary result at University of New Orleans to an Assistant professor at the Civil Engineering Department. He is also the person who is hosting me at UNO. He was satisfied about the progress I made last 10 weeks and found it very promising and was looking forward to the final results of my thesis. With that been said, I went with one of my supervisors to my first draft of my first chapters of my report. Some changes have to be made, but also the report goes in the right direction. I also already get a good understanding on how to calibrate my model for morphological behavior. I hope I can finish the first result of this calibration next week.

Another two weeks to go and enough work that needs to be done. Saints is not playing anymore, so that's a pity. Luckily bands are playing in all sort of bars, I am not getting bored I can tell.

Week 12: January 17 - 23

Almost done! I continued my morphological calibration. I am getting interesting results. The project is still very interesting to work on. It is amazing how well a river like the Mississippi can be modeled. The simulations are meeting the observed data as flow, velocities and sediment transport in the river. Now I have to analyze and interpretate the results, perhaps with some small adjustment I can even improve the model.

Besides that I am still writing on my report. It goes rather slow, but we're getting somewhere. Also my supervisor helps me a lot and reviews all my writings. It helps when people just go to your thought and see if things are missing, which are very obvious to me. If I would only present my work at the end, it could be that my supervisors and I both have different expectation. This way we got rid of that.

Only one week left, so it's all time to have fun. I played a little soccer in park, which was nice and had some beers with the colleagues. Next week I will write something more in my report, I try to finish at least the first 5 chapter of my thesis, so only one is left for the next week back in Holland. And off course I have a presentation to prepare. I will present my work to my colleagues at the USACE and at UNO. I am curious what they think of my work.

Week 13: January 24 - 30

Time goes to fast unfortunately. My time in the US is over. I am already back in the cold and dark Netherlands. To all good things comes an end, as we say it in Dutch. Thank you all for giving me such a good time in the US!

The last week was great, I got a lot of things done and worked almost 24/7. The final result was therefore pretty good. On Friday I had to give two presentations to show my preliminary results of my study. One I gave at the Army Corps of Engineers for 20 Hydraulic Engineers of the department I worked for including the managers. The second I gave at University of New Orleans, for the Associate Professor who hosted me, some of his colleagues and his students. It was an existing day and people where very enthusiastic about my results. They were looking forward to my final results in three months.

Besides the presentation I am also writing my draft report with my work so far. Next week I have to hand in the draft report for review by my Committee. Let's see what they think of my work!

This is also going to be my last official post on my blog. It might post again when my work is finished in three months. I can write how my project is evaluated and what my next plan is. Thanks for reading my blog, feel free to get in contact with me if there are any questions.

Matthijs Bos